2024

Developing Radiosensitizers to Enhance Radiotherapy in Treating Gastroenteropancreatic Neuroendocrine Tumor

Zeta Chow
University of Kentucky, zeta.chow@uky.edu
Digital Object Identifier: https://doi.org/10.13023/etd.2024.177

STUDENT AGREEMENT:

I represent that my thesis or dissertation and abstract are my original work. Proper attribution has been given to all outside sources. I understand that I am solely responsible for obtaining any needed copyright permissions. I have obtained needed written permission statement(s) from the owner(s) of each third-party copyrighted matter to be included in my work, allowing electronic distribution (if such use is not permitted by the fair use doctrine) which will be submitted to UKnowledge as Additional File.

I hereby grant to The University of Kentucky and its agents the irrevocable, non-exclusive, and royalty-free license to archive and make accessible my work in whole or in part in all forms of media, now or hereafter known. I agree that the document mentioned above may be made available immediately for worldwide access unless an embargo applies.

I retain all other ownership rights to the copyright of my work. I also retain the right to use in future works (such as articles or books) all or part of my work. I understand that I am free to register the copyright to my work.

REVIEW, APPROVAL AND ACCEPTANCE

The document mentioned above has been reviewed and accepted by the student's advisor, on behalf of the advisory committee, and by the Director of Graduate Studies (DGS), on behalf of the program; we verify that this is the final, approved version of the student's thesis including all changes required by the advisory committee. The undersigned agree to abide by the statements above.

Zeta Chow, Student

Dr. B. Mark Evers, Major Professor

Dr. Claire Clark, Director of Graduate Studies

Developing Radiosensitizers to Enhance Radiotherapy in Treating Gastroenteropancreatic Neuroendocrine Tumor

---

DISSERTATION

A dissertation submitted in partial fulfillment of the
requirements for the degree of Doctor of Philosophy in the
Department of Clinical and Translational Science
at the University of Kentucky

By

Zeta Chow

Lexington, Kentucky

Director: Dr. B. Mark Evers, Professor of Surgery

Lexington, Kentucky

2024

ABSTRACT OF DISSERTATION

Developing Radiosensitizers to Enhance Radiotherapy in Treating Gastroenteropancreatic Neuroendocrine Tumor

Gastroenteropancreatic Neuroendocrine Tumor (GEP-NET) is a heterogeneous group of malignancies arising from multipotent neuroendocrine stem cells in the gastrointestinal tract. The incidence of GEP-NET continues to rise, possibly due to the advancement of imaging and biomarkers available for diagnosis. However, even though the majority of patients are diagnosed with low-grade and localized disease, a significant percentage of patients present with advanced-stage metastatic disease with poor prognosis in months to a few years. These advanced-stage GEP-NET patients can also present with a variety of debilitating symptoms that significantly impact their quality of life. The role of palliative-intent surgery is limited, and systemic treatment is the mainstay for treating advanced-stage metastatic GEP-NETs. The systemic treatment options include long-acting somatostatin analogs, telotristat ethyl, interferon alpha, anti-angiogenesis agents, immunotherapy, targeted therapy, and conventional chemotherapy.

Radiotherapy is an emerging modality in managing advanced-stage metastatic GEP-NET. The most common type of radiotherapy is the external beam radiation (EBRT), which has been implemented as a palliative measure with reasonable locoregional control. Another novel modality is the Y-90 radioembolization, which is a liver-directed therapy for GEP-NET patients with hepatic metastases. The most widely recognized novel treatment in the modern era is the peptide radionuclide receptor therapy (PRRT). In landmark clinical trials, PRRT has demonstrated an improved objective response rate compared to the standard of care long-acting somatostatin analog systemic treatment. Therefore, it has emerged as the new standard of care in managing advanced-stage metastatic GEP-NETs. Despite its promising outcomes, PRRT failed to demonstrate improved survival, and the objective response rate was still considered suboptimal. One area of active research is the development of combined therapy with PRRT to enhance treatment efficacy, and ultimately improve patient outcomes. Only three anti-neoplastic agents with radiosensitizing property have been established in existing clinical trials, though several therapeutic agents are currently under investigations. This thesis aims to investigate novel radiosensitizing therapeutic agents in preclinical studies and demonstrate their translational values for prospective clinical trials.

The mammalian-targeted rapamycin receptor (mTOR) dysregulation has been established as a crucial therapeutic target for GEP-NET. A study investigated the radiosensitization of PI3K/mTOR dual inhibitor in GEP-NET cell lines (QGP-1, BON, NT-3) in vitro. We assessed the efficacy of PI3K/mTOR dual inhibitor PF-04691502 to inhibit pAkt and to increase apoptosis in GEP-NET cell lines and patient-derived tumor spheroids as a single agent or combined with radiotherapy. Treatment with PI3K/mTOR inhibitor decreased pAkt (Ser473) expression for up to 72h compared with control. Interestingly, simultaneous treatment with PI3K/mTOR dual inhibitor and X-ray ionizing radiotherapy did not induce significant apoptosis; however, the addition of PI3K/mTOR

dual inhibitor 48h after radiotherapy significantly increased apoptosis compared to either PI3K/mTOR dual inhibitor or radiotherapy alone. This result demonstrated that the radiosensitization effect of PI3K/mTOR dual inhibitor is schedule-dependent. Our findings supported that radiotherapy in combination with appropriately scheduled PI3K/mTOR dual inhibitor may be a promising regimen for GEP-NET patients.

Another therapeutic target is the ribonucleotide reductase (RNR), a rate-limiting enzyme that produces deoxyribonucleoside triphosphates, building blocks for DNA synthesis and repair. We explored the radiosensitization effect by inhibiting RNR with a selective RNR M2 subunit (RRM2) inhibitor in metastatic pancreatic neuroendocrine tumor (pNET) cell lines (QGP-1 and BON) in vitro and in vivo. We found that RRM2 inhibition activated DNA damage response pathways by phosphorylating ATM and DNA-PKcs, but not ATR. RRM2 also increased G1 phase cell cycle arrest via Chk1 and Chk2 phosphorylation. The selective RRM2 inhibitor induced more apoptosis when combined with radiotherapy in vitro. We also utilized two metastatic pNET subcutaneous and lung metastasis models. We demonstrated significantly increased apoptosis of BON-cell subcutaneous xenograft and reduced lung metastases burden when combining selective RRM2 inhibitor with radiotherapy in vivo. Together, our findings successfully showed radiosensitization with selective RRM2 inhibitor in treating metastatic pNET and supported future clinical trials utilizing RRM2 inhibitor as a radiosensitizer in treating metastatic pNET.

In conclusion, our preclinical studies suggested that implementing radiosensitizer appropriately could induce more apoptosis, thus effectively reducing disease burden in multiple models in vitro and in vivo. The selection of a radiosensitizer should consider the unique genetics and molecular biomarkers of GEP-NET and proper radiobiology for radiosensitization. Several challenges of radiosensitizer research in GEP-NET include the relative rarity of disease that leads to a lack of preclinical models and slow recruitment in clinical trials, excessive toxicity with current generation radiosensitizers, and diverse tumor biology that renders the “one-fit-for-all” approach ineffective. In response to these challenges, we should consider leveraging modern technologies, such as artificial intelligence, to propel basic and translational GEP-NET research effectively. The future generation of an ideal radiosensitizer for treating GEP-NET is likely safe, effective, and personalized.

KEYWORDS: Gastroenteropancreatic Neuroendocrine Tumor; Peptide Radionuclide Receptor Therapy; Radiosensitizer; Radiotherapy

Zeta Chow

(Name of Student)

04/24/2024

Date

Developing Radiosensitizers to Enhance Radiotherapy in Treating Gastroenteropancreatic Neuroendocrine Tumor

By
Zeta Chow, MD. MS.

B. Mark Evers, MD
Director of Dissertation

Claire D. Clark, PhD. MPH
Director of Graduate Studies

04/24/2024
Date

ACKNOWLEDGMENTS

The following dissertation, while an individual work, benefited from the insights and direction of several people. First, my Dissertation Chair, Dr. Mark Evers, exemplifies the high-quality scholarship to which I aspire. In addition, Dr. Piotr Rychahou provided timely and instructive comments and evaluations at every stage of the dissertation process, allowing me to complete this project on schedule. Next, I wish to thank the complete Dissertation Committee respectively: Dr. Thomas Kelly, Dr. Lowell Anthony, and Dr. Kathleen O'Connell. Everyone provided insights that guided and challenged my thinking, substantially improving the finished product.

In addition to the technical and instrumental assistance above, I received equally important assistance from family and friends. My husband, Patrick Cummins, provided on-going support throughout the dissertation process, as well as technical and financial assistance critical for completing the project in a timely manner.

TABLE OF CONTENTS

LIST OF TABLES

LIST OF FIGURES

CHAPTER 1. INTRODUCTION

1.1 Gastroenteropancreatic neuroendocrine tumor (GEP-NET)

1.1.1 Cell Biology

Gastroenteropancreatic Neuroendocrine Tumor (GEP-NET) is a heterogeneous group of malignancies arising from local multipotent neuroendocrine stem cells in the gastrointestinal tract [1]. It includes both carcinoid tumors and pancreatic neuroendocrine tumors [2]. Carcinoid tumors derive from enterochromaffin cells of the guts, and pancreatic neuroendocrine tumors originate from the islet of the Langerhans [3]. Depending on the location, GEP-NET can be categorized into foregut (esophagus, stomach, proximal duodenum, liver and pancreas), midgut (distal duodenum ileum, jejunum, ascending colon, and proximal two-thirds of transverse colon) and hindgut tumors (distal third of transverse colon, descending colon, sigmoid and rectum) [4]. There are at least 17 types of neuroendocrine cells in the gastrointestinal tract, characterized by their unique morphological and physiological functions [5].

Neuroendocrine tumors (NETs) are characterized by high levels of somatostatin receptors (SSTRs), which are G-protein-coupled receptors. These receptors modulate proliferation and protein synthesis, and regulate hormone secretion by counteracting the prosecretory stimuli deriving from β-adrenoreceptors and adenylyl cyclase [6]. Common biomarkers include chromogranins, a group of acidic proteins contained in the vesicles of neurons and neuroendocrine cells. Chromogranin A is a glycoprotein most neuroendocrine cells express and preserved by malignant tissues. Therefore, it was also used as a biomarker to predict prognosis and monitor disease progression. Other

commonly expressed biomarkers include neuron-specific enolase, a neuron-specific isomer of the glycolytic enzyme 2-phospho-D-glycerate hydrolyase or enolase, and also Synaptophysin, an integral membrane glycoprotein in presynaptic vesicles of neurons [7, 8]. Each subtype of NETs can also express specific biomarkers, such as serotonin by carcinoids, glucagon in glucagonoma, and vasoactive intestinal polypeptide (VIP) in the VIPoma [7].

GEP-NET can be sporadic or associated with inherited genetic syndromes, especially pancreatic neuroendocrine tumors (pNET). Multiple Endocrine Neoplasia type 1 (MEN-1) syndrome is an autosomal-dominant syndrome caused by mutations of the *MEN1* gene and closely associated with pNETs, such as gastrinomas and non-functioning tumors. Other genetic syndromes include Von-Hippel Lindau syndrome, tuberous sclerosis and neurofibromatosis type 1[2, 5]. The pathogenesis of GEP-NET needed to be clearly defined, particularly among the enteral NET subtypes. Genetic mutations implicated in the pathogenesis include *MEN1*, death domain-associated protein/a-thalassemia mental retardation syndrome (*DAXXATRX*), mutY homolog *(MUTYH*), checkpoint kinase 2 (*CHEK2*), breast cancer gene 2 (*BRCA2)*, Kirsten rat sarcoma viral oncogene homolog (*KRAS*), and cyclin-dependent kinase inhibitor 1B (*CDKM1B*) [9-11]. Studies suggested that dysregulation of the mammalian target of the rapamycin (mTOR) pathway was implicated, regardless of its primary site. In addition, whole-genome sequencing study demonstrated possible involvement of DNA damage repair, chromatin remodeling and telomere maintenance pathways [10]. Tumor neo-angiogenesis was also identified as a critical event with evidence of overexpression of proangiogenic factors, such as vascular endothelial growth factor (VEGF) [12].

1.1.2 Epidemiology

In the past four decades, the incidence of GEP-NET increased. According to the Surveillance, Epidemiology, and End Results (SEER) Program, the overall age-adjusted incidence of GEP-NET was 1.05 per 100,000 persons in 1975, which increased to 5.45 per 100,000 persons by 2015, across all age and gender groups. The increase in incidence was the most prominent among localized disease (from 0.32 to 3.28 per 100,000 persons) and World Health Organization grade 1 (WHO G1) GEP-NETs (from 0.03 to 3.5 per 100,000 persons). The 20-year limited-duration prevalence of GEP-NETs also increased significantly, reflecting its increasing incidence and indolence of disease[13].

Patient could present with localized disease (51-53%), locoregional disease (19-20%), or distant metastases (22-27%) at the time of diagnosis [13, 14]. More than half of the patients presented with WHO G1 disease. The most common primary site of GEP-NET was the rectum (28.6%), followed by the small intestine (28.1%), pancreas (16.4%), stomach (9.2%), colon (9.2%) and appendix (8.5%) [13]. It was theorized that advancements in cross-sectional imaging, endoscopy and surveillance programs have increased the detection rate of indolent malignancy [2].

1.1.3 Clinical Presentation

GEP-NET can manifest in a variety of clinical presentations. Functional GEP-NETs are a group of hormone-secreting tumors that cause secondary clinical syndromes. One common subtype of functional GEP-NET is insulinoma, which characteristically presents as symptomatic hypoglycemia, low blood glucose levels, and relief of symptoms after glucose administration [15]. Conversely, glucagonomas presents with

hyperglycemia, weight loss, venous thromboses, glossitis, and necrolytic migratory erythema caused by amino acid or zinc deficiencies [16]. Gastrinomas can cause Zollinger-Ellison syndrome, which manifests as peptic ulceration, heartburn and acidic diarrhea [17]. VIPoma is associated with Verner-Morrison syndrome, profuse watery diarrhea and electrolyte imbalance [18]. Somatostatinoma can cause steatorrhea, achlorhydria, diabetes mellitus and cholelithiasis. Small bowel NETs, especially advanced-stage or metastatic disease, produce serotonin and other vasoactive substances that cause carcinoid syndrome. Symptoms of carcinoid syndrome include diarrhea, flushing, and bronchospasm [2]. Less commonly, GEP-NET can also secrete adrenocorticotropic (ACTH) hormone, parathyroid hormone-related peptide and growth hormone-releasing (GH) hormone to give rise to respective clinical syndromes [19].

Non-functional GEP-NETs do not secrete hormones and, thus, could be asymptomatic. The lack of clinical presentation of a non-functional tumor can lead to delayed diagnosis and, therefore, worse prognosis compared to functional GEP-NETs [2]. Increasing numbers of patients are diagnosed incidentally on radiographic imaging or endoscopic procedures for other indications [20]. The clinical presentation of non-functional GEP-NET largely depends on the size, location and aggressiveness. Duodenal or head of pancreas NETs can cause gastric outlet or biliary obstruction [21]. Aggressive small bowel NET can present with mesentery metastases, bowel obstruction and mesenteric ischemia. Cramping and intermittent abdominal pain are common presentations [2]. Rectal NET may be associated with rectal pain, bleeding, and a change of bowel habit or stool caliber [22].

1.1.4 Diagnosis

Diagnosis of GEP-NET is made based on clinical presentation, respective hormonal markers, and radiographic imaging or endoscopic procedures [2]. We have discussed the clinical presentation of GEP-NET in the previous section. Diagnostic hormonal markers are specific for the subtype of GEP-NETs [5]. For instance, patients who presented with carcinoid syndrome can undergo 24-hour urinary excretion of 5-hydroxyindoleacetic acid (5-HIAA), a breakdown of serotonin, or direct plasma 5-HIAA assay [23]. Other hormonal markers that may help differentiate GEP-NET include insulin, glucagon, VIP, ACTH and GH [5].

Conventional imaging, such as Computed Tomography (CT) and Magnetic Resonance Imaging (MRI), can further localize and characterize the anatomy of disease. Upper and lower endoscopy can provide direct visualization and sampling of the tumor [2]. Functional imaging studies, such as SSTR Indium-111 scintigraphy and Gallium-68-DOTATATE Positron Emission Tomography (PET)/CT scan, is based on the unique SSTR expression of NETs. Both functional imaging studies have excellent sensitivity and specificity for diagnosing GEP-NETs [24]. The level of radiotracer update with functional scan depends on the degree of SSTR expression. Therefore, poorly differentiated and undifferentiated GEP-NETs, which may have lost their SSTR expressions should be imaged with ^{18}F-fluorodeoxyglucose PET/CT scan instead[25].

1.1.5 Prognosis

The prognosis of GEP-NET varies widely, depending on the pathology, grade, and stage of disease. GEP-NETs are relatively indolent with a median overall survival (OS) of 324 months. However, there are also very aggressive subtypes contributing to the mortality of the disease. Rectal and appendiceal GEP-NETs have the best median survival over 10 years, whereas pNETs have the worse survival with a median OS of 67 months. In addition, localized and locoregional diseases have significantly better median OS (>297 months) compared to distant metastatic disease (34 months). Poorly differentiated and undifferentiated grade GEP-NET have a poor median OS of approximately 10 months, while well-differentiated and intermediate-differentiated GEP-NETs have a median OS greater than 324 months. Another independent risk factor is age greater than 60 years old. Of all the prognostic factors, disease stage is the most critical factor. The hazard ratio is 10.32 comparing distant metastatic disease to localized disease [13].

Among patients with distant metastatic disease, small intestine has the best median OS of 96 months. In contrast, patients with colon, stomach, or rectum origin have the worst median OS of 8, 9 and 11 months, respectively. The survival rates for distant metastatic disease in all sites are extremely poor. Even for small intestine GEP-NET with the best prognosis, 3-year and 5-year survival was only 74.9% and 63.2%. Over the past four decades, the prognosis of distant disease has moderately improved. The 3-year and 5-year survival rates have increased from 48.3% and 39.5% in 1975 to 60.9% and 60.9% in 2015, respectively [13].

1.2 Management of GEP-NET

1.2.1 Early Stage and Localized GEP-NETs: Curative-intent Surgery and Close Surveillance

Management of GEP-NET depends on the stage, grade, location, and etiology of disease. Localized disease is primarily managed with surgical resection. The type of operation depends on the anatomy and size of tumor with the goal to obtain complete clearance of disease surgically. For instance, pNET can be managed with either the Whipple procedure or distal pancreatectomy and splenectomy, based on its location. Small pNET can sometimes be managed with enucleation as well [26]. Appendiceal GEP-NET may require simple appendectomy if less than 1 cm, or right hemicolectomy if tumor is greater than 1 cm and other risk factors for recurrence, such as mesoappendix invasion [27]. After definitive surgery, patients were usually surveilled with cross-sectional imaging every 6 months to 2 years, for at least 5 years. Functional imaging study, on the other hand, was not endorsed for surveillance purpose [28].

1.2.2 Advanced Stage, Metastatic GEP-NET: Limited Palliative-intent Surgery

Contrary to the primary role of surgery in early-stage localized GEP-NETs, surgical options in advanced-stage disease are limited and under palliative intent instead. Palliative surgical procedures for advanced-stage GEP-NET include cytoreduction, supportive access, and possibly liver transplantation if indicated. Liver embolization was also an option if the patient had isolated disease progression.

1.2.3 Advanced Stage, Metastatic GEP-NET: Systemic Treatments as the “Backbone”

1.2.3.1 Long-acting Somatostatin Analogs

Locoregional and metastatic diseases usually require systemic treatments. An important development in GEP-NET was the research and clinical utilization of long-acting somatostatin analogs. Somatostatin is a key inhibitory hormone-regulating endocrine and exocrine functions with a short half-life. Therefore, long-acting somatostatin analog (SSA) was fabricated to imitate and improve the pharmacokinetics of somatostatin to provide long-term therapeutic symptom control from advanced-stage and metastatic GEP-NETs. It preferentially binds to the SSTRs, highly expressed in well-differentiated GEP-NETs [6]. The two commonly used SSAs are octreotide and lanreotide. The SSAs are routinely administered to patients with carcinoid syndrome secondary to excessive serotonin and vasoactive substances secreted by GEP-NETs. One of the pioneer trial evaluated long-acting SSA in GEP-NET patients demonstrated rapid relief of symptoms and a corresponding decrease in 5-HIAA levels [29]. It also successfully controlled other hormonal syndromes in pNET patients, such as necrolytic erythema migratory erythema associated with glucagonoma and hypoglycemia related to insulinoma [6]. Long-acting SSA was also proven to have antineoplastic property in GEP-NETs. In the landmark phase 3 PROMID randomized-controlled clinical trial well-differentiated advanced midgut NET patients, SSA significantly improved median time to progression of disease from 6 months to 14.3 months, and disease control rate from 37.2% to 66.7% compared to placebo control [30]. Another crucial CLARINET phase 3 clinical trial randomized low-grade, SSTR-positive, non-functional GEP-NET patients to Lanreotide and placebo and demonstrated nearly doubling of 2-year PFS from 33.0% to 65.1% [31]. These clinical studies have established long-acting SSA as the first-line treatment modality in metastatic GEP-NET patients.

1.2.3.2 mTOR inhibitor (Everolimus)

Another targeted therapy is Everolimus, an oral inhibitor of the mammalian target of Rapamycin (mTOR). The mTOR was found to be dysregulated in GEP-NETs and serves as a target for treatment. The RADIANT series provided strong support for establishing Everolimus as the first line treatment for advanced-stage or metastatic GEP-NETs [32-35]. The first two RADIANT series study established safety profile of combing Everolimus and long-acting octreotide in treating GEP-NETs, which have shown significantly improved survival benefits [32, 33]. RADIANT-3 study provided a strong support for using Everolimus single agent in treating locally-advanced, metastatic pNET patients with a significant progress-free survival of more than 6 months with tolerable toxicities [34]. And RADIANT-4 also demonstrated survival benefit in advanced, non-functional GEP-NETs treated with single agent Everolimus [35]. These well-designed, large-sample, randomized controlled study provided robust and profound evidence for mTOR inhibitors.

1.2.3.3 Anti-angiogenesis agents

Anti-angiogenesis agents include oral tyrosine kinase inhibitor Sunitinib, which targets the PDGF receptor and VEGF1-3 receptors. It was trialed in a phase 3 clinical trial, which demonstrated improved median progression free survival of 12.9 months, overall survival of 54.1 months and objective response rate of 16.7%, compared to placebo in treating advanced pancreatic neuroendocrine tumors [36]. This has not been directly compared with the standard of care treatments, such as Everolimus in prospective studies. However, a retrospective review suggested that Everolimus might have an

improved trend towards better progression free survival and objective response rate compared to Sunitinib, though increased toxicities and higher discontinuation rate were also observed with Everolimus [37]. Given its promising outcome in treating advanced-stage, metastatic pNET patients, Sunitinib is considered a second-line or an alternative for patients who are refractory to first-line systemic treatments.

Sorafenib is another multi-target tyrosine protein kinase and Raf kinase inhibitor, which inhibits angiogenesis and tumor proliferation. It was trialed as a single agent in the MC044h phase II study in treating metastatic GEP-NET and reported modest anti-neoplastic activities, but frequent grade 3+ toxicities [38]. Bevacizumab is a monoclonal antibody against VEGF and has prominent anti-angiogenic property. Bevacizumab as a single agent against GEP-NET was limited due to its dominant cytostatic nature, instead of therapeutic cytotoxic effect resulting in tumor reduction or symptomatic improvement in clinical settings [39]. Therefore, Bevacizumab was frequently combined with another agent in treating metastatic GEP-NETs. Bevacizumab was combined with SSA (i.e. Octretodie), targeted-therapy agent (i.e. Sorafenib, Pertuzumab), mTOR inhibitor (i.e. Temsirolimus, Everolimus), and chemotherapy (i.e. Capecitabine, Temozolomide, Methoxyestradiol) [39-47]. The disease control rate ranged between 80-96% across these clinical trials, though toxicities were frequently reported as well, limiting its application in only clinical trials in managing metastatic GEP-NETs [39].

1.2.3.4 Telotristat Ethyl

Telotristat Ethyl is another inhibitory hormonal treatment option. It works by inhibiting tryptophan hydroxylase, the rate-limiting enzyme that converts tryptophan into serotonin. It is an oral formula that only decreases the production of serotonin in the

gastrointestinal tract without impacting serotonin function in the central nerve system [48]. It can be used to provide symptom control, even in SSA-refractory patients. Two phase 3 clinical trials, TELESTAR and TELECAST, showed that Telotristat ethyl was associated with reduction in 5-HIAA levels and frequency of diarrhea, and efficacious in controlling carcinoid syndrome [49, 50].

1.2.3.5 Interferon alpha

Antiproliferative agent Interferon alpha (IFN) was also trialed as a single agent, or combined with SSA in treating metastatic GEP-NETs. Interferon-alpha is a cytokine with a wide range of anti-viral, anti-proliferative and anti-tumor activities. However, IFN carries a significant side effect profile, such as flu-like symptoms, transaminitis, fever, autoimmune responses, and depression[51]. There were several phase II studies investigating IFNa as a monotherapy in treating metastatic NETs, which has shown reduction of biochemical markers, and mostly stable disease. In addition, IFNa was also combined with SSA. There were three randomized clinical trials, but all of which were underpowered, to detect any differences between treatment groups. The combination treatment with IFNa and SSA did not significantly improve progression-free survival compared to IFNa monotherapy. The combination treatment also did not improve disease progression or overall survival compared to SSA alone. On the other hand, IFNa carries a significant side effect profile, which prevented its further implementation in clinical use. Overall, IFNa may still has a role in managing metastatic NET patients, perhaps most useful among patients with resistance to SSA. There might also be limited role in managing small-volume, low grade disease, or as a bridge therapy to another therapy[52].

1.2.3.6 Chemotherapy

Traditional systemic chemotherapy agents are also options for metastatic GEP-NETs, refractory or contraindicated in other treatments. These cytotoxic chemotherapy agents are frequently used in aggressive, poorly differentiated GEP-NETs. Platinum-based therapies, such as cisplatin and etoposide, and carboplatin, were used in small clinical trials and demonstrated safety and efficacy in treating advanced stage GEP-NETs. In addition, FOLFIRI (5-FU, Leucovorin, Irinotecan) or FOLFIRINOX (5-FU, Leucovorin, Irinotecan, Oxaliplatin) could be used as a second line if patient fails platinum-based treatments. For pNET patients, 5-FU, Capecitabine and Temozolomide were all investigated as either a single agent or combination regimen.

1.2.4 Advanced Stage, Metastatic GEP-NET: Radiotherapy as Emerging and Novel Treatment Modalities

1.2.4.1 Peptide Receptor Radionuclide Radiotherapy (PRRT)

Peptide Receptor Radionuclide Radiotherapy (PRRT) was first developed in Europe more than 20 years ago. The broad concept of PRRT is to deliver targeted short-ranged radiotherapy via a radiolabeled peptide that preferentially binds to tumor cells. Radiolabeled somatostatin analog has been instrumental in developing PRRT in treating GEP-NETs [53]. It is consisted of a radionuclide isotope, an octreotide or octreotate carrier molecule, and a chelator unit to stabilize the compound. It selectively targets cells with high density and overexpression of SSTRs, a hallmark of GEP-NETs [54].

Lutetium-177-DOTATATE (^{177}Lu-DOTATATE) is currently the most widely used PRRT in treating GEP-NETs. Lutetium-177 is a primary beta emitter with a half-life

of 6.7 days. The tissue penetrance ranges from 0.5-2mm [53]. Multiple studies have demonstrated safety and tolerable toxicity profiles. The most common toxicities were nausea/emesis and transient thrombocytopenia and leukopenia. The NETTER-1 is a phase III landmark clinical trial demonstrating the safety and promising efficacy of PRRT compared to long-acting SSA. This study reported an improved objective response rate of 18% in the PRRT arm compared to 3% in the octreotide analog control [55]. Since the publication of this trial, PRRT has become a standard treatment option in many institutions and recommended by the National Comprehensive Cancer Network as an alternative front-line therapy in treating progressive GEP-NETs [56].

Ytterium-90 radiolabeled somatostatin analog (i.e , ^{90}Y-DOTATATE or 90Y-DOTATOC) is another beta particle emitting PRRT in treating GEP-NETs. Ytterium-90 has a half-life of 2.7 days and higher tissue penetrance of 2.5-11mm compared to Lutetium-177. ^{90}Y-DOTATOC was first developed. It had achieved 10-35% partial response and 50% symptom control among GEP-NET patients[57, 58]. Next, the next generation ^{90}Y-DOTATATE replaced ^{90}Y-DOTATOC due to higher binding affinity to SSTR. Studies have shown that Y90-based PRRT was associated with significantly improved objective response and overall survival [59]. A phase 2 prospective clinical trial demonstrated partial response rate of 23% at 6 months post-treatment and tolerable transient gastrointestinal and hematological toxicities. In addition, this study also reported 30% delayed grade 2 renal toxicity at 24 months post-treatment [60]. Though a rare chronic toxicity, it poses a significant risk for patients, especially the ones with baseline renal disease. Therefore, Y90 was not further pursued in large phase III clinical trials due to risks of delayed renal toxicity.

Indium-111 radiolabeled somatostatin analog was one of the first PRRT trials in GEP-NETs. Low-dose Indium-111 octreotide scintigraphy was previously used to diagnose and localize GEP-NET. Indium-111 emits Auger electrons and has a half-life of 2.8 days. It is relatively low in energy and penetrates only 0.25nm - 13.6um [53]. High-activity Indium-111 was built upon the principle of diagnostic imaging to achieve therapeutic effects through dose escalation. A retrospective review has shown that In-111 high-dose activity DOTATATE produced a partial response and achieve disease stabilization. However, the short-range tissue penetrance has limited its efficacy. Therefore, it needs to be further investigated in clinical trials.

Actinium-255-DOTATATE is one of the novel PRRTs used in treating GEP-NET. Actinium-255 has a half-life of 9.9 days and tissue penetrance of 47-85 um [53]. Actinium-255, as an alpha emitter, has the advantage of delivering radiotherapy with higher linear energy transfer and induces more catastrophic dsDNA breaks compared to a beta-emitting PRRT. Preclinical and retrospective review of Actinium-255-DOTATATE showed treatment response and promising results. A prospective phase I/II clinical trial enrolled GEP-NET patients with and without prior ^{177}Lu-DOTATATE treatments. ^{255}Ac-DOTATAE was able to further produce objective treatment response, even in ^{177}Lu-DOTATATE refractory patients [61]. There is a utility of ^{255}Ac-DOTATATE in a selective patient population, and further studies are needed to validate this treatment option.

Bismuth-213 is another alpha-emitting radioactive element experimented in clinical trials only. Bismuth-213 has a half-life of just 45.6 minutes and tissue penetrance of 85 um [53]. It was only used in clinical trial settings. The short half-life of Bismuth-

213 is a major limitation of these radiolabel somatostatin analogs. The therapeutic window is narrow, and patients often require continuous infusions.

Lead-212 is a mixed-energy radioactive element with both alpha, beta and Auger electron activity. The advantage of ^{212}Pb is the high energy and the ability to produce mixed patterns of DNA damages. It has a half-life of 10.6 hours and tissue penetrance between 50-100 um [53]. It has not been used in clinical trials, and future studies should aim to validate this treatment option in human subjects.

1.2.4.2 External Beam Radiation (EBRT)

External beam radiation (EBRT) could be applied in treating either primary or metastatic GEP-NETs, with high rates of local control and symptomatic relief[62]. Several retrospective studies and case reports reported EBRT with a radiosensitizer in treating GEP-NETs [63-66]. Nevertheless, there is no prospective study to validate this approach [62].

EBRT was used to treat pancreaticobiliary neuroendocrine tumors in neoadjuvant, adjuvant and definitive settings. The radiation dose was 45 Gy or above. If a patient receives RT to primary tumor in a definitive fashion, then they received 41.4 Gy in 23 fractions with a 5.4 to 9 Gy boost to the primary disease [67]. In terms of treating anorectal neuroendocrine carcinoma, chemoradiation or radiation alone were found to have similar PFS and OS compared to surgery based on a French multicenter retrospective review. Mean radiation dose was 58 Gy. Chemotherapy options are mostly platinum-based, etoposide, oxaliplatin, 5-FU or capecitabine. Author concluded that chemoradiation could be a reasonable conservative alternative compared to surgery [68].

pNET can also be treated with concurrent chemoradiation with 5-FU or capecitabine, and daily EBRT of 50.4 Gy in 28 fractions. The sample size was only 6 patients, but the objective treatment response was 80% with tolerable toxicities [63]. Another study found adjuvant radiation to pancreatic neuroendocrine tumors with positive surgical margins to provide excellent local control. Half of the patients were given 5-FU or capecitabine concurrently. The radiation dose was 50.4 Gy. In this retrospective review comparing the utility of adjuvant radiation in pNET patients with positive or close margin, patients with large tumor > 3.8 cm and nodal positivity were more likely to receive adjuvant radiation compared to their counterparts. The local recurrence rate was 10% vs. 6% in the radiation group, even though the radiation group had worse tumor characteristics. Most of the patient who failed treatment fail distantly. This study suggested that adjuvant RT may play a role in local control when pNET patients have a positive or close surgical margin [65]. Another study also looked at neoadjuvant and adjuvant radiation in addition to surgery compared to surgery alone in treating pNET patients. This study retrospectively compared patients in the surgery to neoadjuvant radiation followed by surgical resection. It was found that the most common pattern of failure is distal metastases and local failure is less common. Two-year OS and PFS were 77% and 87% respectively. There was no statistical significance between the two comparison arms. Therefore, the author concluded that the additional radiation, either neoadjuvant or adjuvant, had an unclear role in managing pNET patients. The radiation dose was 50.4 Gy in this study [64]. Another study also looked at local control of radiation to both primary and metastatic sites. The overall response rate to radiation was 39%, with 13% complete response, 26% partial response and 56% with stable disease. Therefore, the disease control rate was

96%. 3-year local recurrence rate was approximately 50%. Most importantly, palliation was achieved in 90% of the patients with either improvement or resolution of symptoms. Therefore, radiation was considered an effective modality to achieve local disease control and provide adequate symptom relief for patients [69].

In a systematic review and pooled analysis of external beam radiation in treating GEP-NET patients, the author reviewed 11 retrospective studies and found relatively low disease recurrence of 15% when giving EBRT in neoadjuvant and adjuvant setting to the primary pNET patients after 50.4 Gy radiation. For definitive radiotherapy, the response rate was 46% and acute and chronic toxicities were found to be 11% and 4%. However, the author concluded that the evidence to support EBRT in treating GEP-NET was very limited. There is no prospective study evaluating EBRT in treating GEP-NET and the role remains unclear, though there is some evidence suggesting that EBRT can provide local control either to primary or metastatic disease sites [62].

1.2.4.3 Yttrium-90 Radioembolization (Y-90)

Ytterium-90 (Y-90) radioembolization could be performed in patients with liver metastasis to produce high treatment response rate [70]. The advantage of Y-90 is to deliver a large dose (> 100 Gy) to a confined liver disease. In a phase Ib clinical trial, mTOR inhibitor Everolimus and somatostatin analog Pasireotide were used with Y-90 selective internal radioembolization to achieve disease control in the liver. The phase found the treatment well tolerated and showed promising activity [71]. Another prospective open-label study investigated Y-90 resin Selective Internal Radioembolization (SIR) with concurrent 5-FU infusions in unresectable neuroendocrine tumors with hepatic metastases. In this study, the majority of the patients enrolled had

GEP-NETs. Treatment response was 50% with a promising 18% complete response as well. Symptomatic response was also observed in more than half of the patients, and a significant percentage of patients also had a corresponding decrease in Chromogranin A levels [72]. Other retrospective reviews also showed a disease control rate of 95% (2.7% complete response, 60.5% partial response, and 22.7% stable disease), with a median survival of 70 months. The side effect profile was very tolerable with fatigue being the most common side effect. No radiation-induced liver failure occurred. Very low acute and chronic toxicities or grade 4 events [70]. In another open-label phase II clinical trial, Y-90 radioembolization was used to treat liver metastases from NETs. The disease control rate for SIR was over 90% at 6 months. Dose-limiting grade 3 and 4 toxicities were approximately 15% and there was no difference between glass and resin beads [73]. A large systematic review of Y90 radioembolization revealed that the median disease control rate at 3 months was 86% and the median survival was 28 months. 69% of carcinoid syndrome patient had symptomatic relief. The most common side effects were abdominal pain, nausea, emesis, and fatigue (all around 30%). Therefore, Y-90 radioembolization can be used as an alternative for unresectable liver metastases with good survival rates and tumor response [74]. Large cohort study comparing Trans-arterial Chemoembolization (TACE) and SIR also showed equivalent disease control rate and tumor response rate at 3 months and thereafter. The complication rates were also comparable between the two modalities. Therefore, SIR was considered an equivalent method compared to the TACE [75].

1.3 Challenge in Managing Advanced Stage, Metastatic GEP-NETs in the PRRT Era

Management of advanced-stage metastatic disease is challenging and often time involves multimodality. With continuous evolvement of modern technology and medical research, significant improvements in 5-years OS was observed for distant metastatic disease, increasing from 39.5% in 1975 to 60.9% in 2015 [13]. Treatment options include surgical resection, systemic chemotherapy, hormonal suppression with somatostatin analogs, and also radiotherapy [2]. Radiotherapy has an evolving role in managing advanced stage, metastatic GEP-NETs. Currently, the role of radiotherapy is limited to palliation and disease control. EBRT could be applied in treating either primary or metastatic GEP-NETs, with high local control rates and symptomatic relief. There were several retrospective studies and case reports reporting EBRT with a radiosensitizer in treating GEP-NETs [63-66]. Nevertheless, there is no prospective study to validate this approach[62]. Y-90 radioembolization could be performed in patients with liver metastasis to produce high treatment response rate[70]. Most prominently, radiolabeled somatostatin analogs PRRT has emerged as a vital treatment option for metastatic GEP-NETs.

In the last 20 years, we have experienced the bloom of PRRT in managing advanced stage, metastatic GEP-NETs. The number of studies spiked after 2000. PRRT was first developed in Europe in the 1990s and was trialed in various European institutions. In year 20018, the commercial product Lutethera (^{177}Lu-DOTATATE) obtained FDA approval in the US to treat metastatic GEP-NETs in adults. Ever since then, PRRT research has flourished and continued to gain new indications for additional treatments. Figure 1-1 illustrates timeline of landmark PRRT studies in the past X decades. From bench to clinical practice, PRRT has rapidly gaining popularity due to its

efficacy and low side effect profile. The concept of somatostatin analog based PRRT was appealing in treating GEP-NETs, which leverages the unique SSTR feature of GEP-NET and delivers radiotherapy to selective GEP-NET cells effectively. It offered patients with metastatic GEP-NET, a challenging clinical scenario, another valid treatment options. Currently PRRT (Lutethera) was considered a front-line therapy in many GEP-NET patients. The future of PRRT is promising.

Despite these advancement in treatment for distant metastatic GEP-NETs, current therapy has significant limitations. GEP-NET cell is historically considered a radioresistant cell type due to its indolent nature. PRRT, though extremely promising, has failed to provide a statistically significant 5-year OS benefit, according to the long-term update of the NETTER-1 clinical trial [76]. The response rate with PRRT seems to be improved compared to somatostatin analog control, but still suboptimal to achieve disease control [55]. There is a pressing need to develop new treatment schemes and technology to increase efficacy of the PRRT treatments.

One strategy to enhance efficacy of radiotherapy is administering a radiosensitizer concurrent with PRRT. A radiosensitizer can induce radiosensitization in various cellular pathways including, but not limited to, introducing DNA instability, impairing DNA repair, and impeding signaling of cell survival. Currently, there are much on-going research looking at utility of a radiosensitizing agent to enhance response rate of PRRT in treating GEP-NETs. To understand the current landscape of PRRT research, the next section detailed all 8 prospective clinical trials (Table 1-1) that implemented a radiosensitizer to enhance PRRT in treating GEP-NETs.

1.4 Implement Radiosensitizer to Enhance PRRT in Current Clinical Trials

1.4.1 Capecitabine

Capecitabine is an orally available tumor-selective fluoropyrimidine carbamate, which passes through the intestinal mucosa and is converted into fluorouracil (5-FU) preferentially in tumor tissue by thymidine phosphorylase [77]. 5-FU is metabolized to 5-fluorodeoxyuridine monophosphate, which inhibits thymidylate synthase, an enzyme crucial for converting deoxyuridine monophosphate to deoxythymidine monophosphate for DNA synthesis and repair (Figure 1-2) [78, 79]. Thus, Capecitabine/5-FU sensitizes radiotherapy when cells progress through the S phase during primary DNA synthesis [79]. When administered with ^{177}Lu-DOTATATE, Capecitabine was administered orally either 825 mg/m^2 twice a day for 14 days or 500 mg/m^2 three times a day throughout the cycles [80-82]. Capecitabine was administered at 1,000 mg/m^2 twice a day for 14 days with ^{255}Ac-DOTATATE infusions [61]. Several phase I and II clinical trials have demonstrated safety and well-tolerable toxicity profile [61, 80-82]. The most reported toxicities were mild and transient nausea/emesis and fatigue, likely associated with amino acid and PRRT infusion [80]. Grade 3 or above toxicity was uncommon across all studies [61, 80-82]. One study reported 16.2% hematological toxicities, 5.4% diarrhea and 5.4% asthenia [82].

Capecitabine has shown to enhance ORR with ^{177}Lu-DOTATATE in phase II studies compared to reported historical controls in the NETTER-1 clinical trial [81, 82]. The reported PR ranged from 24-30% and DCR were 85-94% [81, 82]. This was compared favorably to the 18% ORR (17% PR and 1% CR) reported in the ^{177}Lu-DOTATATE arm in the NETTER-1 clinical trial [55]. In addition, Claringbold et al [81]

also reported 70% octreotide uptake reduction 24 hours after infusion, a serial decline in hormonal levels, and 42% symptom remission while maintaining quality of life and overall health at least 6 months after completing treatments. Capecitabine was also used as a radiosensitizer with ^{255}Ac-DOTATATE in treating GEP-NETs regardless of prior ^{177}Lu-DOTATATE treatments. It was particularly worth-noting that Capecitabine along with ^{225}Ac-DOTATATE not only produced an impressive 48% PR, but also achieved CR in 2 out of 91 patients enrolled in the study [61]. The best response (71% ORR) was observed among patients who received prior ^{177}Lu-DOTATATE and achieved disease control. Among ^{177}Lu-DOTATATE naïve patients, ORR was 56% [61].

1.4.2 Capecitabine and Temozolomide (CAPTEM)

The Capecitabine and Temozolomide combination treatment, abbreviated as CAPTEM, has emerged as a doublet combination regimen with PRRT. Temozolomide is hydrolyzed to methyl-triazeno-imidazole-carboxamide spontaneously, which converted to the electrophilic alkylating methyldiazonium cation that transfers a methyl group to DNA strands. This forms the DNA-methyl adducts at the N^7 of guanine, N^3 of adenine, and O^6 of guanine, and contributes to DNA damage and susceptibility (Figure 1-2). Temozolomide sensitizes radiotherapy by further inducing genomic instability, which leads to cell cycle arrest, senescence, and apoptosis [83]. Claringbold et al [84] first investigated the CAPTEM combination in a phase I/II clinical trial. Patients were given Capecitabine 750 mg/m^2 twice a day for 14 days, starting 5 days before ^{177}Lu-DOTATATE infusion, followed by Temozolomide 200 mg/m^2 daily for 5 days at the last 5 days of Capecitabine cycle. The most common grade 1 and 2 toxicities were nausea/emesis (36%), thrombocytopenia (29%), neutropenia (18%) and anemia (11%). A

small percentage (<10%) of patients developed hematological grade 3 toxicities and 2 patients developed angina related to Capecitabine. This regimen was well-tolerated with 89% of patients completing all cycles of treatments, while only 8% and 13% of patients requiring dose reduction of Capecitabine and Temozolomide, respectively [84].

The CAPTEM combination regimen produced an ORR of 56%, particularly with 15% patients achieving CR and only 9% patients showed disease progression. In the subgroup analysis, the CAPTEM combination regimen was found to be more effective in treating pNETs compared to small bowel NETs, achieving slightly higher CR (18% vs. 13%) and significantly better PR (64% vs. 13%) [84]. This led to a sequalae phase II clinical trial investigating CAPTEM with ^{177}Lu-DOTATATE in treating metastatic pNET patients. Not surprisingly, this study showed equally high treatment compliance and patient tolerance, with an impressive 80% ORR and 100% DCR. Patients receiving CAPTEM with ^{177}Lu-DOTATATE had a 2-year OS of 97% and median PFS of 48 months [85].

1.4.3 Everolimus

Everolimus is a potent mammalian target of Rapamycin (mTOR) inhibitor of mTORC1 that induces G1 cell cycle arrest, reduces tumor angiogenesis and enhances apoptosis and sensitivity towards DNA-damaging agent, such as radiotherapy [86]. It was previously investigated in the RAD001 In Neuroendocrine tumor (RADIANT) clinical trial series and had shown significant survival benefit in treating advanced-staged, metastatic NETs [87-90]. The mTOR Complex 1 (mTORC1) is part of the PI3K-Akt-mTOR feedback axis. Everolimus specifically inhibits the mTORC1 complex, which initiates phosphorylation of S6 and 4EBP1, two key downstream effectors to promote cell

survival and growth (Figure 1-2) [91]. Everolimus was combined with PRRT in treating unresectable low grade NETs in two phase I clinical trials [92, 93]. Everolimus was administered daily throughout all cycles of ^{177}Lu-DOTATE infusions. Both clinical trials found significant dose limiting toxicities at 10 mg daily and patient often required dose de-escalation or cessation of therapy [92, 93]. Alijubran et al [93] reported grade 3 toxicity of 36%, including infection, fatigue, pneumonitis, and neutropenia. Other common toxicities include grade 1 and 2 mucositis (90.9%), transient nausea/emesis (72.2%) and fatigue (63.6%). Due to insufficient patient accrual, this clinical trial was terminated early [93]. The NETTLE study was another concluded phase I clinical trial that recommended 7.5mg daily Everolimus with PRRT. The overall PR was 44%, 1-year and 2-year OS were 88% and 63% respectively [92].

1.5 PI3K/Akt/mTOR pathway inhibition induces radiosensitization

1.5.1 PI3K/Akt/mTOR pathway in GEP-NET

PI3K/Akt/mTOR is a crucial cell survival pathway involved in pathogenesis of various cancers. The PI3 kinase can get activated via many mechanisms, such as epidermal growth factor receptor (EGFR), integrins, G-protein-coupled receptors and Ras-oncogene. PI3K then phosphorylates the D3 position on phosphoinositides to generate PI(3,4,5,)P3 and PI(3,4)P2 proteins, which bind to the serine/threonine site of kinase Akt and translocate this protein to the cell membrane for activation [94].

Akt activation can result in several downstream substrates, which control key cellular processes such as apoptosis, cell cycle progression, transcription and translation. One of a well-known downstream substrate of Akt activation is the mTOR, either directly

or indirectly by phosphorylating and inactivating TSC2 [95]. It is important to recognize that mTOR exists in two metabolically distinctive complexes, the mTORC1 complex that binds to Raptor and the mTORC2 complex that binds to Rictor. The mTORC1 complex signals to downstream effector S6 and 4EBP-1 to control protein translation. The S6 effector protein S6 kinase-1 provides an inhibitory phosphorylation to PI3K via insulin receptor substrate proteins as a negative feedback mechanism [96]. On the other hand, mTORC2 complex, though a substrate of Akt, can also activate Akt and thus provide a positive feedback mechanism to enhance Akt activation of the mTOR pathway [97].

The mTOR has been recognized as a master regulator and involved in the pathogenesis of neuroendocrine tumors. Patients with TSC2 gene defect, and thus upregulation of mTOR, are known to develop islet cell tumors [98]. Another example is the loss of NF-1 gene can result in mTOR activation and development of carcinoid tumors in the ampulla of Vater and duodenum [99, 100]. Tissue examination of GEP-NET patient tumor samples revealed that high level of mTOR activation was observed primarily in the foregut neuroendocrine tumors. In addition, activation of mTOR pathway and expression of downstream effectors were correlated with enhanced proliferative index [101]. These studies formed the basis of targeting mTOR in treating GEP-NETs. Nowadays, the mTOR inhibitors, Everolimus and Sirolimus, were used either as a single agent or combined with Octreotide in treating GEP-NET patients. It is recognized as the first-line treatment for metastatic GEP-NETs. Not to mention the RADIANT series, which firmly demonstrated the benefit of mTOR inhibitor in treating GEP-NETs.

1.5.2 Mechanism of radiosensitization

Ionizing radiation can activate the PI3K/Akt/mTOR pathway through various mechanisms, such as the DNA-damage repair signaling, HIP-1a activation, RTK, and EGFR signaling [102, 103]. The complex interplay of ionizing radiation and activation of the PI3K/Akt/mTOR lead researchers to believe that inhibition of the PI3K/Akt/mTOR axis can enhance cytotoxicity of radiation. It was previously demonstrated in preclinical studies that PI3K/Akt/mTOR signaling pathway inhibitors enhanced radiosensitivity in cancer cells *in vitro* and *in vivo* [104]. Though the mechanism of radiosensitization by inhibiting the PI3K/Akt/mTOR is not completely understood and remains an area of active research. Here are several proposed mechanisms of radiosensitization by inhibiting PI3K/Akt/mTOR pathway.

First, ionizing radiation causes sublethal, potentially lethal and lethal damages to DNA, it contributes to genomic instability and DNA replication stress, and subsequently activation of the PI3K/Akt/mTOR pathway. The PIK kinase family has a role in mediating the DNA damage response (DDR). Specifically, radiation can induce DNA-PK, ATM and ATR activation to signal DNA repair, and directly or indirectly trigger the PIK kinases and its downstream pro-survival mechanisms. By combing with a PI3K/Akt/mTOR inhibitor such as Rapamycin, irradiated cells will not be able to undergo DNA repair, thus prompting cells to undergo autophagy, cell cycle arrest and apoptosis radiation [105]. A PI3K inhibitor, Wortmannin, potentially targets the DDR and has been shown to have a radiosensitization effect [103].

A second mechanism pertains to Ras-mediated radioresistance. Ionizing radiation was shown to activate Akt in a K-Ras dependent fashion and hyperactive Akt signaling

promotes tumorigenic cell behaviors by increasing cell survival, proliferation, invasion and angiogenesis [106]. Previously, the study found that inhibition of the PI3K pathway could reverse Ras-mediated radioresistance. PI3K inhibitor has shown to reduce tumor cell clonogenicity synergistically and delay tumor regrowth *in vivo* [107]. Inhibition of Akt signaling was also found to sensitize cells with intact K-rad function to ionizing radiation. Inhibition of Akt reduced motility and invasiveness of tumor cells *in vitro* and demonstrated prolonged survival in xenograft *in vivo* [99].

Lastly, the PI3K/Akt/mTOR pathway is involved in the angiogenesis and radioresistance of tumors. It has been shown that ionizing radiation phosphorylates HIP-1a, a downstream effector of PI3K/mTOR activation and regulates vascular radiosensitivity in tumors. Radiation also induces Vascular Endothelial Growth Factor (VEGF) expressions to promote angiogenesis and cell survival. Precious study revealed that PI3K/mTOR pathway inhibition overcame radioresistance and increased radiosensitivity of multiple cells types via suppression of the HIF1-a/VEGF pathway [108]. Rapamycin inhibited angiogenesis by decreasing the production and response to VEGF [99]. Another study also demonstrated that PI3K inhibitor enhanced radiation-induced obliteration of tumor vasculature, resulting in enhanced tumor growth delay [109].

1.5.3 PI3K/mTOR dual inhibition

To further enhance and explore the therapeutic benefit of mTOR inhibition, researchers realized that the traditional mTOR inhibitor, such as Everolimus, has limited activity against the mTORC1 complex but not the mTORC2 complex. Previous studies suggested that inhibition of mTORC1 alone allows for feedback Akt activation mediated

through the mTORC2 complex. The mTORC2 complex permitted an escape mechanism and feedback to stimulate Akt activation. Therefore, a new class of PI3K/mTOR dual inhibitor was designed to provide more robust inhibition of the PI3K/Akt/mTOR axis and overcome drug resistance of mTOR inhibitor.

Several candidates have entered clinical trials in treating patients with various malignancies [110]. Voxtalisib, a selective inhibitor of class I PI3 kinases and mTOR inhibitor, demonstrated safety and association with stable disease against advanced solid tumors in a phase I clinical trial [111]. Paxalisib, a dual inhibitor capable of crossing the blood brain barrier, was evaluated in treating MGMT unmethylated glioblastoma and preliminary analysis demonstrated prolonged survival in an ongoing phase II study [112]. Moreover, Samotolisib was used to treat metastatic castrate-resistance prostate cancer patients in phase Ib/II clinical trial [113]. This PI3K/mTOR dual inhibitor was also selected to treat pediatric patients with advanced solid tumors or lymphoma with TSC or PI3K/mTOR mutations in the ongoing NCI-COG pediatric MATCH trial [114]. These new pharmaceuticals have demonstrated promising results and the potential to serve as the next-generation anti-neoplastic therapy.

1.6 RNR inhibition induces radiosensitization

1.6.1 RNR and role in GEP-NET

The ribonucleotide reductase (RNR) is an evolutionary conserved rate-limiting enzyme for producing deoxyribonucleoside triphosphates (dNTPs), substrates for DNA repair and synthesis. The RNRs found in human cell lines are categorized as largely Class I RNR, based on their requirement for oxygen to generate tyrosyl radicals. Each RNR

contains two dimeric subunits, RRM1 and RRM2. Upon activation of the RNR catalysis, the smaller RRM2 subunit with a Fe-O-Fe center continuously produces and shuttles tyrosyl radicals to a cysteine of the larger RRM1 subunit. The RRM1 contains both the catalytic site for reducing ribosides and the allosteric sites for regulation [115]. The enzyme activity is tightly regulated by ATP/dATP binding to RRM1, as well as an unique allosteric mechanism to maintain equal pool sizes of each dNTP for DNA synthesis. The activity of RNR is also highly adaptive to the cell cycle. In eukaryotes, RNR activity is low in the G0/G1 phase and ramps up in the S phase. When examining specific subunit, researchers found that RRM1 subunit has constant expression throughout the cell cycle, while RRM2 expression varies. RRM2 mRNA transcription is blocked during G1 phase and reversed when entering S phase. Further research also revealed that RRM2, but not RRM1, is associated with cyclin-dependent kinases and phosphorylation of RRM2 results in degradation of RRM2 during G2 phase [116]. This suggested that the RRM2 subunit is crucial in cell cycle progression and regulation.

Numerous studies have found that the cell cycle dependent RRM2 expression is associated with malignant potential of many types of cancer [117-121]. Over-expression of RRM2 is known as a predictive biomarker for poor prognosis [122-124]. Given its ubiquitous expression and implication in tumorigenesis in mammalian cells, RRM2 became a therapeutic target in treating a variety of solid tumors [125-128]. Most recently, researchers discovered a small subunit of RNR called p53R2. As previously mentioned, RRM2 subunit is exclusively expressed during S-phase, followed by phosphorylation and degradation during G2 phase. When the RRM2 unit is unavailable during the cell cycle, the R1 associates with the p53R2 subunit instead to form an active RNR to supply cells

with dNTPs for repair and synthesis [129]. The p53R2 and RRM2 subunits are structurally similar but regulated through different mechanisms. The p53R2 was known to be induced by p53, p21, and p73, which play crucial roles as guardians of the genome and prominent tumor suppressors [130, 131]. Not surprisingly, p53R2 expression was found to be associated with tumor progression, metastasis and poor prognosis [132-134]. Currently, active research is exploring the therapeutic potential of p53R2 [131].

The role of RNR in neuroendocrine tumor was previously explored only in models of small-cell lung cancer. Both RRM1 and RRM2 were reported to be over-expressed in the SCLC models, contributing to increased proliferation and disease progression [135, 136]. There is little knowledge about the role of RNR in GEP-NET. One genome-wide study identified RRM2 as a gastrin-response gene in gastrointestinal tumor cells, suggesting its role in tumor biology, and thus, a potential therapeutic target [137]. Future research is warranted to identify the role of RNR in GEP-NETs.

1.6.2 Mechanism of radiosensitization

Radiation universally causes DNA damage in cells, which can be effectively repaired through various mechanisms, such as NHEJ and HR repair. However, regardless of the mechanisms, dNTPs are building blocks fundamental to de novo DNA synthesis and repair. RNR, the rate-limiting enzyme of dNTP synthesis, becomes essential. Radiation-induced DDR can increase RNR activity through the regulatory function of RRM2/p53R2. RRM2 overexpression is also associated with radioresistance by increasing dNTPs available for prompt DNA repair[138, 139]. Conversely, inhibition of RNR impedes the ability to repair DNA damages, resulting in increased cell death.

Various RNR inhibitors, targeting either RRM1 or RRM2 subunit, have demonstrated increased radiosensitivity in preclinical studies[140].

1.6.3 RNR inhibitors

There are many RNR inhibitors targeting different functional units of the RNR compound. It can be categorized as either RRM1 or RRM2 inhibitors. Majority of RRM1 inhibitors are nucleoside analogs, which directly inhibit RNR activity and get incorporated into DNA. This combined effect leads to the termination of DNA elongation and inhibition of DNA repair and synthesis, leading to apoptosis eventually [141]. Examples of RRM1 inhibitors include Gemcitabine, Tezacitabine, Cytarabine, Flutarabine, Cladribine, and Clofarabine [142]. Of these mentioned nucleoside analog RRM1 inhibitors, Gemcitabine is the most widely used anti-neoplastic therapy clinically. It was used either as a single agent or combined regimen in treating pancreatic, lung, breast and many other malignancies [143-146]. Gemcitabine is also a well-established potent radiosensitizer in treating many malignancies[147]. Its cytotoxicity profiles and chemoresistance often limit the use of RRM1 inhibitors. In addition to inhibiting RRM1 activity, they are also known to inhibit other off-targets, such as DNA polymerase, which ultimately contributes to its escalated toxicity[148]. Another limitation of nucleoside analog RRM1 inhibitors is the development of chemoresistance. Take Gemcitabine as an example, upregulation of multi-drug resistance (MDR) genes was observed in pancreatic cancer cells treated with Gemcitabine. The MDR genes can promote drug efflux, thus lowering Gemcitabine concentration within tumor cells and rendering the treatment ineffective [149].

On the other hand, RRM2 inhibitors are non-nucleoside analogs and have diverse functions. The RRM2 inhibitor may function as a radical scavenger, metal chelator, or agent that disrupt interaction between RRM1 and RRM2 subunits[148]. Hydroxyurea is an example of radical scavenger RRM2 inhibitor, which quenches the tyrosyl radicals and prevents RNR catalysis and activation[150]. It was one of the early and widely used anti-neoplastic compound in treating solid and hematological malignancies[151]. It was also used as a radiosensitizer in several head and neck and cervical cancer clinical trials [152, 153]. Unfortunately, the clinical use of Hydroxyurea was limited mainly by its poor efficacy and treatment resistance in patients [154]. The next group of RRM2 inhibitors are metal chelators that interfere with the Fe-O-Fe compound in the center of the RRM2 subunit to prevent appropriate functioning and activating of RNR. Metal chelator RRM2 inhibitors include Triapine, Didox, Trimidox, Desferrioxamine, and Gallium complexes [148]. Some of these RRM2 inhibitors, such as Triapine, have secondary function as a DNA damaging agent [155]. Many of them have been evaluated as radiosensitizers in clinical trials. Triapine was mainly used with concurrent cisplatin and radiotherapy in treating gynecological and head and neck cancer patients [156-158]. Motexafin Gadolinium was used as a radiosensitizer in treating brain metastasis and pediatric intrinsic pontine gliomas [159, 160]. The third group of RRM2 inhibitor belongs to a novel development and encompasses a wide range of mechanism of actions for RRM2 inhibition. The primary principle of this class of RRM2 inhibitors involves the disruption of binding between RRM1 and RRM2 subunits [148]. COH29, a small compound bound to the C-terminal tail of RRM2, is an example [161]. Another novel development is the

antisense oligonucleotide, such as GTI-2040, targeting the mRNA of RRM2 expression [162]. These RRM2 inhibitors are currently under clinical investigation.

RNR inhibitors have a wide range of anti-neoplastic agents with both chemosensitizing and radiosensitizing properties. They were either used as monotherapy or commonly combined with another DNA-damaging modality to induce a synergistic effect. Each class of RNR inhibitors has its own limitations. Nucleoside analog RRM1 inhibitors regularly exhibit drug resistance, whereas the RRM2 inhibiting radical scavengers and metal chelators lack targeting specificity [148]. The next generation RNR inhibitor is currently under investigation. Active research should be dedicated to designing the "perfect" on-target specific RNR inhibitor that is highly effective and resilient to drug resistance.

1.7 Hypothesis

Radiation is an emerging modality in treating GEP-NETs with novel developments in radiopharmaceuticals, such as PRRT. Implementing a radiosensitizer is a valid strategy to enhance the therapeutic ratio of its treatment. Appropriate DNA repair mechanisms are fundamental in restoring genomic instability when DNA sustains damages from ionizing radiation. The inability to repair DNA damages can result in cell cycle arrest, autophagy, quiescence, and apoptosis, which clinically manifest as control or regression of disease. Therefore, I firmly believe that implementing a therapeutic agent that interferes with the DNA repair mechanism is a successful strategy to achieve radiosensitization. By carefully reviewing the tumor biology of GEP-NETs, two specific agents were thought to be promising candidates as radiosensitizers with a vast clinical

translational value in treating GEP-NETs. Here, I proposed two specific hypotheses in my thesis statement:

1. The PI3K/Akt/mTOR pathway is implicated in the tumor biology of GEP-NETs. Therefore, I hypothesize that inhibiting the PI3K/Akt/mTOR pro-survival pathway with a dual PI3K/mTOR inhibitor dampens DNA repair mechanism and sensitizes pancreatic neuroendocrine tumor cells to radiation-induced DNA damages, and thus increased apoptosis.
2. The RNR is a ubiquitously expressed rate-limiting DNA synthesis and repair enzyme implicated in many malignancies. Particularly, RRM2 upregulation was found to be associated with poor prognosis and radioresistance. I hypothesize that selective RRM2 inhibition decreases dNTP supplies and renders DNA synthesis and repair ineffective in a S-phase cell cycle-dependent fashion, thus sensitizes pancreatic neuroendocrine tumors to ionizing radiation via S-phase cell cycle arrest, increased apoptosis, and tumor regression.

Table 1-1 Prospective clinical trials combining a radiosensitizing agent with PRRT

Clinical trials	Phase	Radiosensitizer	Radiotherapy
Van Essen 2007 [80]	I	Capecitabine 825 mg/m^2 B.I.D[a] x 14 days	^{177}Lu-DOTATATE 7.4 GBq[b] x 4 cycles, every 6-10 weeks
Claringbold 2011 [81]	II	Capecitabine 825 mg/m^2 B.I.D x 14 days	^{177}Lu-DOTATATE 7.8 GBq x 4 cycles, every 8 weeks
Claringbold 2012 [84]	I/II	CAPTEM[c] 750 mg/m^2 B.I.D x 14 days + 200mg/m^2	^{177}Lu-DOTATATE 7.8 GBq x 4 cycles, every 8 weeks
Claringbold 2015 [92]	I	Everolimus 7.5 mg daily x 24 weeks	^{177}Lu-DOTATATE 7.8 GBq x 4 cycles, every 8 weeks
Claringbold 2016 [85]	II	CAPTEM 750 mg/m^2 B.I.D x 14 days + 200mg/m^2	^{177}Lu-DOTATATE 7.9 GBq x 4 cycles, every 8 weeks
Nicolini 2021 [82]	I/II	Capecitabine 500 mg/m^2 T.I.D[d] x 40 weeks with inter-cycle metronomic taper	^{177}Lu-DOTATATE 5.5 GBq x 5 cycles, every 8 weeks
Alijubran 2022 [93]	I	Everolimus 10 mg daily x 24 weeks	^{177}Lu-DOTATATE 3.7 – 7.4 GBq x 4 cycles, every 8 weeks
Ballal 2022 [61]	I/II	Capecitabine 1000 mg/m^2 B.I.D x 14 days	^{225}Ac-DOTATATE 100-120 kBq/kg[e] every 8 weeks

a, twice-a-day; b, Giga-Becquerel, radiation dose unit; c, Capecitabine and Temozolomide combination treatment.

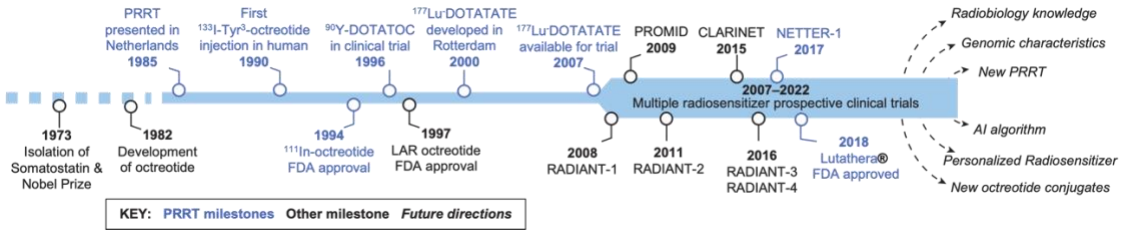

Figure 1-1 Timeline of landmark discoveries and clinical trials in PRRT research

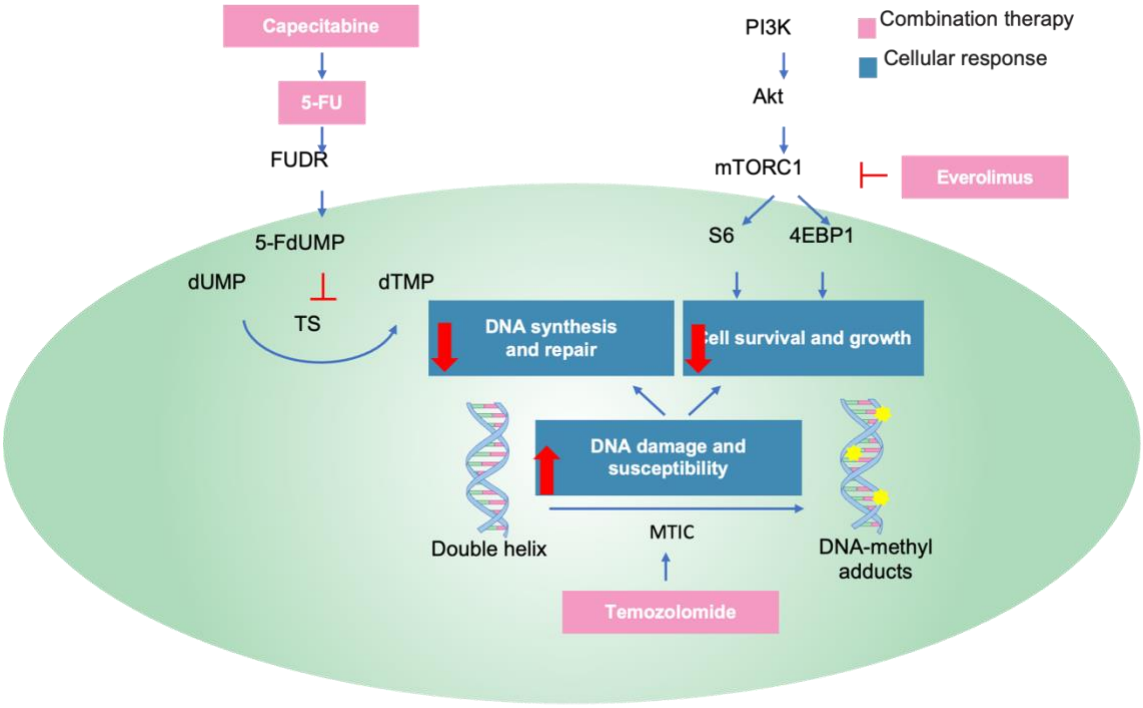

Figure 1-2 Mechanisms of action of Capecitabine, Temozolomide and Everolimus
Capecitabine metabolizes to Fluorouracil (5-FU), then 5- fluoro-2′-deoxyuridine (5UDR) and 5-fluorodeoxyuridine monophosphate (5-FdUMP), which inhibits thymidylate synthase (TS), an enzyme that converts deoxyuridine monophosphate (dUMP) to deoxythymidine monophosphate (dTMP) for DNA synthesis and repair. Temozolomide hydrolyzes to methyl-triazeno-imidazole-carboxamide (MTIC), which induces DNA-methyl adducts in DNA strands that contribute to DNA damage and susceptibility. Everolimus inhibits the mTORC1, a key regulator of the PI3K-Akt-mTOR axis. The mTORC1 phosphorylates S6 and 4EBP1, two key downstream regulators of cell survival and growth. Together, increasing DNA damage and susceptibility, decreasing DNA synthesis, repair, cell survival and growth contribute to radiosensitivity of the cell.

CHAPTER 2. PI3K/MTOR DUAL INHIBITOR PF-04691502 IS A SCHEDULE-DEPENDENT RADIOSENSITIZER FOR GASTROENTEROPANCREATIC NEUROENDOCRINE TUMORS

2.1 Abstract

Patients with advanced stage gastroenteropancreatic neuroendocrine tumors (GEP-NETs) have a poor overall prognosis despite current treatment options that include chemotherapy and radiotherapy (e.g., peptide receptor radionuclide therapy [PRRT]). Better treatment options are needed to improve disease regression and patient survival. The purpose of this study was to examine a new radiotherapy strategy for NETs combining PI3K/mTOR dual inhibition and radiotherapy. As a first step, we assessed the efficacy of two PI3K/mTOR dual inhibitors, PF-04691502 and PKI-402, to inhibit pAkt and increase apoptosis in NET cell lines (BON and QGP-1) and patient-derived tumor spheroids as single agents or combined with radiotherapy (XRT). Treatment with PF-04691502 decreased pAkt (Ser473) expression for up to 72 h compared with control; in contrast, decreased pAkt expression was noted for less than 24h with PKI-402. The IC-50 for PF-04691502 was 48.3nM and 138.7nM in BON and QGP-1 cells, respectively, at 96 h. Simultaneous treatment with PF-04691502 and XRT did not induce apoptosis in NET cells; however, the addition of PF-04691502 48 h after XRT significantly increased apoptosis compared to PF-04691502 or XRT treatment alone. Our results demonstrate that schedule-dependent administration of a PI3K/mTOR inhibitor, combined with XRT, can enhance cytotoxicity by promoting radiosensitivity of NET cells. Moreover, our findings suggest that radiotherapy, in combination with timed PI3K/mTOR inhibition, may be a promising therapeutic regimen for patients with GEP-NET.

2.2 Introduction

Gastroenteropancreatic neuroendocrine tumors (GEP-NETs) are heterogeneous clinical and pathological subsets of NETs arising from the gastrointestinal tract. Historically, NETs have been considered an "orphan" disease [163]. However, the incidence of these tumors has increased approximately 6.4-fold from 1973 to 2012, which is likely attributed to advanced imaging and earlier diagnosis [14]. Among all NETs, GEP-NETs have the highest incidence of 3.56 per 100,000 population [14]. In addition, many patients experience diagnostic delays due to the lack of specific presenting symptoms. In contrast to these early stage asymptomatic patients, symptomatic patients are often diagnosed with advanced or metastatic disease and have a poor overall prognosis[164].

Peptide receptor radionuclide therapy (PRRT) has emerged as an effective therapeutic modality for treating GEP-NETs, with clinical trials showing increased progression-free survival and overall survival in patients [165-169]. Somatostatin receptors are highly expressed in 80-100% of GEP-NETs [170, 171]. Synthetic somatostatin analogues, which have a high affinity to GEP-NETs, and coupled with a radioactive element, facilitate uptake into cells to deliver targeted intracellular radiation [168, 170]. The PRRT compounds currently available in the United States and approved for treatment of GEP-NETs include ^{177}Lu-Octreotide, ^{90}Y-DOTATOC, and ^{111}In-DTPA-octreotide [170]. ^{177}Lu-Octreotide has achieved partial and minor response rates of 29% and 16%, respectively, and improved progression-free survival and overall survival in the

NETTER-1 phase III clinical trial, thus indicating the utility of PRRT as a potential treatment option for inoperable or metastatic disease [169, 170]. Another evolving approach in cancer treatment is to utilize a multimodal regimen to enhance the effects of single agents for tumor regression. For example, radiosensitizers, such as 5-FU, capecitabine, and temozolomide, have been tested in conjunction with PRRT [172-174].

The mammalian target of rapamycin (mTOR) and the PI3K/mTOR/Akt signaling pathway play a role in tumor proliferation, survival and angiogenesis[175]. Treatment with everolimus, a potent inhibitor of the mTORC1 subunit, significantly improved progression-free survival in the RAD001 in advanced neuroendocrine tumors (RADIANT) clinical trials [34, 35, 176-179]. Of particular interest, mTOR inhibitors have been tested *in vitro* as a radiosensitizer in combination with PRRT [180]. Recently, PRRT combination therapy with everolimus has entered phase I/II clinical trials [92, 181]. Although this combination therapy has demonstrated an improved treatment response rate of 44%, serious side effects, such as neutropenia and renal function impairment, occurred in 8 out of 11 patients in one study, requiring dose reduction [92, 181]. New combination strategies may improve patient tolerance to PI3K/mTOR, such as inhibiting PI3K/mTOR pathway only when cancer cells experience radiation-induced stress, which may offer short-term synergistic effects combined with radiotherapy.

Novel and promising PI3K and mTOR dual inhibitors with advanced antineoplastic properties, such as PF-04691502 and PKI-402, inhibit multiple targets in the PI3K/mTOR/Akt pathway and may be superior therapeutic agents compared to everolimus [182]. PI3K/mTOR dual inhibitors have been assessed in several clinical trials as treatment for various advanced cancers, but rarely GEP-NET[183-187].

Furthermore, little is known about the effect of PI3K/mTOR inhibition and radiosensitization of GEP-NET cells. In this study, we evaluated the response of GEP-NET cells to the combination of a novel PI3K/mTOR inhibitor in conjunction with radiotherapy. Our results show that schedule-dependent administration of a dual PI3K/mTOR inhibitor and radiotherapy can improve treatment response by increasing apoptosis *in vitro*. Furthermore, our results suggest that this combination strategy may be a potential treatment to improve disease regression and progression-free survival among GEP-NET patients.

2.3 Materials and Methods

2.3.1 Reagents, Supplements and Antibodies

Tissue plates were from Olympus: 6-well flat bottom tissue culture plate (25-105), 96-well flat bottom tissue culture plate (25-109); Corning: 24-well low attachment plates (CLS3473) and Millipore Sigma: collagen IV-coated plates (collagen from human placenta; C7521). Cell culture medium and reagents included: Roswell Park Memorial Institute (RPMI) 1640 medium (Gibco, 11875085), DMEM/F12-GlutaMAX^{TM} medium (Gibco, 10565018), HyClone™ HEPES (GE Healthcare; SH30237.01), IntestiCult organoid growth medium (Stemcell Technologies; 06010), recombinant human FGF-basic (Peprotech, 100-18B), epidermal growth factor (BioVision; 4022), non-essential amino acid solution (Millipore Sigma; M7145), sodium pyruvate solution (Millipore Sigma; S8636), MEM vitamin solution (Millipore Sigma; M6895), Liberase DH (Roche Applied Science, 05401054001), collagenase/hyaluronidase (StemCell Technologies,

07912), trypsin-EDTA solution (Sigma-Aldrich, SLCB7154), antibiotic-antimycotic 100X (Gibco, 15240-062), fetal bovine serum (FBS) (Sigma-Aldrich, 12303C-500).

PI3K/mTOR dual inhibitors used in this study were PF-04691502 (Selleckchem, S2743) and PKI-402 (Selleckchem, S2739). Drugs were diluted in dimethyl sulfoxide (DMSO) (Fisher Scientific, D128-500) and stored at -80ºC prior to use. Cell media mixture with DMSO only was added to cells in the control group.

Western blot materials included: Dulbecco's phosphate buffered saline (PBS) (Sigma-Aldrich, D8637-500), RIPA buffer 10X (Cell Signaling, 9806S),

protein assay dye (Bio-Rad, 5000006), MOPS SDS running buffer 20X (Invitrogen, NP0001-02), Tris-Glycine 10X transfer buffer solution (Fisher Scientific, BP1306-1), TBS buffer 20X (VWR, J640-4L), Tween 20 (Fisher Scientific, BP337-500), NuPAGE™ 4-12% Bis-Tris Gel 1.0 mm x 10 well (Invitrogen, NP0321B0X), NuPAGE™ LDS sample buffer 4X (Invitrogen, NP0007), NuPAGE™ sample reducing agent (Novex, NP0009), phenylmethanesulfonyl fluoride (PMSF) solution 100X (Sigma-Aldrich, 93482-50), Precision Plus Protein™ dual color standards (Bio-Rad, 161-0374), sodium azide (Fisher Scientific, S2271-100), non-fat dry milk (Lab Scientific, M0841), methanol (VWR, BDH1135-4LP), Amersham ECL prime western blotting detection reagent (GE Healthcare Life Sciences, RPN2209), Immobolin western (Millipore, WBKLS0500). The following primary antibodies were from: 1) Abcam: anti-chromogranin A (ab45179, 1:500), recombinant anti-cyclin D1 antibody (ab134175, 1:5000); 2) Santa Cruz: SSTR2 antibody (A-8) (SC-365502, 1:100), SYP antibody (4H255) (SC-58301, 1:100); 3) Cell Signaling: phospho-Akt (Ser473) (D9E) XP ® rabbit mAb (4060, 1:1000), phospho-4E-BP1 (Thr37/46) (236B4) rabbit mAb (2855, 1:1000), phospho-S6 ribosomal protein

(Ser235/236) (D57.2.2E) XP ® rabbit mAb (4858, 1:2000), cleaved PARP (Asp 214) (D64E10) XP® rabbit mAb (5625, 1:1000), PARP (46D11) rabbit mAb (9532, 1:1000). Secondary antibodies are from Santa Cruz: mouse anti-rabbit IgG-HRP (SC-2357), and m-IgGk BP-HRP (SC-516102).

Proliferation and clonogenic analyses were performed with CytoScan™ SRB Cell Cytotoxicity Assay (G-Biosciences, 786-213) [188].

2.3.2 Cell Culture

The BON cell line was derived from a human pancreatic neuroendocrine tumor and previously characterized [189, 190]. QGP-1, a pancreatic neuroendocrine cell line purchased from Japan Health Sciences Foundation [191], was maintained in ATCC-formulated RPMI 1640 medium with 10% fetal bovine serum and 1% 100x penicillin antibody solution. The NT-3 cells, derived from a human pancreatic NET, was a kind gift from Dr. Jörg Schrader (University Medical Center Hamburg-Eppendorf, Hamburg, Germany) [192]. All cells were cultured in a humidified incubator at 37°C and 5% CO_2. QGP-1 cells were cultured in RPMI-1640 + 10% FBS + 1% 100x penicillin antibody solution. BON cells were cultured in a 1:1 mixture of DMEM F1/2 GlutaMAX supplemented with 10% fetal bovine serum and 1% 100x penicillin antibody solution in 5% CO_2 at 37°C. NT-3 cells were cultured in RPMI medium supplemented with 10% FBS, 10 mM HyClone™ HEPES, 1X antibiotic-antimycotic, 20 ng/ml epidermal growth factor, 10 ng/ml recombinant human FGF-basic. NT-3 cells were cultured on collagen IV-coated plates. Collagen IV solution was prepared in PBS for coating cell culture plates at 50 µg/ml concentration [192].

2.3.3 GEP-NET Tumor Spheroids

The original patient NET tumor (F0 generation) was divided into 2-mm^3 pieces and digested in 50 µg/ml Liberase DH (100 µl) and 0.5X collagenase/hyaluronidase (250 µl), diluted in 5 mL of DMEM/F12 serum free media for 4h at 37°C with gentle agitation by a magnetic stirring bar. Liberase DH was resuspended in sterile water (2.5 mg/ml concentration) and stored in single-use 100 µl aliquots at -80°C. Collagenase/hyaluronidase was aliquoted into single-use 250 µl aliquots and stored at -80°C. Digested cells were washed twice with complete cell culture media and transferred into 24-well low attachment plates in 10% DMEM/F12 FBS, 1X MEM non-essential amino acid solution, 10 mM sodium pyruvate solution, 1X MEM vitamin solution, 10 mM HyClone™ HEPES. Cell culture media was supplemented with 1X antibiotic-antimycotic, 20 ng/ml epidermal growth factor, 10 ng/ml recombinant human FGF-basic. IntestiCult organoid growth medium was added to each well of the 24-well plates in a 1 to 4 proportion to culture media.

2.3.4 Immunohistochemistry

GEP-NET patient tissue samples (n=39) were identified by the Markey Cancer Center Biospecimen Procurement and Translational Pathology Shared Resource Facility. Immunohistochemistry (IHC) was performed as previously described [193]. Briefly, slides were deparaffinized in xylene, rehydrated, incubated for 15 min with fresh 0.3% hydrogen peroxide, washed with PBS, and heated to 95°C for 30 min in sodium citrate buffer (10mM Sodium Citrate, 0.05% Tween 20, pH 6.0).

Endogenous peroxidase activity was blocked with Bloxall blocking solution (Vector Laboratories, SP-6000). Next, sections were blocked for 1h with 2.5% normal horse serum (Vector Laboratories; S-2012). pAkt (Ser473) antibody was diluted in Dako background reducing antibody diluent (Agilent Dako; S3022). Primary antibody was incubated with slides for 12h at 4°C in a humidifier chamber, washed with TBST (Tris-Buffered Saline and Tween 20) and incubated with ImmPRESS universal antibody IgG polymer detection kit (Vector Laboratories, MP-7500) for 1h at room temperature. Antibody reaction was visualized with Immpact DAB EqV peroxidase substrate (Vector Laboratories, SK-4103). All sections were counterstained with hematoxylin (VWR, 95057-844) and observed by light microscopy. For negative controls, primary antibody was omitted from the above protocol.

The number of positive cells was visually evaluated in each core by a pathologist (EL), and the staining intensity was classified using a semi-quantitative seven-tier system developed by Allred et al. [194, 195]. The system assesses the percentage of positive cells (none=0; <10%=1; 10% to 50%, =2; >50%=3) and intensity of staining (none=0; weak=1; intermediate=2; and strong=3).

2.3.5 Immunoblotting

Cells were seeded on plates in equal density. To determine inhibition of the mTOR/pAkt pathway, cells were treated with either PKI-402 (50 to 1000nM) or PF-04691502 (100 to 10000nM) for 24, 48, and 72h and selected tumor spheroids were treated with PF-04691502 (500nM) for 24h prior to lysis. To examine markers for NET origin, selected tumor spheroids were incubated in humidified 37ºC 5% CO_2 incubator for 7d prior to lysis. To determine the synergistic effect on apoptosis, cells were treated

by radiotherapy or radiotherapy combined with PF-04691502 as described above, prior to lysis. The immunoblotting for individual experiments was performed as previously described [196].

2.3.6 Sulforhodamine B (SRB) Proliferation Assay

Cells were seeded in equal density and treated with PF-04691502 (100nM to 10,000nM), followed by incubation in a humidified 37ºC 5% CO_2 incubator for 72, 96 and 120h. Cells were then fixed, stained, and quantified following the Cytoscan™ SRB Cell Cytotoxicity Assay protocol [188].

2.3.7 Colony Formation Assay

Cells were seeded in equal density and treated with PF-04691502 (25nM to 500nM), followed by incubation in a humidified 37ºC 5% CO_2 incubator for 14d. Cells were then fixed and stained followed by quantification per Cytoscan SRB cell cytotoxicity assay protocol [188].

2.3.8 Radiotherapy

Cells were irradiated using a Precision X-Ray irradiator (X-RAD-225XL, North Branford, CT, USA) at the X-ray Service Center of the Department of Toxicology and Cancer Biology of the University of Kentucky (Ref: 32438621 and 30673636). The energy of the X-ray used was 225 kV at a dose rate of approximately 1.7 Gy/min. Accurate absorbed doses were calculated by considering the impact of backscattering as previously described [197]. To determine radiation dose-dependent apoptosis, cells were irradiated (2, 4, and 8 Gy) once, followed by incubation for 48, 72, and 96h. To assess the synergistic effect of radiotherapy and PF-04691502, cells were irradiated (2 Gy) once,

incubated for 48, 72, and 96h, followed by PF-04691502 treatment (500nM or 1000nM) for 24h. Finally, to determine the synergistic effect of simultaneous radiotherapy and PF-04691502, cells were irradiated (2 and 4 Gy), immediately treated with PF-04691502 (500nM or 1000nM), followed by incubation for 24h.

2.3.9 Statistical Analysis

Descriptive statistics, including means and SD, are presented in each experimental group and displayed in bar graphs. Percentage inhibition was calculated compared to control of each experiment and plotted against concentrations in a logarithmic scale. The standard curves and absolute maximal inhibitory concentration (IC-50) values were generated using SigmaPlot software version 14 (Systat Software Inc., San Jose, CA, USA). Immunohistochemistry scores were summarized descriptively. Comparisons of SRB absorbance, proliferation and colony formation assays were performed using one and two-way analysis of variance (ANOVA) with Holm's adjustment for multiple testing between groups. $p<0.05$ was considered to indicate a statistically significant difference. Statistical analyses were performed using SAS software version 9.4 (SAS Inc., Cary, NC, USA).

2.4 Results

2.4.1 pAkt (Ser473) expression in GEP-NET tumors

The PI3K/Akt/mTOR pathway has been implicated in GEP-NET development and improvement of progression-free survival [198, 199]. pAkt expression was analyzed in 39 GEP-NET tumor samples; 88% of the samples stained strongly positive (score 5 or 6). The staining intensity was weak in 2% (score 3 or less) and intermediate in 10% of

cases (score 4) (Figure 2-1. 2-2). Positive cytoplasmic staining was observed in all patient samples with positive pAkt staining. Although the sample number was somewhat limited, these results suggest increased Akt activation in a majority of GEP-NETs.

2.4.2 Cellular profiling of PI3K/mTOR inhibitors, PF-04691502 and PKI-402, in GEP-NET cancer cell lines

To determine the activity of the novel PI3K/mTOR inhibitors on NETs, three well-established human GEP-NET cell lines (QGP-1, BON, and NT-3), were treated with various concentrations (50-1,000nM) of either PKI-402 or PF-04691502 over a defined time period. PKI-402 (500 and 10,000nM) completely inhibited pAkt expression at 4h in both QGP and BON cells (Figure 2-3). However, this effect was not prolonged as noted by attenuation of pAkt expression at 24h with only the highest concentration (i.e., 1000nM) (Figure 2-4A). In contrast, PF-04691502 potently inhibited pAkt expression in both QGP-1 (at concentrations of 100 to 10,000nM) and BON (at concentrations of 500 to 10,000nM) cell lines at 24h after treatment (Figure 2-4B).

Next, we treated QGP-1 and BON cells with PF-04691502 (500nM) to test the duration of PI3K pathway inhibition (Figure 2-4C). The expression of pAkt was inhibited in both QGP-1 and BON cells at 24, 48 and 72h. Similarly, expression of pS6(Ser235/236), which is a key regulator of 40S ribosome subunit biogenesis, was inhibited in both cell lines. Finally, we assessed expression of p4EBP-1(Thr37/46), which plays a critical role in translational mRNA complex assembly, and found that PF-04691502 (500nM) inhibited expression of this protein at all time points; p4EBP-1 expression was markedly attenuated at 24 and 48h and completely inhibited at 72h. A single treatment with PF-04691502 not only demonstrated sustained inhibition for the

24h period in QGP-1 and BON cells (Figure 2-4B), but also attenuated pAkt, pS6 and p4EBP-1 at 24h in NT-3 cells (data not shown). Moreover, these results demonstrate that PF-04691502 can effectively inhibit PI3K/mTOR pathway components in both QGP-1 and BON cells for at least 72h.

To determine the effect of PF-04691502 on GEP-NET cell proliferation, we treated QGP-1 and BON cells with concentrations ranging from 100nM to 10000nM for 72, 96, or 120h. The percentage of cell inhibition was plotted against concentration of PF-04691502 on a logarithmic scale, and a standard curve was fitted to calculate the absolute IC-50 values. As shown in Figure 2-5A&B, a dose-dependent increase in percentage inhibition of cellular proliferation was observed in both QGP-1 and BON cells. The absolute IC-50 value, defined as 50% inhibition compared to control, ranges from 127.8 nM to 168 nM for QGP-1 cells and from 48.3 nM to 127.8 nM for BON cells.

Next, we evaluated the effect of PF-04691502 on QGP-1 and BON cell colony formation. Cells were treated with PF-04691502 (from 25 to 500nM) and clonogenicity was quantified as previously described. We noted a statistically significant decrease in clonogenicity at dosages of 250 and 500nM for both QGP-1 and BON cells (Figure 2-5C). These results demonstrate significant antiproliferative activity of PF-04691502 in GEP-NET cell lines, particularly at a dosage of 500nM.

2.4.3 Cellular profiling of PF-04691502 in patient-derived tumor spheroid model

Developing new preclinical models for GEP-NET has been a well-known challenge as slow growth and genetic stability limit availability of NET cell lines, PDX and metastatic models [200]. We have developed and evaluated 3D patient-derived NET

spheroids to perform rapid and reliable evaluation of therapeutics *in vitro*. As shown in Figure 2-6A, GEP-NET tumor samples M1893 primary (pT3N2Mx, well-differentiated small intestinal NET) and M3210 primary (pT3N2M1a, well-differentiated small intestinal NET), with their respective lymph node (LN) metastasis were established and cultured as tumor spheroids. Neuroendocrine origin of the tumor spheroids was confirmed by immunoblotting analysis of neuroendocrine biomarkers: chromogranin A (CgA), somatostatin receptor 2 (SSTR2), and synaptophysin (SYP) (Figure 2-6B). After confirming these patient-derived spheroids were indeed neuroendocrine in origin, we treated the spheroids with PF-04691502 (500nM) for 24h and determined expression of pAkt, pS6, and p4EBP-1 (Figure 2-6C). Similar to GEP-NET cell lines, we observed inhibition of pAkt, pS6, and p4EBP-1 expression in both spheroid samples at 24h. These results demonstrate both the validity of our NET spheroid model as a reproducible tool for the evaluation of novel therapeutics and the anti-proliferative effect of PF-04691502 on GEP-NETs.

2.4.4 Enhanced radiosensitization of GEP-NET cells via schedule dependent PF-04691502 treatment

Radiotherapy, namely PRRT, has emerged as the next generation treatment for GEP-NET patients [201, 202]. Here, we tested the hypothesis that combination of a PI3K/mTOR inhibitor with radiotherapy may enhance therapeutic effects in GEP-NETs. As shown in Figure 2-7A, radiotherapy alone resulted in a dose-dependent increase in cleaved PARP expression, a marker of apoptosis, in both QGP-1 and BON cells. Notably, cleaved PARP expression was detected at least 48h after radiation in QGP-1 cells and 72h after radiation in BON cells, suggesting delayed radiation-induced apoptosis in GEP-

NET cells. Therefore, we hypothesized that NET cells are most sensitive to PI3K/mTOR inhibition after radiotherapy. Next, QGP-1 and BON cells were irradiated (2 Gy) and then treated with PF-04691502 (500 or 1000nM) for 24h at 48h, 72 or 96h after radiation. As shown in Figure 2-7B, we observed a significant increase in cleaved PARP expression in cells treated with a combination of radiation and PF-04691502 at 48 and 72h post-radiation in QGP-1 cells and 96h post radiation in BON cells. In contrast, increased cleaved PARP expression was not noted in cells treated with 4 Gy radiation, immediately followed by PF-04691502 (500nM or 1000nM) treatment for 24h (Figure 2-8). Our findings suggest that delayed treatment with a PI3K/mTOR inhibitor after radiotherapy can result in increasing cytotoxic effects compared to either drug or radiotherapy alone. Most importantly, our data demonstrates a schedule dependence of apoptosis induction after radiation and PI3K/mTOR inhibition in GEP-NET cells. Therefore, our results suggest the use of a PI3K/mTOR inhibitor in combination with radiotherapy in a delayed fashion as a possible treatment strategy to prevent disease progression and to promote disease regression in NET patients, as proposed in the schematic diagram (Figure 2-7C).

2.5 Discussion

GEP-NET is a subset of aggressive gastrointestinal NETs, often diagnosed as advanced disease with poor prognosis[164]. Improved treatment options are needed, as a third of GEP-NET patients do not respond to current regimens [14, 164, 179]. Radiotherapy and mTOR inhibition are two promising therapies that have improved treatment outcomes, such as progression-free survival [35, 165, 166, 177, 181]. PRRT is a form of targeted radiotherapy, coupled with either an alpha-emitter or beta-emitter and a somatostatin analog to induce DNA damage in targeted GEP-NETs overexpressing

somatostatin receptors [165, 170]. It has become a prevalent treatment among patients with inoperable and metastatic somatostatin receptor positive GEP-NETs [165, 170, 203], with clear progression-free survival benefit and improved quality of life among patients [204, 205]. Despite the fact that the initial PRRT treatment resulted in stable disease in up to 80% of patients, all patients eventually progressed over time [165, 166, 170, 203, 205].

Our study explored the therapeutic potential of inhibiting the PI3K/mTOR/Akt pathway, which plays a crucial role in NET pathogenesis [175, 206]. The mTOR pathway, one of the most significant targets in modern cancer treatment[175, 207], is triggered by growth factors and is responsible for cell survival, proliferation and angiogenesis[175]. There are multiple downstream targets of the mTOR pathway, such as the ribosomal protein S6 kinase 1 (S6K1) and eukaryotic translation initiation factor 4E (eIF4E)-binding protein 1 (4E-BP1)[208]. The S6 protein is a key regulator of 40S ribosome subunit biogenesis and 4E-BP1 has a critical role in translational mRNA complex assembly [207, 209, 210]. Together, these two proteins are phosphorylated by mTORC1 to promote translation and protein synthesis[207, 210]. Clinically, inhibition of S6 and 4E-BP1 phosphorylation are two important therapeutic targets for multiple malignancies[208, 209, 211, 212]. Everolimus, a rapamycin analog and potent mTORC1 inhibitor[213], was used to treat GEP-NETs in the RADIANT clinical trial series[34, 35, 176-179]. Though Everolimus showed improved progression free survival in short term, only 10% of patients had disease regression [176]. This could be secondary to the negative feedback loop of the mTORC2/Akt pathway [214]. The protein S6K inhibits the mTORC2 complex and Akt, which forms the negative feedback loop. Therefore, inhibition of S6K by mTORC1 inhibitor could result in Akt pathway activation through

mTORC2 signaling, thus providing an escape mechanism and incomplete inhibition of downstream effectors[214]. Therefore, a new class of PI3K/mTOR dual inhibitors was developed to provide complete inhibition of mTOR/Akt pathway [182, 212].

In contrast to Everolimus, the PI3K/mTOR dual inhibitors, PF-04691503 and PKI-402, tested in this study, primarily inhibit PI3K and Akt phosphorylation, an upstream mediator of both mTORC1 and mTORC2 complexes[182]. Inhibition of Akt results in dual inhibition of the mTORC1 and mTORC2, thus preventing the escape negative feedback loop [212]. Our study identified abundant expression of pAkt in the cytoplasm of GEP-NET, which is the primary target of the PI3K/mTOR dual inhibitor, as shown in Figure 1. We also demonstrated significant and prolonged attenuation of pAkt, pS6, and p4EBP-1 expression and antiproliferative properties of the PI3K/mTOR dual inhibitors *in vitro*. This is consistent with previous studies where PI3K/mTOR dual inhibitors have shown antineoplastic properties in various cancer cell lines [215-219]. Despite the abundant supporting evidence for their antineoplastic properties, multiple clinical trials of PI3K/mTOR dual inhibitors have reported unacceptable toxicity resulting in the early termination of trials, including one phase II study in pNET [184, 187, 220, 221]. Thus, it has a limited role in cancer treatment as a single agent [182, 183, 214]. However, its role as a radiosensitizer has not been previously studied.

Radiotherapy, which utilizes ionized radiation, directly or indirectly damages cellular DNA in cells undergoing rapid division and activates cell survival pathways [222, 223]. The ionizing energy can break double helix DNA structure, which subsequently results in programmed cell death if not repaired successfully, or induce single strand DNA break, which leads to prolonged cell autophagy or cell cycle arrest

[223]. When cells sustain DNA damage, the Non-Homologous End Joining (NHEJ) or Homologous Recombination (HR) repair pathways become activated and phosphorylate ATR, ATM and DNA-PK to promote cell survival [222, 223]. The PI3K/mTOR/Akt pathway responds to ATM and DNA-PK phosphorylation through AMPK signaling, and triggers its downstream effectors to promote survival, proliferation and angiogenesis as described previously [222]. This forms the basis for our hypothesis that PI3K/mTOR dual inhibitor could enhance the cytotoxic effect of radiotherapy.

Our laboratory recently showed that Akt1 expression plays a major role in radiosensitivity of triple negative breast cancer [196]. Therefore, we hypothesized that combining radiotherapy and PI3K/mTOR dual inhibitor could prevent cell survival response to DNA damage from radiation therapy, thus achieving synergistic cytotoxic effect through a multimodal approach. We used PI3K/mTOR dual inhibitors, which prevent re-activation of mTOR through negative feedback, and combined it with radiotherapy to induce synergistic apoptosis in GEP-NET cell lines. In addition to the radiosensitization by PI3K/mTOR inhibitions, our study identified a schedule-dependent induction of apoptosis. Pre-radiation and simultaneous treatment with PF-04691502 did not increase apoptosis, while PF-04691502 administered post-radiation produced a synergistic induction of apoptosis compared to either PF-4691502 or radiation alone. Moreover, cells did not undergo apoptosis immediately after radiation. In contrast, there was a delayed apoptotic response at 48h and at longer time points. Prior preclinical studies have also noted a schedule-dependent radiosensitization using sorafenib and erlotinib [224, 225]. One study suggested that this variation could be due to PI3K signal transduction and its regulatory effects [225]. Schedule-dependent PI3K/mTOR inhibition

has a potential to reduce the frequency of side effects observed after PI3K/mTOR pathway inhibition by reducing number of administered doses required to achieve cytotoxic effects in cancer cells.

In summary, we demonstrate that PF-06491502 is a long-acting PI3K/mTOR inhibitor with antineoplastic activity, which can also potentiate radiotherapy when administered in a schedule-dependent fashion. Our findings suggest that PI3K/mTOR inhibitors should be administered for short term after radiation therapy to potentiate radiotherapy and to improve clinical outcomes in GEP-NET patients. Short term exposure of PI3K/mTOR inhibitor administration in this setting could prevent toxicity of inhibitors associated with long term treatment.

2.6 Acknowledgement

The Markey Cancer Center's Research Communications Office helped prepare the manuscript and figures. The Biostatistics and Bioinformatics Shared Resource Facility of the Markey Cancer Center conducted formal statistical analyses. The Biospecimen Procurement & Translational Pathology Shared Resource Facility of the Markey Cancer Center acquired and stained tissue sections. Shared Resource Facilities of the Markey Cancer Center are supported by P30CA177558. Dr. Quan Chen (Department of Radiation Medicine) assisted with radiation treatment of cells. Dr. Zeta Chow was supported by National Institute of Health T32 training grant CA160003. Ms. Carrigan Wasilchenko and Mr. Matthew Melton were supported by the Appalachian Career Training in Oncology program (R25 CA221765). This project was supported by a generous donation from the Amanda W. Lockey Foundation.

2.7 Citations

1. Chow, Z., Townsend, C., Evers, B. M., & Rychahou, P. (2020). Effect of novel mTOR-PI3K dual inhibitors on neuroendocrine tumor cell proliferation and apoptosis. *Cancer Research*, *80*(16_Supplement), 676-676.
2. Chow, Z., Johnson, J., Chauhan, A., Izumi, T., Cavnar, M., Weiss, H., ... & Rychahou, P. (2021). PI3K/mTOR dual inhibitor PF-04691502 is a schedule-dependent radiosensitizer for gastroenteropancreatic neuroendocrine tumors. *Cells*, *10*(5), 1261.

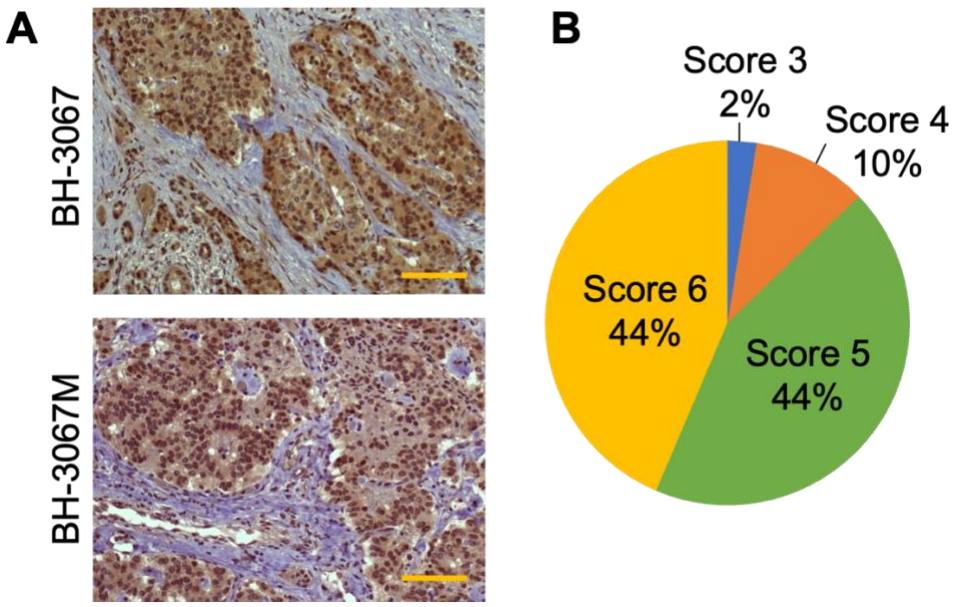

Figure 2-1 Analysis of pAkt (Ser473) expression in GEP-NET patient samples
(A) Representative pAkt (Ser473) immunohistochemistry staining of patient neuroendocrine tumor samples. Positive staining was observed in the cytoplasm. Patient GEP-NET samples (n=39) were prepared by pathologist and scored in abundance and intensity as described. (B) Percentage distributions of cytoplasmic expression of pAkt (Ser473) scored by abundance and intensity is shown in the pie chart.

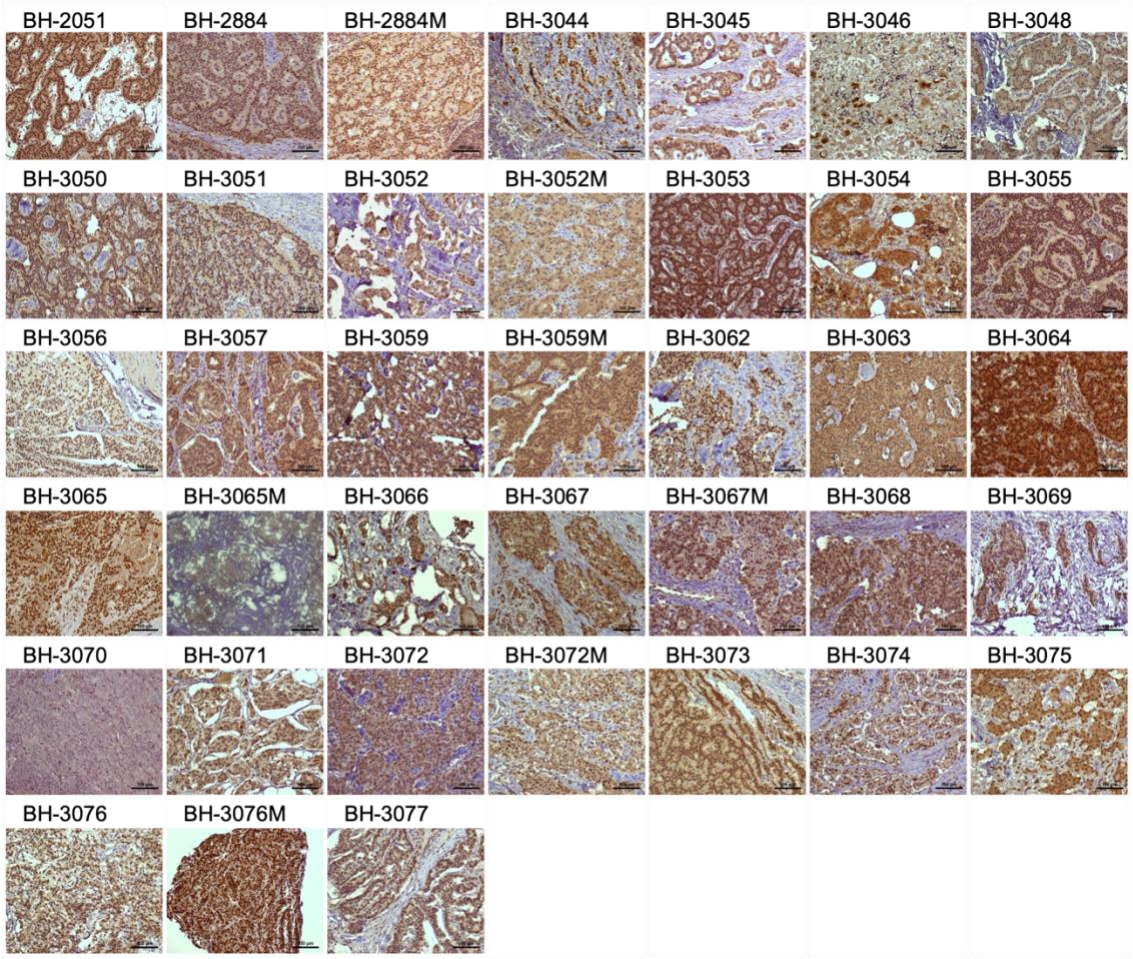

Figure 2-2 . pAkt (Ser473) expression GEP-NET patient tumor samples
IHC staining of pAkt (Ser473) in pNET primary and metastatic tumor samples. Samples were scored on scales of 0-3 for both intensity and distribution percentage and then added together (n = 38).

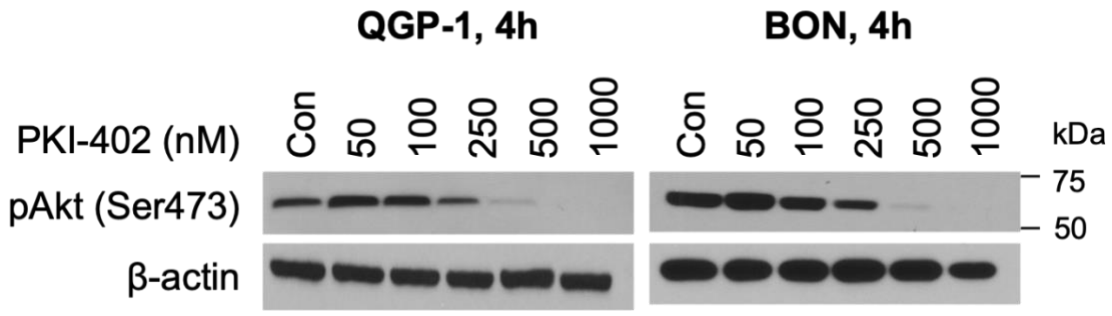

Figure 2-3 pAkt (Ser473) inhibition by PKI-402 in NET cell lines at 24h
(A) QGP-1 (left) and BON (right) cells were seeded in a 6-well plate at 800,000 cells per well density and treated with PKI-402 from 50nM to 1,000nM, and collected at 4h. Immunoblotting was performed to confirm PI3K/Akt pathway inhibition at 4h. β-actin was used as loading control.

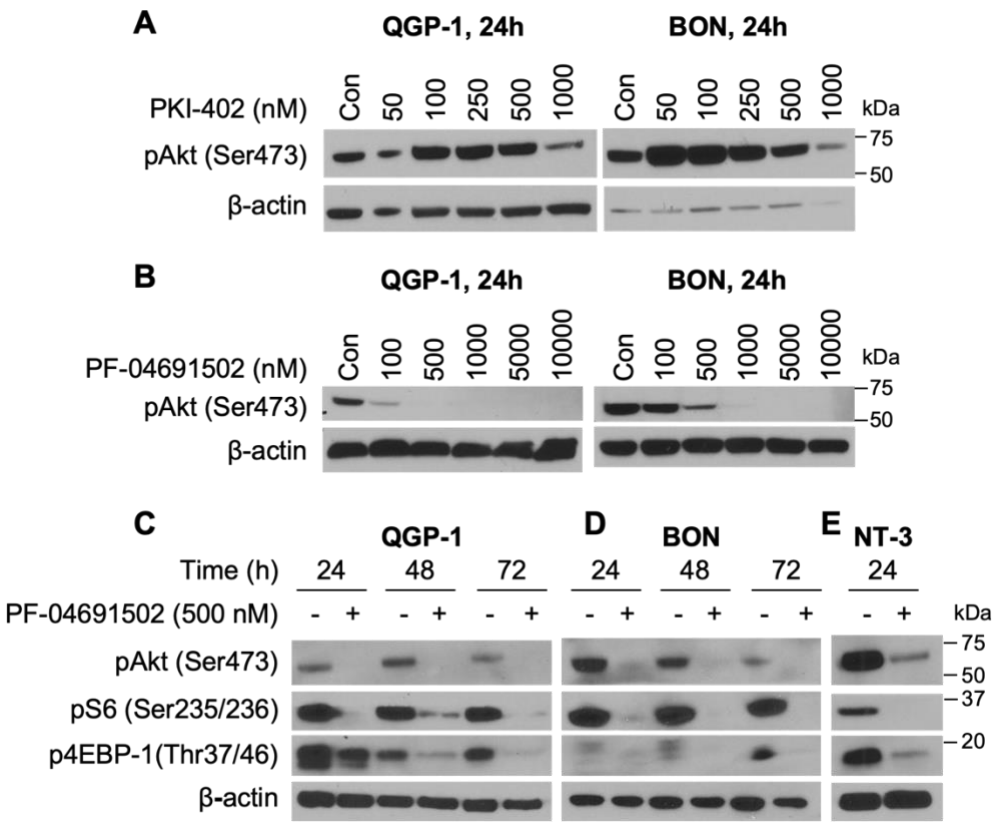

Figure 2-4 pAkt (Ser473) inhibition by PKI-402 and PF-04691502 in NET cell lines
(A) QGP-1 and BON cells were seeded in a 6-well plate at 800,000 cells per well and treated with PKI-402 from 50nM to 1,000nM, and collected at 24h. Western blot analysis was performed to confirm PI3K/Akt pathway inhibition at 24h (B) QGP-1 and BON cells were seeded 6-well plate at 800,000 cells per well and treated with PF-04691502 from 100nM to 10,000nM, and collected at 24h. Western blot analysis was performed to confirm PI3K/Akt pathway inhibition. (C) QGP-1 (D) BON and (E) NT-3 cell lines were seeded in 6-well plate at 800,000 cells per well and treated with 500nM PF-04691502. Protein was collected at 24h, 48h, and 72h. In addition to pAkt (Ser473) inhibition, downstream targets of PI3K/Akt pathway, pS6(Ser235/236) and p4EBP-1(Thr37/46) inhibition were confirmed with western blot analysis. β-actin was used as loading control.

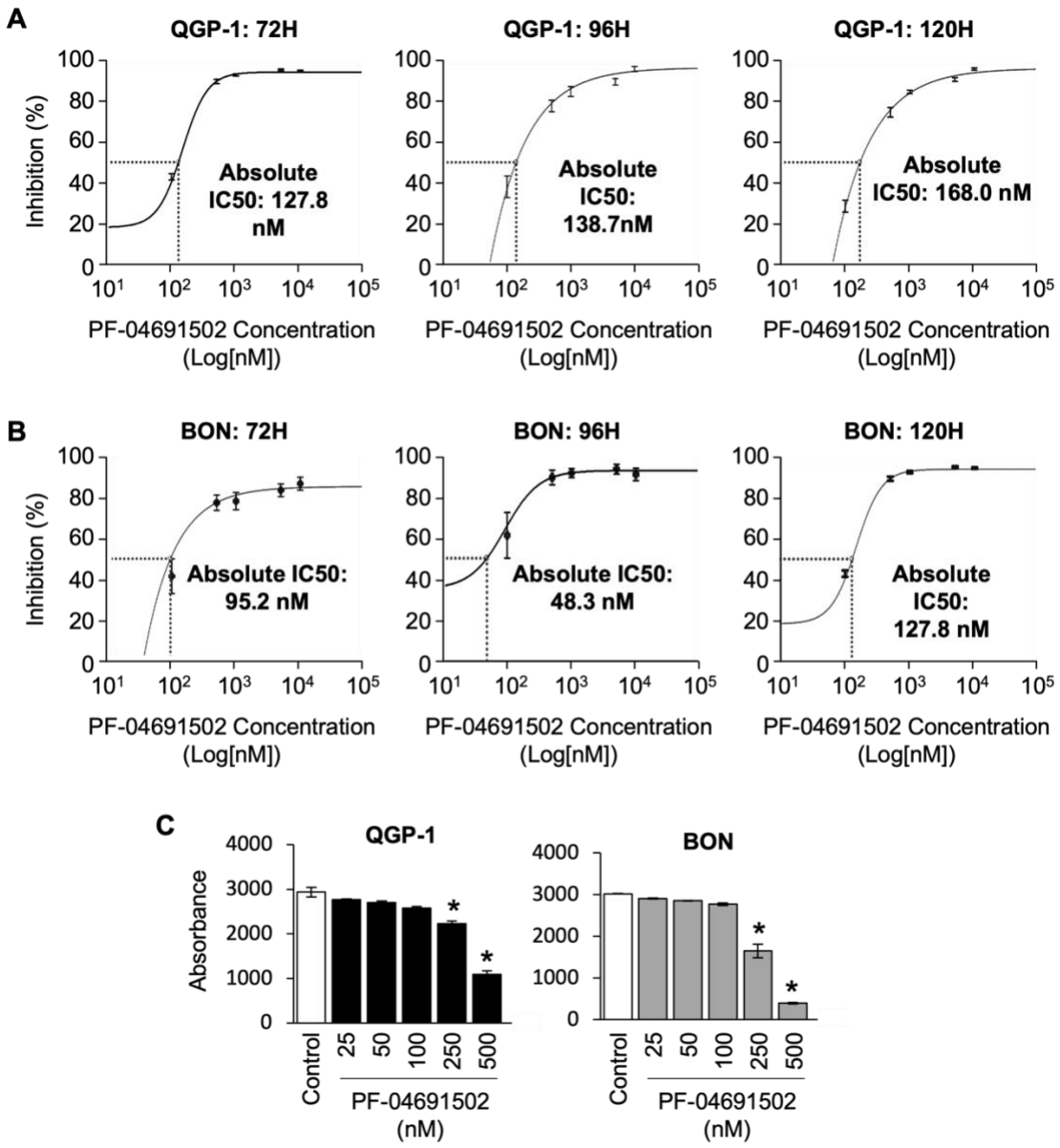

Figure 2-5 Analysis of QGP-1 and BON cells proliferation and clonogenicity after PF-04691502 treatment

(A) QGP-1 and (B) BON cells were seeded in 96-well plate at 5,000 cells per well density (n=6 per group) and treated with PF-04691502 from 100nM to 10,000nM for 72, 96, and 120h. Cell proliferation was analyzed with SRB assay as described. Percentage inhibition of proliferation was plotted against concentrations of PF-04691502 in logarithmic scale. Absolute IC-50 was denoted by dashed line and labeled, respectively. (C) QGP-1 and BON cells were seeded in 96-well plate at 200 cells per well density (n=6 per group) and treated with PF-04691502 from 25nM to 500nM. Cell colonies were fixed and stained according to SRB protocol 14d later. *, $p<0.01$ versus control clonogenicity by one-way ANOVA analysis.

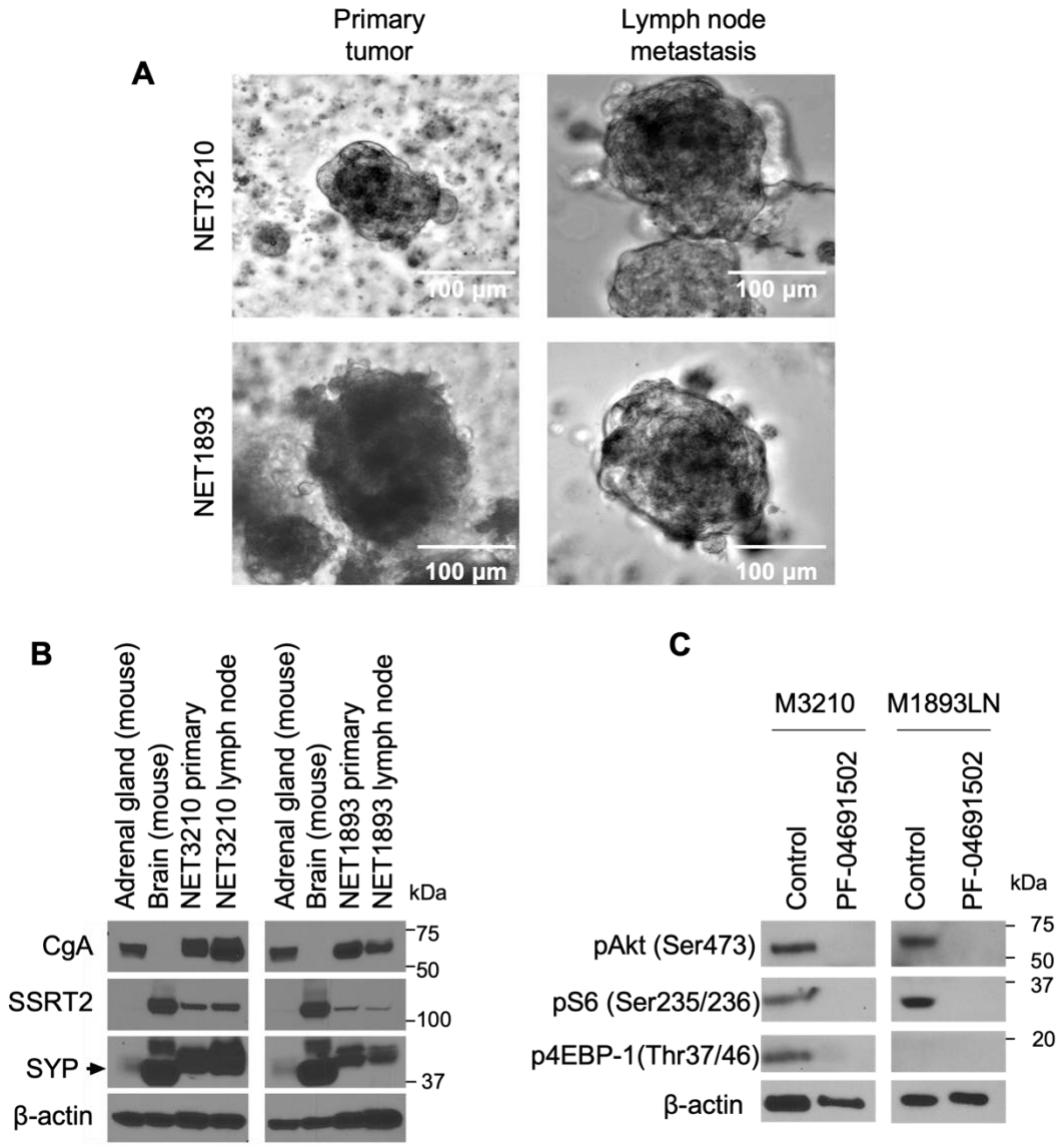

Figure 2-6 Patient-derived GEP-NET tumor spheroids treatment with PF-04691502
(A) Photographs of tumor spheroids in low-attachment plates. GEP-NET patient tumor sample M3210 was a pT3N2M1a, grade 2 tumor ileal neuroendocrine tumor, and tumor sample M1893 was pT3N2Mx small intestinal neuroendocrine tumor. (B) GEP-NET tumor spheroids were plated in low-attachment plates and 7d later protein lysates were collected for GEP-NET origin confirmation by western blot. Mouse brain and mouse adrenal glands were used as positive controls for SYP and CgA, correspondingly. (C) GEP-NET tumor spheroids were seeded in low-attachement plates with equal density and treated with 500nM PF-04691502 for 24h. Protein lysates were collected to confirm PI3K/Akt pathway inhibition by pAkt (Ser473), pS6(Ser235/236) and p4EBP-1(Thr37/46) by immunoblotting. β-actin was used as loading control.

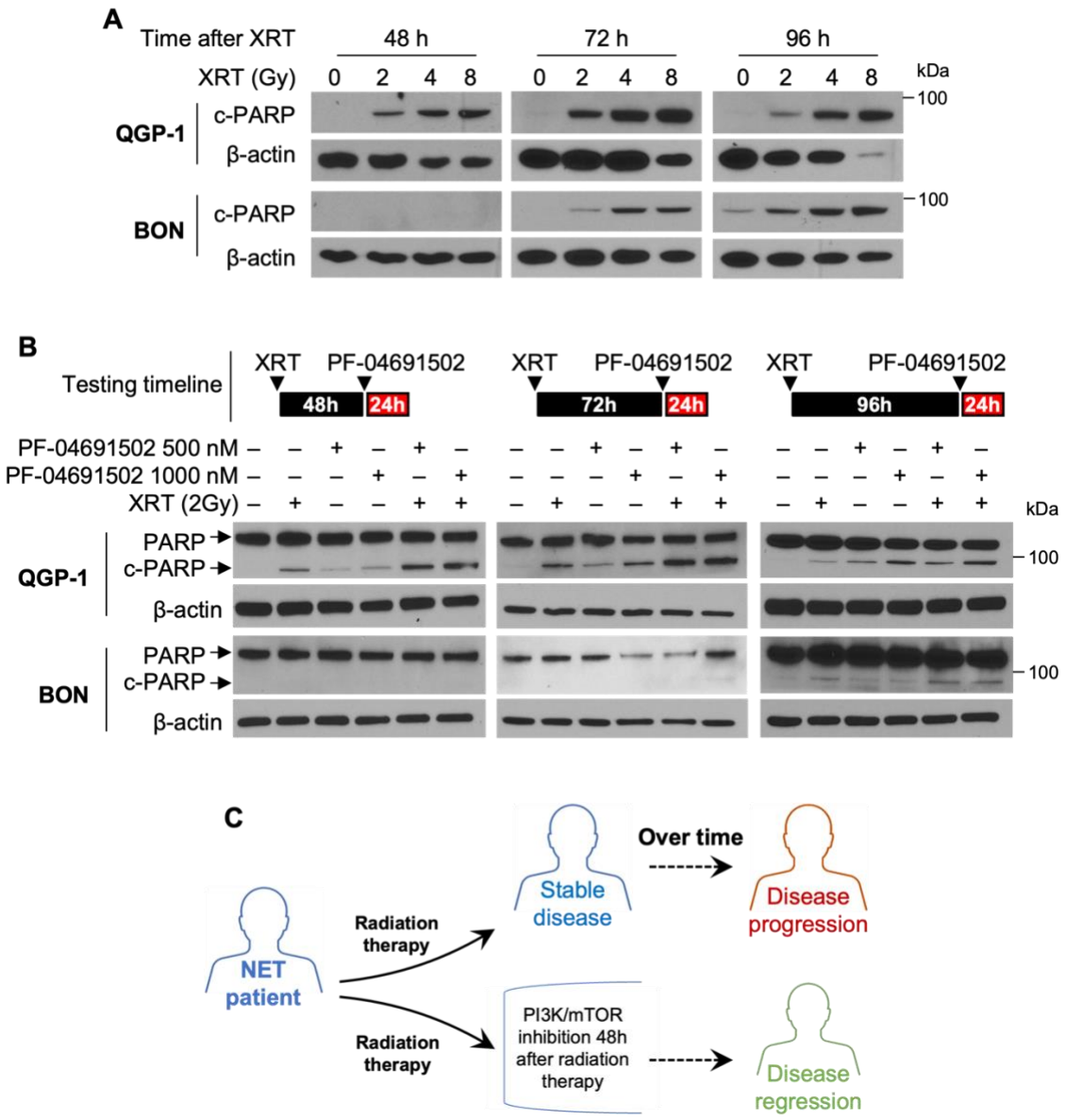

Figure 2-7 Radiotherapy and schedule-dependent PF-04691502 therapy in NET cells (A) QGP-1 (top) and BON (bottom) cells were seeded in 6-well plate at 800,000 cells per well density. Cells were then exposed to either control (0Gy), 2Gy, 4Gy, or 8Gy X-ray radiation. Protein lysates were collected at 24h, 48h, 72h, and 96h after radiation exposure and analyzed for cleaved-PARP expression by immunoblotting. β-actin was used as loading control. (B) QGP-1 (top) and BON (bottom) cells were seeded in 6-well plate at 800,000 cells per well density and exposed to 2 Gy X-ray radiation. Cells were incubated for either 48h, 72h, or 96h and then treated with PF-04691502 at 500nM or 1,000nM for 24h prior to protein lysates collection. Cleaved-PARP expression was determined by immunoblotting analysis. β-actin was used as loading control. (C) Schematic diagram for schedule-dependent PI3K/mTOR inhibition after radiotherapy in NET patients

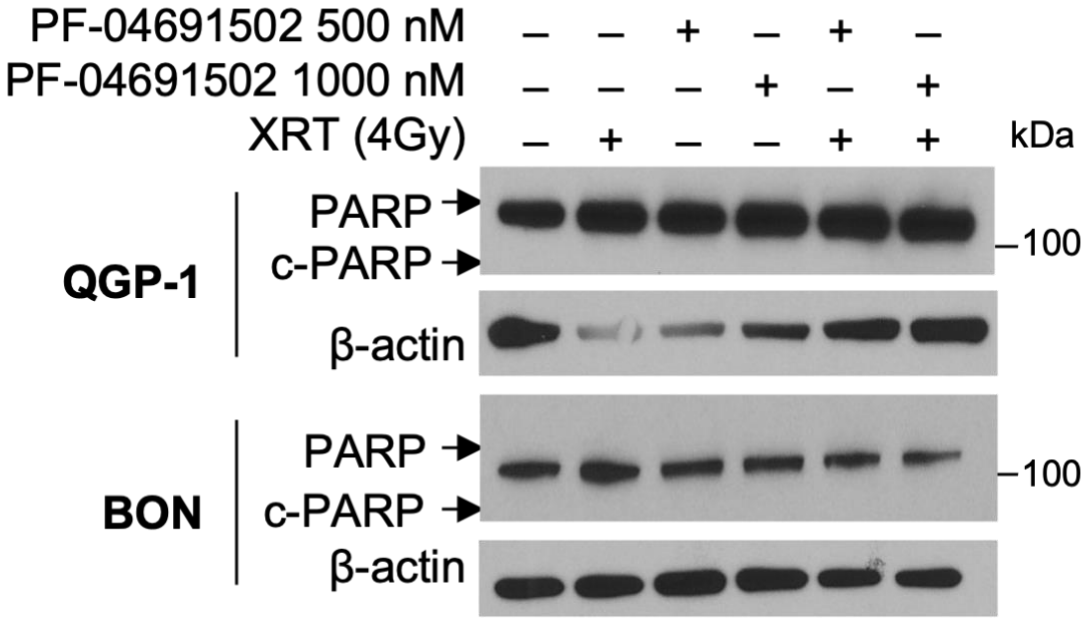

Figure 2-8 Simultaneous XRT and PF-04691502 therapy in NET cell lines
QGP-1 (top) and BON (bottom) cells were seeded in 6-well plate at 800,000 cells per well density and exposed to 4 Gy X-ray radiation. Cells were then immediately treated with PF-04691502 at 500nM or 1,000nM for 24h prior to protein collection. Cleaved-PARP expression was determined by immunoblotting. β-actin was used as loading control.

CHAPTER 3. INHIBITION OF RIBONUCLEOTIDE REDUCTASE SUBUNIT M2 ENHANCES THE RADIOSENSITIVITY OF METASTATIC PANCREATIC NEUROENDOCRINE TUMOR

3.1 Abstract

Ribonucleotide Reductase (RNR) is a rate-limiting enzyme in the production of deoxyribonucleoside triphosphates (dNTPs), which are essential substrates for DNA repair after radiation damage. We explored the radiosensitization property of RNR and investigated a selective RRM2 inhibitor, 3-AP, as a radiosensitizer in the treatment of metastatic pNETs. We investigated the role of RNR subunit, RRM2, in pancreatic neuroendocrine (pNET) cells and responses to radiation in vitro. We also evaluated the selective RRM2 subunit inhibitor, 3-AP, as a radiosensitizer to treat pNET metastases in vivo. Knockdown of RNR subunits demonstrated that RRM1 and RRM2 subunits, but not p53R3, play significant roles in cell proliferation. RRM2 inhibition activated DDR pathways through phosphorylation of ATM and DNA-PK protein kinases but not ATR. RRM2 inhibition also induced Chk1 and Chk2 phosphorylation, resulting in G1/S phase cell cycle arrest. RRM2 inhibition sensitized pNET cells to radiotherapy and induced apoptosis in vitro. In vivo, we utilized pNET subcutaneous and lung metastasis models to examine the rationale for RNR-targeted therapy and 3-AP as a radiosensitizer in treating pNETs. Combination treatment significantly increased apoptosis of BON (human pNET) xenografts and significantly reduced the burden of lung metastases. Together, our results demonstrate that selective RRM2 inhibition induced radiosensitivity of metastatic pNETs both in vitro and in vivo. Therefore, treatment with the selective RRM2 inhibitor, 3-AP, is a promising radiosensitizer in the therapeutic armamentarium for metastatic pNETs.

3.2 Introduction

Pancreatic neuroendocrine tumors (pNETs) are a subset of gastroenteropancreatic neuroendocrine tumors (GEP-NETs) originating from the islet of the Langerhans within the pancreas [3]. Metastatic pNETs carry a poor prognosis with a median survival of 24 months and a 5-year overall survival (OS) rate of 28.6% [13]. Peptide receptor radionuclide therapy (PRRT) has emerged as an effective treatment for metastatic pNETs, with studies showing increased progression-free survival and OS [85, 226]. In a retrospective analysis, metastatic pNET patients treated with ^{177}Lu-DOTATATE infusions had an objective response rate (ORR) of 57.4% and a disease control rate of 85.3%. The median OS was 53 months, significantly improved from the 24 months reported using historical controls [13, 226]. Utilization of a radiosensitizer concurrently with PRRT has further enhanced the effectiveness. Claringbold et al. [85] combined radiosensitizing capecitabine and temozolomide with ^{177}Lu-DOTA-octratate (DOTATATE) in the treatment of metastatic pNET patients, and noted that the ORR was further improved to 83%. However, the complete response rate was only 13%. Currently, there is a pressing need to explore new therapeutic targets to further improve the treatment response of PRRT.

Ribonucleotide reductase (RNR) is the rate-limiting enzyme responsible for the de novo conversion of ribonucleotides to deoxyribonucleotides, substrates for DNA polymerase and production of deoxyribonucleoside triphosphates (dNTPs) [227, 228]. RNR consists of two larger ribonucleotide reductase subunit M1 (RRM1) and two smaller ribonucleotide reductase subunit M2 (RRM2) with two isoforms, RRM2 and RRM2B, encoded by *RRM2* and *p53R2* genes, respectively [227]. The RRM2 subunit

was found to be among the top 10% most overexpressed genes in 73 out of 168 cancers, and among the top 1% most overexpressed in pancreatic cancer [229]. Multiple studies have found that RRM2 overexpression was associated with chemoresistance and poor prognosis in various cancers, whereas RRM2 suppression could overcome resistance [230-232]. Recently, RRM2 inhibition was found to be associated with enhanced radiosensitivity in the treatment of glioblastoma and esophageal cancer [233, 234]. These studies suggest that RRM2 is an important therapeutic target to enhance DNA damage-based therapy.

Selective RRM2 inhibitors have been developed to specifically target the small regulatory subunits [235]. Of all the RRM2 inhibitors, 3-AP has a 1000-fold greater potency in both enzyme and tumor cell growth inhibition than hydroxyurea [236]. In addition, 3-AP is a DNA damaging agent and causes cell cycle arrest and apoptosis [235]. 3-AP has shown promising results in prospective clinical trials [237-239]. Remarkably, a 96% complete metabolic response was noted 3 months post-treatment in a phase II clinical trial evaluating 3-AP with concurrent cisplatin-based chemoradiation in treating cervical and vaginal cancer patients [237].

The purpose of our current study was to investigate the role of the RRM2 subunit in pNET radiosensitivity and to evaluate a selective RRM2 inhibitor, 3-AP, as a radiosensitizer in treating metastatic pNET. We found that suppression of RRM2 alone has a profound cytostatic effect; however, when combined with radiotherapy, the RRM2 inhibitor 3-AP significantly potentiated apoptosis in vitro and in vivo. Our findings demonstrate that RRM2 is an effective therapeutic target, and that 3-AP is a promising radiosensitizer in the treatment of metastatic pNETs

3.3 Materials and Methods

3.3.1 Cell lines and cell culture supplies

The BON cell line was derived from a human metastatic carcinoid of pancreas in a peripancreatic lymph node and previously characterized [240]. QGP-1, derived from a human somatostatin-producing pancreatic carcinoma of islet cell origin, was purchased from Japan Health Sciences Foundation [241]. The NT-3 cells, derived from a human well-differentiated metastatic insulinoma, was a kind gift from Dr. Jörg Schrader [242]. Materials and techniques for maintaining the cell cultures were described previously [243].

3.3.2 Selective RRM2 inhibitor, 3-AP

RRM2 inhibitor, 3-AP (Triapine®; PAN-811; OCX191; HY-10082), used for in vitro studies was purchased from MedChemExpress®. Drug was diluted in dimethyl sulfoxide (DMSO), aliquoted and stored at -20°C; DMSO served as control. 3-AP used for in vivo studies was obtained from the National Cancer Institute Cancer Therapy Evaluation Program and stored as a powder at -20°C. Drug was resuspended in 0.9% normal saline (NS) and mixed thoroughly, prior to intra-peritoneal (i.p.) administration to mice. 3-AP (10 mg/kg) was administered to mice 30 min before radiation therapy; NS was used as control.

3.3.3 radiotherapy in vitro

Cells were irradiated at the X-ray Service Center (XSC) of the Department of Toxicology and Cancer Biology at the University of Kentucky. Briefly, cells were placed on the X-RAD 225XL orthovoltage X-ray platform (Precision X-ray, Madison, CT) with

an aluminum filter and received a dose rate of approximately 2.0 Gy/min. Absorbed doses were calculated with consideration of the impact of backscattering as previously described [197].

3.3.4 Radiotherapy in vivo

Prior to the radiation procedures, the mice (control and treated groups) were anesthetized by i.p administration of (10 mg/kg; AnaSed xylazine, NADA 139-236, Akorn, IL) and ketamine (100 mg/kg; Ketathesia Ketamine hydrochloride, Henry Schein Animal Health, Dublin, OH). The tumor sites of mice were precisely positioned on the X-RAD 225 XL platform for the X-ray exposure with the adjustable collimator [244, 245]. The tumor sites were then irradiated with a copper filter and a dose rate of approximately 1.6 Gy/min.

3.3.5 Western Immunoblotting

Firstly, we examined RNR subunit expression and efficiency of siRNA knockdown in pNET cell lines. Cells, with or without siRNA knockdown, were seeded in 6-well plates at 800,000 cells/well density, incubated overnight, and analyzed for RRM1, RRM2, p53R2 expression. GAPDH was used as loading control. Secondly, we evaluated markers for DNA Damage Response (DDR) and cell cycle arrest after RRM2 inhibition. Cells with RRM2 knockdown were seeded in 6-well plates at 800,000 cells/well density, incubated overnight and analyzed for RRM2, pDNA-PK (S2056), DNA-PK, pATM (S1981), ATM, pATR (S428), ATR, pChk-1(S345), Chk1, pChk-2 (T68), Chk2, and cyclin D1 expression. Cells were also treated with 3-AP (DMSO control, 2,500 nM and 5,000 nM) for 16h, and harvested for the same protein analysis, except for RRM2

expression. β-actin was used as loading control. Lastly, we evaluated the radiosensitization effect of RNR inhibition in vitro and in vivo, using PARP/cleaved PARP (c-PARP) as markers for apoptosis. Cells were either transfected with RRM2 siRNA for 72h to establish knockdown or treated with 3-AP (DMSO control or 2,500 nM) for 16h, followed by radiotherapy as described above. Cells were then incubated in fresh medium for 96h prior to analysis of cleaved PARP expression. β-actin was used as loading control. Lastly, BON xenograft tumors were excised from the left flank of mice, minced and placed into 1x lysis buffer (Cell Signaling Technology, Danvers, MA) supplemented with proteinase inhibitors (Thermo Scientific; #A32955). Tumor tissues were homogenized with stainless steel beads (0.9-2 mm blend, #SSB14B) on Bullet Blender homogenizer (Next Advance, Troy, NY). Protein lysates were separated by centrifugation and analyzed for total PARP and c-PARP expression. β-actin was used as loading control. The materials and western blot techniques were performed as described previously [243]. The primary and secondary antibodies used in this study are noted in Table 3.1

3.3.6 Immunohistochemistry

The pNET patient tissue samples (n=36) were identified by the Markey Cancer Center Biospecimen Procurement and Translational Pathology Shared Resource Facility. IHC was performed as previously described [246]. The IHC slides were evaluated by a pathologist, who classified staining positivity and intensity using a semi-quantitative seven-tier system developed by Allred et al. [247]. The system assesses the percentage of positive cells (none=0; <10%=1; 10% to 50%, =2; >50%=3) and intensity of staining (none=0; weak=1; intermediate=2; and strong=3).

3.3.7 siRNA transfection

RRM1, RRM2 and p53R2 subunit siRNA were purchased from Santa Cruz: siRNA RRM1 (SC-37640), siRNA RRM2 (SC-36338), and siRNA p53R2 (SC-36158); transfection reagent was purchased from Invitrogen: Lipofectamine™ RNAiMax (56532). Cells were seeded at 100,000 cells/mL density in 12-well plates, transfected with siRNAs (NTC, RRM1, RRM2, or p53R2) and incubated for 48 and 72h. The final siRNA concentration was 100nM for each experiment. siRNA transfection was performed as previously described [196].

3.3.8 Cell counting assay

Cells were seeded at 100,000 cells/2mL density in 12-well plates and siRNA knockdown was performed as described above. Cells were seeded in 6-well plates at 800,000 cells/2mL, transfected with NTC, RRM1, RRM2, and p53R2 siRNA for 24h and re-plated in 48-well plates at 20,000 cells/0.5 mL (n=6 wells). Cells were counted at 48 and 72h after siRNA transfection with an automated cell counter (Beckman Coulter, Vi-Cell Blue Cell Counter).

3.3.9 Confocal imaging

QGP-1 and BON cells were plated onto gelatin coated (0.1% gelatin in deionized H_2O) glass coverslips and treated with 3-AP at 2500 nM 24h later. Cells were fixed with 4% paraformaldehyde (Pierce, #28908, ThermoFisher Scientific) and probed with p-Histone H2A.X antibody (Ser 139, 1:250, Santa-Cruz Biotechnology, #sc-517348) at 4°C overnight. Cells were washed and incubated with secondary antibody DyLight™ 594 horse anti-mouse antibody protected from light (ready to use, Vector Laboratories, #DI-

2794-15). F-actin was visualized with phalloidin staining (ThermoFisher Scientific, #A12379, 1:4000, 20 min RT) and coverslips were mounted with antifade mounting medium with DAPI (Vector Laboratories; #H-1800).

3.3.10 Clonogenic assay, cell proliferation assay and low cell density survival assay

For proliferation analysis, cells were seeded at 5,000 cells/100µL (15625/cm^2) in 96-well plates and treated with 3-AP (DMSO control, 1,000nM to 5,000nM) for 96h. SRB Cell Cytotoxicity Assay (G-Biosciences, #786-21) was used to measure cell proliferation as previously described [243].

For clonogenic assay, cells were seeded in a 6-well plate at density of 1000 cells/well (104 cells/cm^2) for both QGP-1 and BON cells (n=3 wells for each group). Cells were treated with 3-AP (DMSO control or 2,500nM) and 14d later fixed with 10% trichloroacetic acid (TCA) for 1h at 4°C. Next, cells were stained with 0.4% sulforhodamine B (SRB) for 30 min, excess dye was removed with 0.1% acetic acid wash and dye was released from colonies with 10mM Tris base solution. The absorbance of aliquots from each well of a 6-well plate (200 µl) was measured by photospectrometry (540 nm).

For the low cell density survival assay, cells were seeded at 500 cells/100µL (1562/cm^2) in 96-well plates and treated with 3-AP (DMSO control or 2,500nM) for 16h, irradiated (control, 2Gy and 4Gy), then media with 3-AP and DMSO control was removed and replaced with fresh media. Cells were fixed 14d later, stained, and analyzed following the SRB Cell Cytotoxicity Assay protocol (G-Biosciences, #786-21) [248]. Absorbance was measured with Varioskan LUX microplate reader (ThermoFisher

Scientific). *Cell cycle analysis.* Cell cycle analysis was performed with a Cell Cycle Kit (Beckman Coulter, C03551). Cells were seeded at 800,000 cells/2 mL in 6-well plates overnight and treated with 3-AP (DMSO control or 2,500 nM) for 16h (n=4). Cells were then fixed with 70% ethanol at 4°C overnight, and stained for analyses as described in the manufacturer's protocol [249]. Propidium iodide fluorescence intensity was analyzed with a Becton Dickinson FACSymphony cell sorter (Becton Dickinson FACS Systems, Sunnyvale, CA) in the Flow Cytometry and Immune Monitoring Core at the University of Kentucky. Cell cycle was analyzed by ModFit LT™ Cell Cycle Analyses Software Version 2.0 (Verity Software House Inc., West Lafayette, IN).

3.3.11 Annexin V FIT-C apoptosis assay

Annexin V FIT-C apoptosis assay was performed with a FIT-C Annexin V Apoptosis Detection Kit with Propidium Iodine (Biolegend, 640914). Cells were seeded at 800,000 cells/2mL in 6-well plates and treated with 3-AP (DMSO control or 2,500nM) for 16h, irradiated, then incubated in fresh medium for 96h. Cells were collected and analyzed via flow cytometry as described above and in the manufacturer's protocol [250]. Data were analyzed by BD FACSDiva™ Software Version 9.1 (BD Bioscience, San Jose, CA).

3.3.12 BON Xenograft mice model

The NOD.Cg-*Rag1*^{tm1Mom} *Il2rg*^{tm1Wjl}/SzJ strain, immunodeficient mice with a recombination activation gene 1 mutation and a complete null receptor common gamma chain, was obtained from the Jackson Laboratory (Strain #:007799; 8 wks) and housed in a clean, pathogen-free room with controlled temperature (27°C), humidity, and a 12h

light/dark cycle. The mice were fed standard chow and tap water ad libitum and allowed to acclimate for 1 wk. All animal experiments were approved by the Institutional Animal Care and Use Committee at the University of Kentucky and conducted in accordance with guidelines issued by the National Institutes of Health (NIH) for the care of laboratory animals.

BON tumor cells were implanted subcutaneously (s.c.) by methods previously described [251]. After recovery from the implantation procedure and visible tumor (~1cm) observed, mice were randomized to the treatment groups. Mice in the experiment arm (n=5) received i.p. injection of 3-AP (10 mg/kg) daily for 5 days, 30 min before radiotherapy (4 Gy). Radiotherapy was administered in the first 3 days concurrently with 3-AP i.p. administration. Mice in the control arm (n=5) received i.p. injection of NS prior to radiotherapy. All mice were euthanized 24h after the last dose of 3-AP or NS injection. The tumors implanted in the left flank were retrieved en bloc for western blot as described above.

3.3.13 BON G-LungM3 mice model

The same NOD.Cg-*Rag1*^{tm1Mom} *Il2rg*^{tm1Wjl}/SzJ strain mice were used to establish the BON lung metastasis model. First, BON cells with stable expression of Green Fluorescent Protein (GFP) and firefly luciferase, trained to colonize lungs with high efficiency, were injected into mice intravenously (i.v.) via tail vein. Mice were anesthetized using isoflurane (3% in oxygen at 0.6 L/min flow rate), placed on a prewarmed (42°C) surgical bed and injected with cells (100 µl, 1×10^6 cells, PBS). Lung metastatic tumors were collected 90d after cancer cell injections for LungM1, 60d for LungM2 and 30d for LungM3. Collected tumor tissues were placed into serum free cell

culture media supplemented with 1X Gibco® Antibiotic-Antimycotic (15240-062; Life Technologies) for transportation. Metastatic tumors were minced and digested in liberase DH (50 µg/ml, 100 µl) and 0.5X collagenase/hyaluronidase (250 µl), diluted in 5 mL of McCoy5A serum free media for 4h at 37°C with gentle agitation. Digested cells were washed twice with complete cell culture media and transferred into 10% FBS McCoy5A media supplemented with 1X Gibco® Antibiotic-Antimycotic and 100 µg/ml Primocin (ant-pm-1; InvivoGen). Cells harvested from the first-generation mice were injected i.v. into the next generation of mice. The third-generation mice with lung metastatic cells, denoted as BON G-LungM3, were selected to establish the BON-cell lung metastasis model.

A total of 16 BON G-LungM3 mice were randomized to receive control (i.p. NS; no radiotherapy), 3-AP (i.p. 10mg/kg, every 48h, 3 treatments), radiotherapy (2 Gy, every 48h, 3 treatments), or combination modality (i.p. 10mg/kg 3-AP administered 30 min prior to radiotherapy, every 48h for a total of 3 treatments). One wk after cancer cell injection, mice were treated as defined by treatment groups (n=4). Four wks after cancer cells injections, mice were euthanized, and lung tissues were removed from mice to quantify metastatic burden by *ex-vivo* luciferase macroscopic optical imaging. The total bioluminescent emission intensity reflected remaining active disease in the tissues. Bioluminescent imaging was carried out using a Lago SII station (Spectral Instruments Imaging; Tucson, AZ). Composite images obtained were comprised of black and white digital photos with an overlay of images reflecting fluorescent activity. The density map, measured as photons/second/cm2/steradian (p/s/cm2/sr), was created using the Aura

software (Spectral Instruments Imaging; Tucson, AZ) and represented as a color gradient centered at the maximal spot.

3.3.14 Statistical analysis

IHC scores were summarized descriptively. Descriptive statistics (i.e., means and standard deviation) were presented in cell counting assays, cell cycle analyses, colorimetric proliferation assays, colorimetric cell survival assays, Annexin V FIT-C apoptosis assays, and GPF bioluminescence intensity of lung metastases, and displayed in bar graphs, pie charts and linear graphs. In the colorimetric proliferation assay, the ratio of absorbance relative to control (percentage of cell proliferation inhibition) was plotted against concentrations to generate the standard curves. The standard curves and absolute IC-50 values were calculated using SigmaPlot software version 14 (Systat Software Inc., San Jose, CA, USA). Comparisons of colorimetric proliferation assay, colorimetric survival assay, Annexin V FIT-C apoptosis assay, and GPF bioluminescence intensity of lung metastases were performed using one and two-way analysis of variance (ANOVA) with Holm's adjustment for multiple testing between groups. P-value <0.05 was considered to indicate a statistically significant difference. Statistical analyses were performed using SAS software version 9.4 (SAS Inc., Cary, NC, USA).

3.4 Results

3.4.1 RRM2 expression in pNET tumors

Increased RRM2 expression is associated with poor prognosis in various cancers [230-232]. We analyzed RRM2 expression in 36 pNET tumor samples by IHC. RRM2 expression was present in tumors with a spectrum of Ki-67 status (Figure 3-1A, 3-2).

Positive cytoplasmic staining was present in all tumor samples, while nuclear staining was present in 69% of tumors (Figure 3-1B). The elevated cytoplasmic expression of RRM2 in pNETs was designated as strongly positive in 69% of cases (score 5 or 6) and intermediate in 31% of cases (score 3 or 4). Nuclear staining was not only less abundant, but also weaker in intensity, with only 21% of cases stained strongly positive (score 5 or 6); 73% of samples had intermediate signal (score 3 or 4), and 8% stained weakly (score 2) (Figure 3-1C). RRM2 expression was also present in QGP-1 and BON xenograft tumors (Figure 3-3). RRM2 expression in vitro was strong in QGP-1 and BON cell lines, but nearly absent in NT-3 cells (Figure 3-1D). These findings demonstrate high protein expression levels of the RRM2 subunit in a majority of pNET patient samples, xenografts, and cell lines.

3.4.2 Role of RRM1, RRM2, and p53R subunits in QGP-1 and BON cells proliferation

To examine the role of RNR subunits in pNET cell proliferation, we utilized QGP-1 and BON cell lines with reliable expression of all RNR subunits. First, we established knockdown of RRM1, RRM2, and p53R2 subunits at 48 and 72h post transfection. RRM1 and RRM2 expression was markedly attenuated in QGP-1 and BON cells at both 48 and 72h, while p53R2 expression was significantly decreased at 72h in QGP-1 and at 48h in BON cells. The effect of p53R2 knockdown was still present, but less attenuated at 72h in BON cells (Figure 3-4A). Therefore, we could expect knockdown of RRM1, RRM2 and p53R2 to persist for 72h after siRNA transfection.

To determine the effect on cell proliferation, QGP-1 and BON cells with RRM1, RRM2 and p53R knockdown were counted at 48 and 72h after transfection. RRM2 knockdown resulted in a 32% and 58% reduction of cell counts compared to NTC control

at 72h in QGP-1 and BON cells, respectively. Similarly, RRM1 knockdown resulted in a 37% and 54% decrease in cell counts at 72h in QGP-1 and BON cells, respectively. However, knockdown of p53R2 demonstrated discrepant results with a non-significant increase in QGP-1 cells and a minor 21% decrease in BON cells at 72h (Figure 3-4B). These findings demonstrate that both RRM1 or RRM2 subunits play critical roles in RNR function, and RRM1 and RRM2 subunit knockdown reliably inhibit proliferation in both pNET cell lines. Conversely, the p53R2 subunit may not directly impact RNR activity since we did not observe a similar anti-proliferative effect with p53R2 knockdown.

Next, we tested the anti-proliferative effect of the selective RRM2 inhibitor, 3-AP, on QGP-1 and BON cells. A dose-dependent increase in percentage inhibition of cell proliferation was observed. The absolute IC-50 value, defined as 50% inhibition compared to control, was 1240nM and 1297nM for QGP-1 and BON cells, respectively. The fitted standard curves were sigmoid-shaped, with the maximum inhibitory effect plateau between 70-80% at approximately 2,500 nM in both cell lines (Figure 3-4C). The anti-proliferative effect of 3-AP is concordant with results observed after RRM2 subunit knockdown on pNET cells.

3.4.3 RRM2 inhibition activated DNA-PK and ATM pathways

DNA damage repair is a crucial mechanism of chemoresistance or radioresistance that is regulated by a complex network of DDR protein kinases, Ataxia Telangiectasia Mutated (ATM), Ataxia Telangiectasia and Rad3-related (ATR) and DNA-dependent Protein Kinase (DNA-PK) pathways [252]. Next, we examined how RRM2 inhibition affects DDR pathways in pNET cells. RRM2 knockdown resulted in increased phosphorylation of DNA-PK at the Ser2056 site and ATM at the S1981 site in both cell

lines. In contrast, we did not observe any change in ATR phosphorylation at the S428 site (Figure 3-5A). RRM2 inhibition by 3-AP showed concordant phosphorylation of DDR protein kinases and that 3-AP (2,500 nM) was adequate to induce phosphorylation of these DDR protein kinases in both cell lines (Figure 3-5B).

Phosphorylation of H2AX occurs rapidly in response to DNA damage and contributes to repair protein recruitment, checkpoint activation, cell cycle arrest and cell death. Here, we surveyed DDR in QGP-1 and BON cells after 3-AP treatment with confocal microscopy and observed strong phosphorylation of H2AX 48h after 3-AP treatment in both pNET cell lines (Figure 3-5C. Together, our results demonstrate that RRM2 inhibition decreases the deoxyribonucleotides pool available for DNA damage repair, and subsequently activates the DNA-PK and ATM pathways (Figure 3-5D).

3.4.4 RRM2 inhibition induced cell cycle arrest

RRM2 inhibition results in decreased proliferation in both QGP-1 and BON cells as demonstrated previously. Therefore, we examined important cell cycle checkpoint regulators, Chk1 and Chk2, and conducted cell cycle analyses to identify points of cell cycle arrest. First, we observed strong induction of Chk1 phosphorylation at the S345 site after RNR inhibition with 3-AP treatment in both cell lines (Figure 3-6A). We also observed phosphorylation of Chk2 at the T68 site after 3-AP treatment in both cell lines (Figure 3-6A). These findings demonstrate that both Chk1 and Chk2 pathways are both activated after RRM2 inhibition. Next, we analyzed colony survival after 3-AP inhibition in QGP-1 and BON cells. As shown in Figure 3-6B, 3-AP treatment significantly inhibited QGP-1 and BON colony formation; treatment of both cell lines resulted in >95% reduction in colony formation. RNR inhibition in pNET cells delays mitosis and

arrests the cell cycle progress in G1 phase (Figure 3-6C). Together, RNR inhibition by selective RRM2 inhibitor 3-AP or siRNA RRM2 knockdown decreases deoxyribonucleotide pool, which increases genomic instability and triggers DDR pathways, evidenced by phosphorylation of ATM and DNA-PK. DDR activation further results in cell cycle arrest and checkpoint activation. Simultaneously, decreased deoxyribonucleotide supply increases replication stress and synergistically causes cell cycle arrest at G1 phase, evidenced by decreased CD1 expression and increased Chk1 and Chk2 phosphorylation (Figure 3-6D).

3.4.5 RRM2 inhibition potentiated pNET cells radiosensitivity in vitro and in vivo

Next, we tested the hypothesis that RRM2 inhibition could enhance radiotherapy treatment of pNETs. First, RRM2 knockdown resulted in minimal PARP cleavage in both cell lines. Cells treated with 3-AP resulted in more PARP cleavage (c-PARP), thus apoptosis, compared to cells treated with RRM2 knockdown, in respective cell lines (Figure 3-7A&B). This could be due to the DNA-damaging property and mild cytotoxic effect of 3-AP [235]. Secondly, a radiation dose of 2 Gy minimally induced PARP cleavage, whereas 4 Gy was associated with strong increase of c-PARP expression in both cell lines (Figure 3-7A&B). Lastly, when RRM2 inhibition was combined with radiotherapy, c-PARP expression increased significantly compared to either radiotherapy or RRM2 inhibition alone, particularly in the 2 Gy combination group. This was additionally demonstrated in the Annexin V FIT-C apoptosis assays using BON cells, where combination treatment resulted in increased percentage of apoptotic cells compared to either radiotherapy or 3-AP treatments alone (Figure 3-8). These findings suggest that RRM2 inhibition potentiates radiotherapy, as noted by increased apoptosis in

pNET cells. We also performed colorimetric survival assays to investigate cell survival after combining 3-AP and radiotherapy. Not surprisingly, we observed a corresponding reduction of cell survival with either 3-AP or radiotherapy alone, and further reduction with the combination modality (Figure 3-7C). In summary, our findings demonstrate that RRM2 inhibition sensitizes pNET cells to DNA-damaging radiotherapy to induce apoptosis and reduce survival in vitro.

To further extend our in vitro findings we next examined the effect of RNR inhibition, in combination with 3-AP, on pNET radiosensitivity in vivo utilizing two animal models (i.e., a subcutaneous xenograft model and a novel lung metastasis model). The BON lung metastasis model was established as described above (Figure 3-9A). First, we determined whether combining radiotherapy with 3-AP could induce apoptosis in tumor xenografts. Mice were treated as previously described. Combining radiotherapy with 3-AP resulted in strong PARP cleavage compared to radiotherapy alone (Figure 3-9B). Next, we evaluated the effect of combining radiotherapy with 3-AP on BON lung metastases. Metastatic burden was reduced by 41% with 3-AP treatment compared to control. Radiotherapy reduced metastatic burden by 52% compared to control. Most impressively, metastatic burden was further reduced by 93% in the combination modality group, indicating a strong potentiation effect with the combination of 3-AP and radiation (Figure 3-9C). Together, the strong induction of PARP cleavage with the combination modality in both animal models demonstrate that selective RRM2 inhibition by 3-AP induces radiosensitivity and significantly increases metastatic pNET cell apoptosis. Therefore, we conclude that RRM2 inhibition is a valid strategy to induce

radiosensitization and that the selective RRM2 inhibitor, 3-AP, is a promising radiosensitizer in the treatment of metastatic pNET.

3.5 Discussion

Metastatic pNET can present as an aggressive disease with a poor prognosis [13]. The development of peptide receptor radionuclide therapy (PRRT) is considered a major advancement in the treatment of metastatic pNET [85, 226]. Implementation of a radiosensitizer is a valid strategy to further improve PRRT treatment effectiveness [85]. The current radiosensitizer, such as Everolimus, incurs a high rate of toxicity and warrants novel radiosensitizer agent used with PRRT [93]. RNR is an important therapeutic target in anti-cancer research, and RRM2 was found to have oncogenic properties with overexpression of RRM2 associated with a poor prognosis in various cancers [230-232]. Previous genomic analyses showed that overexpression of RRM2 was frequently present in pancreatic cancers; however, the study did not specify whether pNETs were included in the analysis [229]. Our study showed that pNETs have abundant and strong RRM2 expression, with a spectrum of Ki-67 proliferation status, suggesting that RRM2 is ubiquitously expressed and can serve as an effective therapeutic target in the treatment of pNETs. In this study, we explored the role of RRM2 inhibition in cell cycle progression, phosphorylation of DDR protein kinases, and radiosensitization of pNETs. We found that RRM2 inhibition resulted in phosphorylation of ATM and DNA-PK protein kinases and G1/S phase cell cycle arrest. Sensitization of pNETs by RRM2 inhibition, combined with DNA-damaging radiotherapy, significantly enhanced pNET cell death.

The DDR signaling pathways can be activated by ionizing radiation, oxidative and replication stress, resulting in cell cycle arrest, DNA repair, senescence, and apoptosis [253-256]. For instance, ATM phosphorylation is associated with radiation-induced DNA double-stranded break and the presence of reactive oxygen species [253]. Besides DNA damage, DNA-PK can be activated through DNA-independent protein-protein interactions, such as heat shock transcription factor 1 [256]. We observed an increased phosphorylation of ATM and DNA-PK with RRM2 inhibition in our study. RRM2 inhibition could result in the inactivity of RNR with decreased dNTPs available for DNA synthesis, leading to genomic instability and replication stress [257]. This could potentially explain phosphorylation of ATM and DNA-PK, though the specific mechanism of activation was not investigated in this study. Surprisingly, we did not observe any change in phosphorylation of ATR since single-stranded DNA break repair is often induced with replication stress during S phase [254]. We hypothesize that ATR activation is RRM2-independent, though the latter is a downstream effector of ATR activation.

RRM2 inhibition is known to induce cell cycle arrest in the late G1 and early S phases of the cell cycle, since the RRM2 subunit is differentially expressed during late G1 and S phases [258]. When DNA damage occurs, upregulation of RRM2 expression coordinates with the S phase checkpoint to facilitate DNA damage repair and recovery from replication stress by supplying sufficient deoxyribonucleotides [257]. In response to genotoxic stress, such as decreased dNTP pool, Chk1 and Chk2 are phosphorylated to induce cell cycle arrest [259]. Previously, Chk1 and Chk2 were thought to be closely associated with ATR and ATM activation, respectively [260, 261]. However, recent

study suggests that activation of Chk1 could be an independent process [262]. In our study, we observed increased Chk1 phosphorylation without a change of ATR phosphorylation status with RRM2 inhibition. This finding is consistent with a recent study by Corrales-Guerrero et al. [262] demonstrating Chk1-dependent RRM2 upregulation in glioblastomas after RRM2 inhibition.

Ionizing radiation causes DNA damage and results in prolonged autophagy, cell cycle arrest, DNA damage repair, and programmed cell death if not repaired successfully [223]. In this study, we tested the hypothesis that RRM2 inhibition sensitizes DNA-damaging radiotherapy to further enhance apoptosis. Here, we propose a plausible mechanism of radiosensitization through RRM2 inhibition. First, RRM2 inhibition causes cell cycle arrest in relatively radiosensitive late G1 phase prior to entering S phase, and cells are more likely to sustain lethal DNA damage from ionizing radiation. Next, RRM2 inhibition decreases the dNTP pool available for DNA damage repair, thus further contributing to genomic instability. Concurrently, DDR protein kinases, ATM and DNA-PK, are already activated after RRM2 inhibition prior to sustaining significant DNA damage. Cells, which are already under significant replication and repair stress, are prompted to undergo programmed cell death after sustaining radiation-induced DNA damage. Our results support our proposed mechanism of radiosensitization and exhibit induction of apoptosis with this combination modality. Notably, we utilized two animal models to demonstrate efficacy in the treatment of both xenograft tumors and lung metastases. Our results have significant translational value in the treatment of metastatic pNETs.

There are several limitations of this study. First, one active research area is the role of p53R2 in RNR activity and its potential as a therapeutic target. However, we are limited by the number of pNET cell lines available for in vitro experiments, and the two cell lines utilized in our study are both p53-mutant. Thus, we were not able to adequately evaluate the radiosensitization property of this RRM2 isoform. Also, we observed DDR pathway activation with RRM2 inhibition, especially phosphorylation of DNA-PK with RRM2 inhibition, which has not been reported previously. However, little is known regarding the pathway leading up to protein kinase phosphorylation. These results are intriguing and deserve attention in future studies.

In summary, RRM2 inhibition produces a profound anti-proliferative effect in pNET cells and activates DDR, specifically the ATM and DNA-PK pathways, resulting in cell cycle arrest during the radiosensitive late G1 phase. RRM2 inhibition potentiates radiotherapy and results in increasing apoptosis through the DDR signaling cascade. We conclude that RRM2 inhibition is an important therapeutic target and 3-AP may serve as a potential radiosensitizer to enhance radiotherapy efficacy in the treatment of metastatic pNET tumors.

3.6 Acknowledgements

We thank Donna Gilbreath from the Markey Cancer Center (MCC) Research Communications Office for manuscript preparation; the Flow Cytometry and Immune Monitoring, Biospecimen Procurement and Translational Pathology and Biostatistics and Bioinformatics Shared Resource Facilities of the MCC (supported by National Cancer Institute grant P30 CA177558). This study was further supported by the NIH National

Center for Advancing Translational Sciences (grant number UL1TR001998) and GI Cancer and Radiopharmaceutical Alliance grants from the University of Kentucky College of Medicine and MCC. Dr. Zeta Chow was supported by an NIH postdoctoral training grant T32 CA160003. The content is solely the responsibility of the authors and does not necessarily represent the official views of the NIH.

3.7 Citations

1. Chow, Z., Johnson, J., Chauhan, A., Izumi, T., Anthony, L., Townsend, C. M., ... & Rychahou, P. (2021). Abstract PO-014: 3-Aminopyridine-2-carboxaldehyde thiosemicarbazone (3-AP): A promising radiochemotherapy for gastroenteropancreatic neuroendocrine tumors. Clinical Cancer Research, 27(8_Supplement), PO-014.
2. Chow, Z., Johnson, J., Chauhan, A., Izumi, T., Cavnar, M., Weiss, H., ... & Rychahou, P. (2022). Inhibition of Ribonucleotide Reductase Subunit 2 (RRM2) Induces Radiosensitization in Gastroenteropancreatic Neuroendocrine Tumors. International Journal of Radiation Oncology, Biology, Physics, 114(3), S160.

Table 3-1 Primary and secondary antibodies used for IHC and western blot analysis

Primary Antibodies	Catalog Number	Concentration
RRM1 (A-10)	SC-377415	1:1000
RRM2 (A-5)	SC-398294	1:1000
p53R2 (F-9)	SC-376973	1:1000
ATM (D2E2) rabbit mAb	2873S	1:1000
pATM (S1981) (D25E5) rabbit mAb	13050S	1:1000
ATR rabbit mAb	2790S	1:1000
pATR (S428) rabbit mAb	2853S	1:1000
DNA-PK	ab70250	1:1000
pDNA-PKcs (S2056) rabbit mAb	056344	1:1000
Chk-1 (2G1D5) mouse mAb	2360S	1:1000
pChk-1 (S345) (133D3) rabbit mAb	2348T	1:1000
Chk-2 antibody	2662	1:1000
pChk-2 (T68) (C13C1) rabbit mAb	2197T	1:1000
Recombinant anti-cyclin D1	ab134175	1:5000
Total PARP	9542	1:1000
Cleaved PARP (Asp 214) (D64E10) XP rabbit mAb	5625	1:1000
GADPH (14C10) rabbit mAb	2118	1:1000
β-actin (8H10D10) mouse mAb	3700	1:5000
Secondary Antibodies		
Mouse anti-rabbit IgG-HRP	SC-2357	1:5000
M-IgGk BP-HRP	SC-516102	1:5000

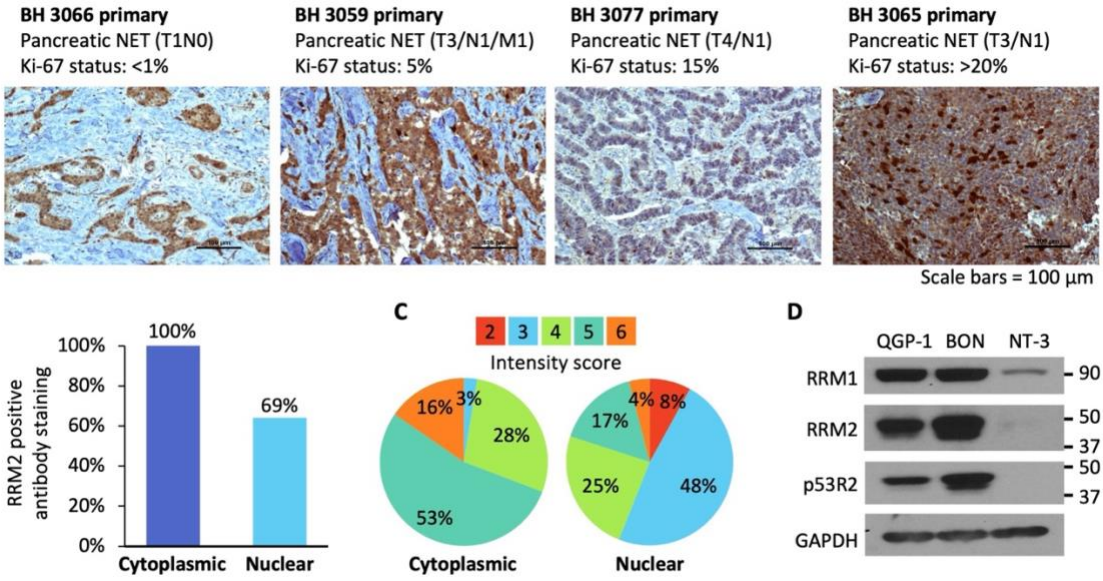

Figure 3-1 RRM2 expression in pNET patient tumor samples and pNET cell lines
(A) RRM2 IHC staining of pNET patient tumor samples (n=36). RRM2 expression was present in a spectrum of Ki-67 status, from low (<1%) to high (>20%) Ki-67 positive pNET tumors. (B) Analysis of RRM2 cytoplasmic and nuclear expression in pNET patient tumor samples (n=36). (C) Analysis of RRM2 cytoplasmic and nuclear intensity in pNET patient tumor samples (n=36). (D) RRM1, RRM2 and p53R2 subunit expression in QGP-1, BON and NT-3 cells. GAPDH was used as loading control.

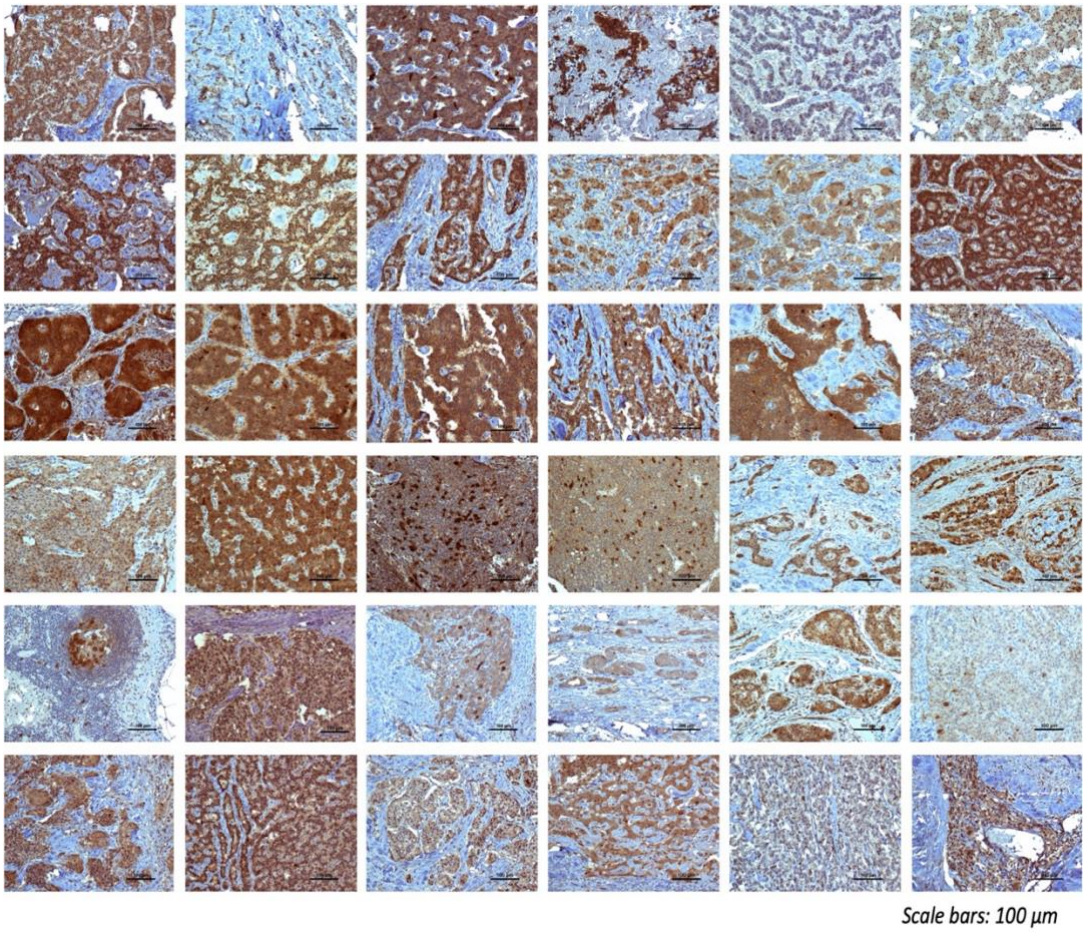

Figure 3-2 RRM2 expression by IHC staining in pNET patient samples (n=36)

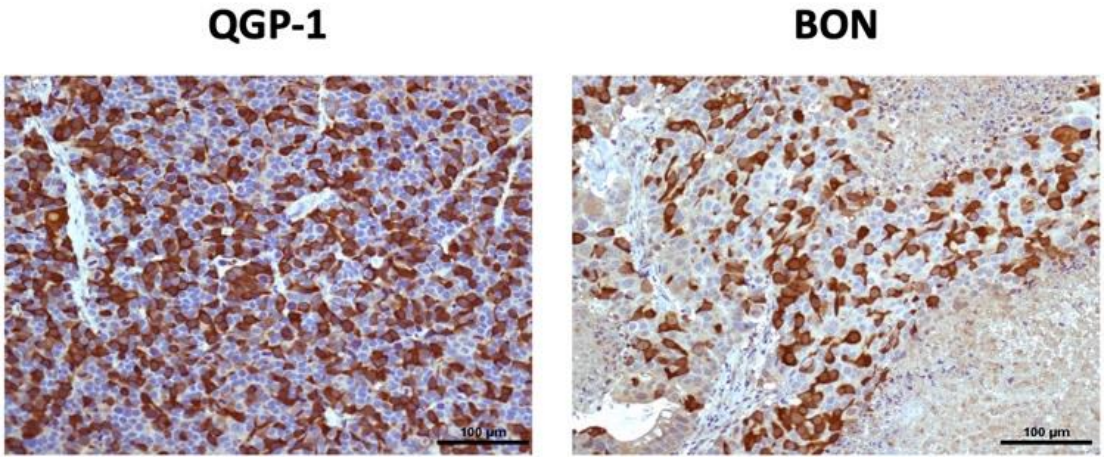

Figure 3-3 RRM2 antibody IHC staining in QGP-1 and BON xenograft model

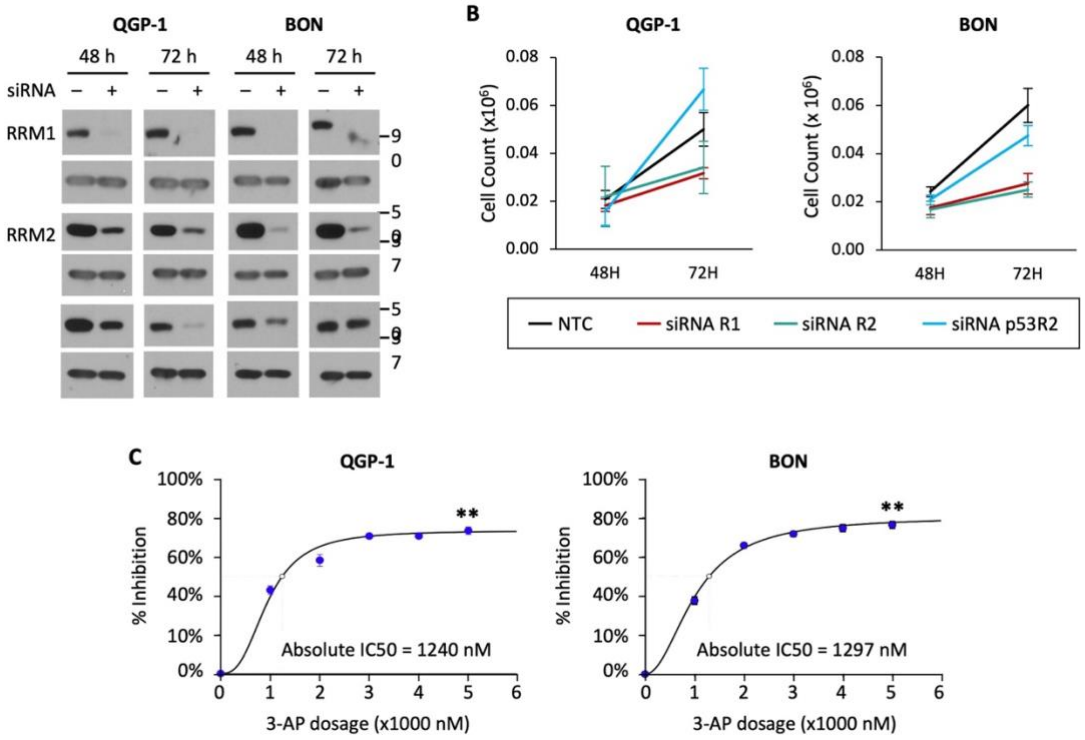

Figure 3-4 Inhibition of RRM2 inhibits cell proliferation

(A) siRNA knockdown in cell lines. QGP-1 and BON cells were transfected with NTC, RRM1, RRM2, and p53R2 siRNA. Cell lysate was collected 48 and 72h after transfection for WB analysis. (B) Cell counting assay. QGP-1 and BON cells were transfected and collected at 48 and 72h after siRNA transfection. The average numbers of cells and corresponding standard deviations per group were plotted at 48 and 72h. (C) Colorimetric proliferation assay. The percentage inhibition was determined as the ratio relative to control and plotted against concentrations to generate standard curves. Absolute IC50 was defined as concentration required to reduce cell density by 50%. ** denotes p-value < 0.0001.

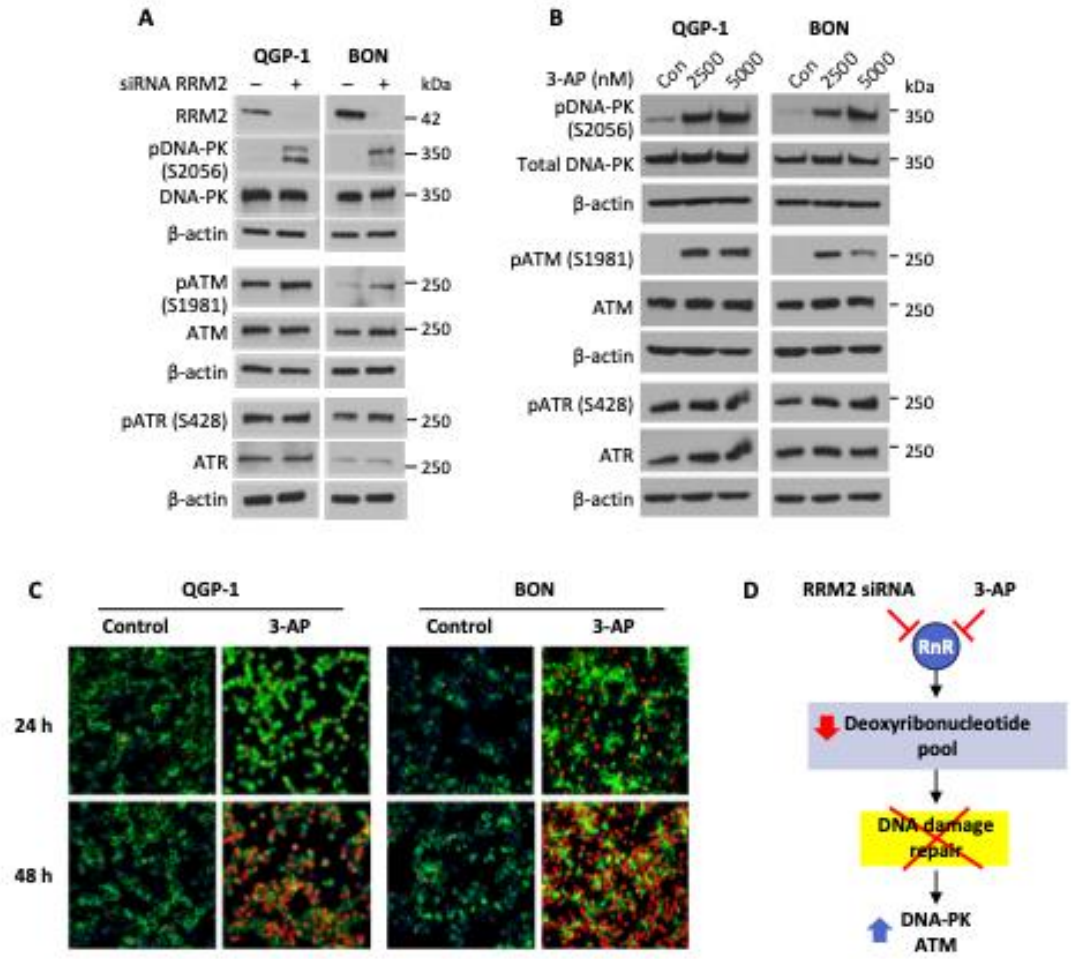

Figure 3-5 Inhibition of RRM2 increases phosphorylation of DNA-PK and ATM, but not ATR

(A) QGP-1 and BON cells were transfected with siRNA RRM2 and collected at 72 h post-transfection to examine the effect of RRM2 knockdown on DNA-PK, ATM and ATR activation. β-actin was used as loading control. (B) QGP-1 and BON cells were treated with 3-AP (2,500 or 5,000 nM) for 16 h prior to protein collection to determine effect of RNR inhibition on DNA-PK, ATM and ATR activation. β-actin was used as loading control. (C) QGP-1 and BON cells were treated with 3-AP for 24h and 48h (2500 nM) and analyzed for yH2AX expression by confocal microscopy (blue, Dapi, green, phalloidin; red, yH2AX). (D) Schematics for RRM2 inhibition and downstream signaling. RRM2 siRNA and 3-AP inhibit RNR activity, which resulted in decreased deoxyribonucleotide pool available for DNA damage repair and phosphorylation of DNA-PK and ATM pathways.

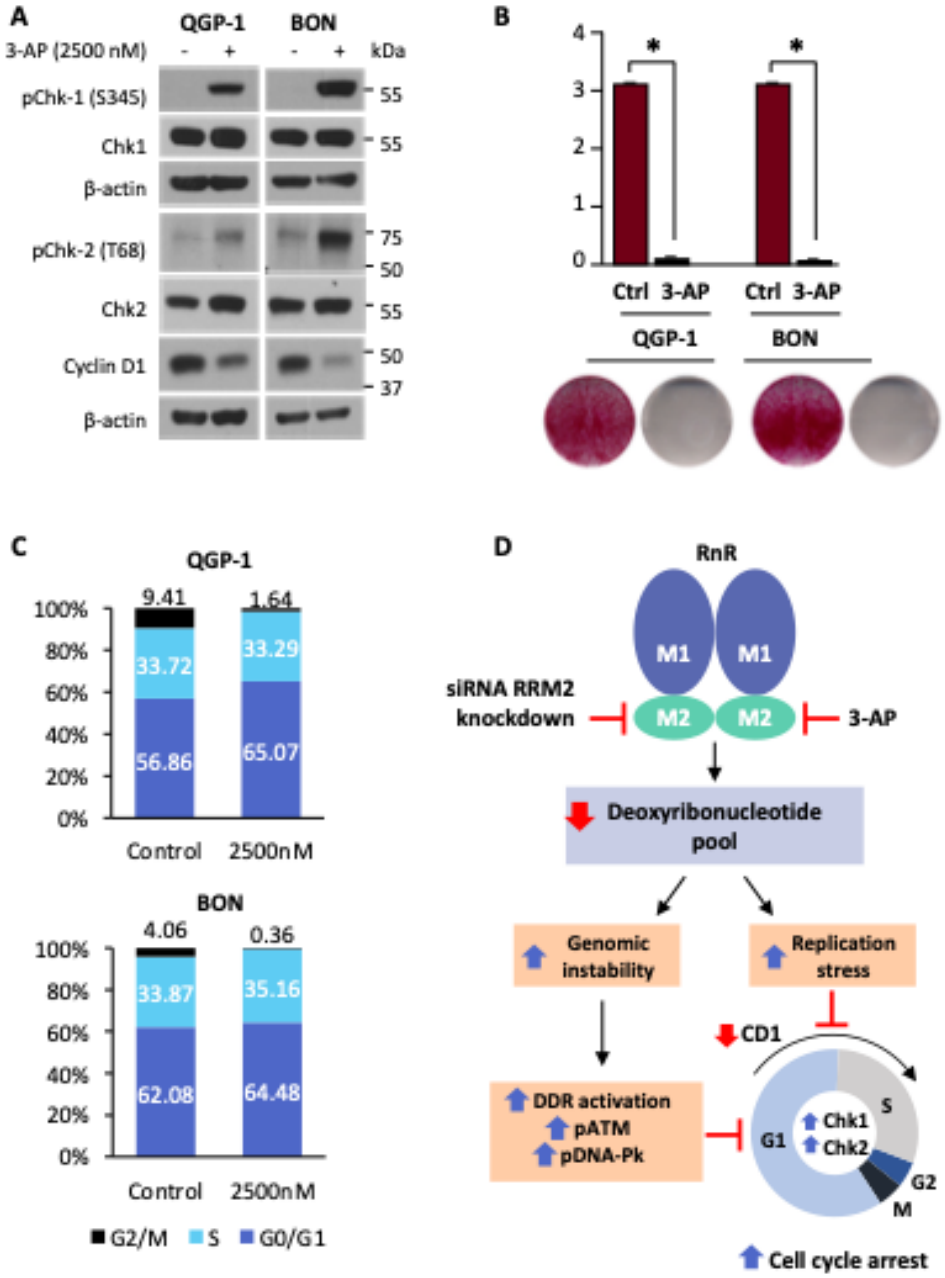

Figure 3-6 RNR inhibition by 3-AP induces cell cycle arrest at G1/S phase

(A) QGP-1 and BON cells were treated with 3-AP (2,500 nM) for 16 h for cell cycle arrest markers, pChk-1, pChk-2, p-cdc-2 and cyclin D1. β-actin was used as loading control. (B) Colony formation was assessed with clonogenic assay in QGP-1 and BON cells (6-well plate; 1000 cells, 14d) treated with 2500 nM 3-AP. (C) Cell cycle analyses. QGP-1 and BON cells (n=4) were treated with 3-AP (2,500 nM) for 16 h, then collected, fixed, stained and analyzed via flow cytometry. The average percentages of cells in G0/G1, S, and G2/M phase were quantified, plotted and labeled as bar graphs in each group. (D) Schematic of RNR inhibition on G1/S phase cell cycle arrest.

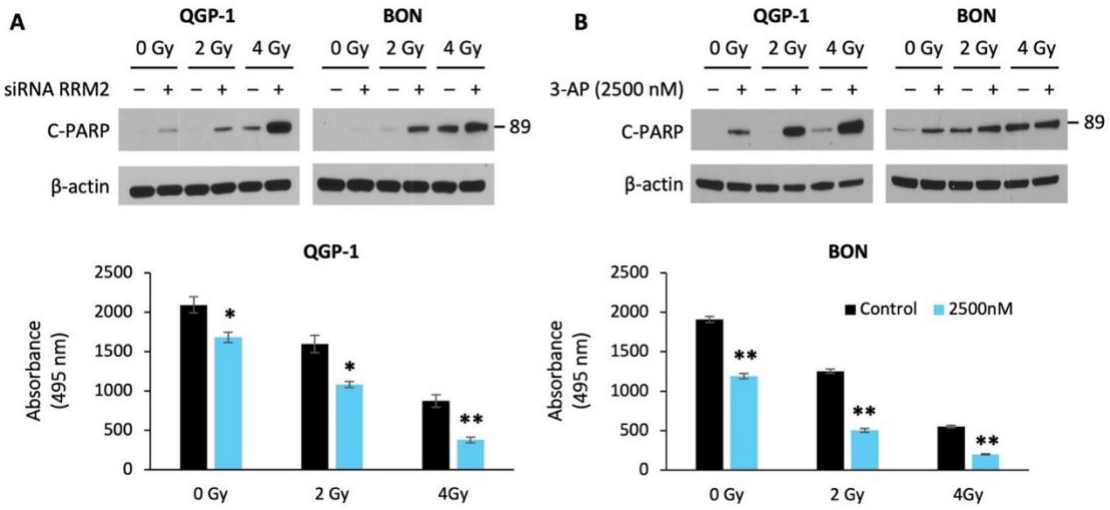

Figure 3-7 RNR inhibition enhances apoptosis with radiotherapy in vitro

(A) QGP-1 and BON cells were transfected with either NTC or siRNA RRM2, irradiated 72h post-transfection (control, 2 or 4 Gy), incubated in fresh medium for 96 h prior to WB analysis for c-PARP expression. β-actin was used as loading control. (B) QGP-1 and BON cells were treated with 3-AP (DMSO control or 2,500 nM) for 16h, irradiated (2 or 4 Gy), incubated in fresh medium for 96h before WB analysis for c-PARP expression. β-actin was used as loading control. (C) Colorimetric cell survival assay. QGP-1 and BON cells (n=6) were treated with 3-AP (DSMO control or 2,500 nM) for 16h, followed by irradiation (control, 2 or 4 Gy), and incubated in fresh medium for 14 days before quantification. The average absorbance at 495 nm and its standard deviations were compared and plotted against radiation doses. * Denotes p-value < 0.05; ** p-value <0.0001.

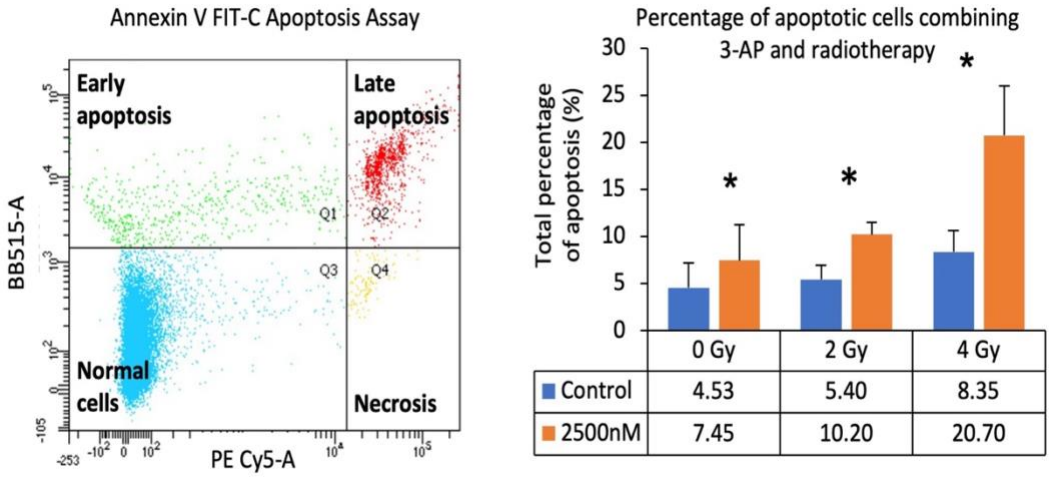

Figure 3-8 Inhibition of RRM2 by 3-AP potentiates radiotherapy to induce apoptosis
BON cells were treated with 3-AP (DMSO control or 2,500 nM) for 16h, followed by irradiation (control, 2 or 4 Gy), and incubated in fresh medium for 96h. Cells were then analyzed and quantified via flow cytometry. Q1, Q2, Q3, Q4 represent early apoptosis, late apoptosis, normal cell, and necrosis. The percentage of total apoptosis consisted of both early and late apoptosis. * denotes p-value <0.05.

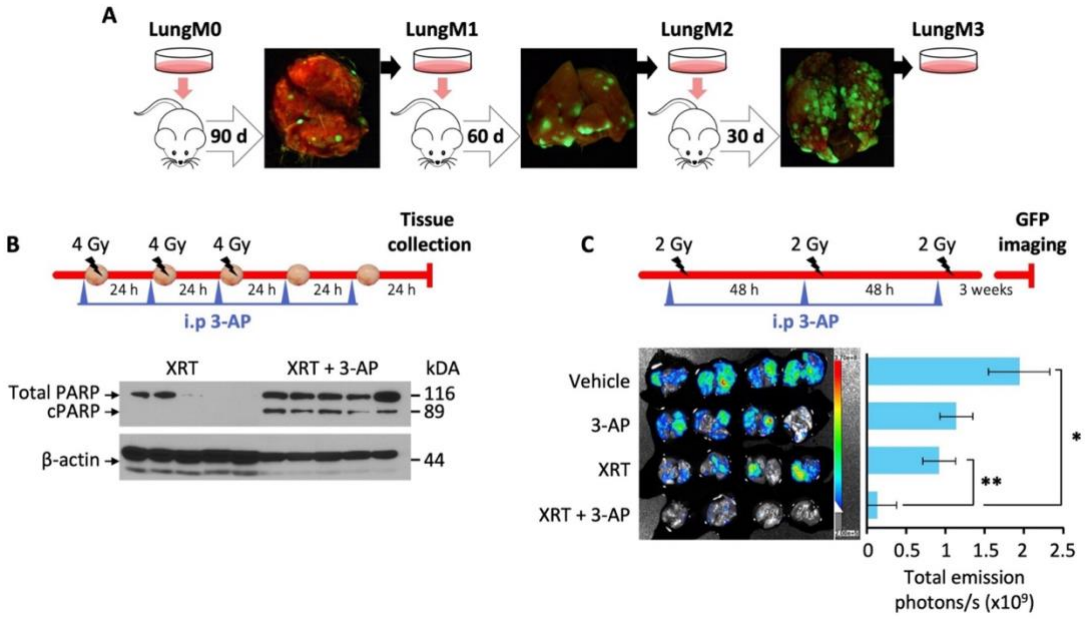

Figure 3-9 RNR inhibition enhances radiation therapy against pNETs in vivo

(A) Mice were injected with BON G-LungM0 cells ($1x10^6$; 100 µl), metastatic tumors were isolated from lungs 90 days later and enzymatically digested to establish BON G-L LungM1 cell line. The process was repeated until BON G-L LungM3 cell line establishment. (B) Mice (n=5) with subcutaneous BON xenografts were treated with i.p injection of 3-AP (10 mg/kg; daily) and irradiated (4 Gy q24h, first 3d). Tumors were collected 24h after last 3-AP treatment and protein lysate was analyzed by western blot for cleaved PARP. β-actin was used as loading control. (C) Mice (n=4) were injected i.v with BON G-L LungM3 cells ($1x10^6$; 100 µl); 7d later, mice were treated with 3-AP (i.p; 10 mg/kg) 30 min before irradiation and irradiated (2 Gy, q48h). Lung metastasis burden was evaluated and quantified with *ex-vivo* GFP imaging. The average emission densities and standard deviations of each group were plotted. * Denotes p-value < 0.05; ** p-value <0.0001.

CHAPTER 4. CONCLUSIONS

4.1 How to choose a radiosensitizer

The radiosensitizers used in clinical trials are cytotoxic chemotherapy agents that also possess radiosensitizing property. Everolimus has shown to potentiate radiotherapy effect in NET cell lines[91]. Capecitabine is used as a radiosensitizer for concurrent neoadjuvant chemoradiation in treating locally advanced rectal cancer[263-265]. Temozolomide is used concomitantly with daily EBRT in treating glioblastoma[266]. Out of the three regimens, CAPTEM produced the best radiosensitization effect when combined with PRRT in treating metastatic GEP-NETs, particularly in pNET patients. The 2-year survival was a stunning 97% and median PFS was 48 months[85]. It not only induced a high 67% PR, but also achieved 13% CR, thus an ORR of 80%. This is compared superior to the 1% CR, 17% PR, and 18% ORR in the PRRT arm of the landmark NETTER-1 study[55, 85]. This treatment regimen has significantly extended patient survival compared to the SEER database for metastatic GEP-NETs decades ago. Retrospective study has also suggested that CAPTEM is an effective radiosensitizing regimen when combined with PRRT, achieving 38-55% disease control and median PFS of 25 months in the population that had failed multiple lines of treatments[267]. In addition, there are several on-going clinical trials investigating CAPTEM in treating metastatic GEP-NETs, including the first randomized phase II clinical trial CONTROL NET (NCT04194125, NCT05247905). Though the final manuscript is not available, preliminary analysis of the CONTROL NET suggests that PRRT/CAPTEM has durable treatment response and superior PFS in treating pNET patients and recommends phase III

clinical evaluation[268]. We patiently await results of these upcoming studies for potential practice changing recommendation.

One may notice that concurrent PRRT and CAPTEM did not work uniformly for all GEP-NETs and only showed superior radiosensitization in the pNET population. One study suggested that the difference could be due to the lack of MGMT enzyme in most pNET cells, while enteral NETs usually express high level of MGMT. Similar to Temozolomide in treating MGMT-methylated patients in glioblastoma, lack of MGMT enzyme in pNET allows temozolomide to alkylate DNA strands without prompt DNA repair, thus inducing greater DNA damage and instability with concurrent PRRT radiotherapy[85]. This highlights the importance to appropriately select radiosensitizer in GEP-NETs based on distinctive cell biology. GEP-NET is a heterogenous entity and harbors unique genetic mutation, and molecular biology based on specific cell type. For instance, insulinomas have very unique genomic features compared to other types of pNETs with gain-of-function mutations in the Yin Yang 1 (YY1) gene in 30% of samples[269]. Small bowel carcinoids are characterized by global DNA hypomethylation, which also predicts clinical aggressiveness[270]. Poorly differentiated neuroendocrine carcinomas exhibit loss of retinoblastoma (Rb) and mutations of Kirsten rat sarcoma viral oncogene homolog (KRAS) in half of patients, and these molecular alterations seem to predict response to platinum-based chemotherapy[271]. It is crucial to consider these unique genetic and molecular hallmarks when selecting the suitable radiosensitizer.

Another consideration in choosing a radiosensitizer is to ensure radiosensitization with the modality of radiotherapy. Majority of the radiosensitizer research was conducted

with EBRT and the concept of radiosensitization with PRRT was largely extrapolated from EBRT. There are fundamental differences between EBRT and PRRT, including the nature of ionizing radiation, dose rate, dose distribution and interval fractionations[272]. EBRT is produced artificially via a linear accelerator and delivers homogeneous, high-dose, and conformal photon (X-ray) radiation on a scheduled basis. On the other hand, PRRT delivers either α, β, or γ emitters intracellularly, and produces a relatively heterogenous, low dose and continuous radiotherapy throughout the decay period of the conjugated radioactive element[272]. The difference in radiobiology and kinetics can impact the effectiveness and delivery of a radiosensitizer. One study found that ^{177}Lu-DOTATATE exhibited delayed cytotoxic response, transient and low-level reactive oxygen species production, lack of H2A Histone Family Member X (H2AX)/Ataxia telangiectasia mutated(ATM) phosphorylation peak but prolonged γH2AX foci presence in human cell lines[272]. This implies that radiosensitizer should be given continuously fashion with PRRT rather than a single-dose exposure within hours of high-dose radiotherapy. When comparing different PRRTs, ^{225}Ac-DOTATATE, an α-particle radiolabel analog with higher linear energy transfer, induced greater double-strand DNA (dsDNA) break per cell, evidenced by higher fractions of cells expressing γH2AX foci compared to ^{177}Lu-DOTATATE, a primary β-particle emitter[273]. We could hypothesize that a radiosensitizer that impedes single-stranded DNA repair may not be effective when using α-particle PRRT that induces more dsDNA damage. Therefore, we not only have to identify a valid mechanism of radiosensitization in the GEP-NETs, but also select based on the appropriate radiobiology of the radiotherapy modality.

4.2 On-going clinical trials

In addition to the prospective trials reviewed in this article, clinical trials are actively being recruited round the world as PRRT gains more ground in clinical practice. Besides the combination therapies mentioned previously, other agents currently being evaluated in clinical trials include PARP inhibitors (i.e., Olaparib, NCT05870423, NCT05053854, NCT04375267, NCT04086485), tyrosine kinase inhibitors (i.e., Suntinib, NCT05687123; Cabozantinib, NCT05249114, NCT04893785), immune checkpoint inhibitors (i.e., Pembrolizumab, NCT03457948; Nivolumab, NCT04525638), and DNA repair enzyme inhibitors (i.e., Triapine, NCT04234568, NCT05724108; Peposertib, NCT04750954) (Table 4-1). Moreover, there are abundant preclinical studies evaluating potential radiosensitizing agents in NETs, such as the Heat Shock Protein 90 (HSP90) inhibitor [264], Phosphoinositide-3-kinase/mTOR dual inhibitor [234], topoisomerase inhibitor [265], and smoothened antagonist [266]. Out of these potential radiosensitizers, the strategy to prevent DNA damage repair appears promising, such as the PARP inhibitor and DNA-PK inhibitors. The PARP inhibitor, Olaparib, has shown a synergistic radiosensitization effect in multiple human NET cell lines [267, 268]. DNA-PK inhibitor, AZD7648 has also shown significant potentiation in treating neuroendocrine tumor cells in vitro and in vivo [269]. These radiosensitizers have also entered phase I/II clinical trials in treating NETs.

4.3 Challenges in GEP-NET radiosensitizer research

There are several challenges in GEP-NET research. First, GEP-NET is a rare cancer that makes up only 2% of all gastrointestinal malignancy [1]. Recruitment in clinicals trial may be prolonged due to a lack of patient enrollment or require extensive

collaboration among multiple high-level referral centers and organizations. The largest prospective clinical trial reviewed in this article contained only 91 patients and took almost 4 years to complete patient enrollment [61]. Another example of phase III RADIANT-4 clinical trial enrolled over 300 patients from 97 centers across 25 countries worldwide [90]. Based on statistically powered prospective study, It will likely take years to make any practice changing recommendations. Second, current radiosensitizers used with PRRT or EBRT are mostly cytotoxic chemotherapy agents with significant toxicity. Everolimus, for instance, caused grade 1 and 2 gastrointestinal and hematological toxicities in almost all patients and dose-limiting grade 3 and 4 toxicities in 36% of patients, who ultimately required dose reduction or cessation of treatment [92, 93]. Patient tolerance of these agents could be a challenge, aside from the additional toxicity of radiotherapy. Third, GEP-NET is a highly diverse and complex entity with 14 different subtypes. Each of them possesses unique genetic variations and molecular biology [1]. Indeed, there is a common pathogenesis of GEP-NET, such as dysregulation of the mTOR pathway [2]. But more is needed to explain the differences in behavior and response to radiotherapy. The interaction between GEP-NETs and radiotherapy, either EBRT or PRRT, is still largely unknown and requires in-depth research to understand the underlying biology. The “one-fit-for-all” approach to select a radiosensitizer is likely unpractical due to the heterogeneity of GEP-NET.

4.4 Potential solutions and opportunities

Modern technology has gradually transformed basic and clinical translational science and provided answers to some challenges. Whole exome genomic sequencing has involved and becomes more readily available in clinical setting. Currently, the Next

Generation Sequencing (NGS), also known as massively parallel sequencing, allows researcher to sequence the entire genome within a single day [274]. National-wide initiative network in cancer research, such as the Oncology Research In Exchange Network Total Cancer Care program, has the capability to provide a large clinically-annotated genomic data. These novel technologies open the opportunity to acquire large amount of genome-wide information in relatively rare and heterogenous cancer, such as GEP-NETs. This can further facilitate the identification of therapeutic targets, even personalized radiosensitizers in treating these patients. Another rapidly progressing field in research and medicine is utilization of artificial intelligence (AI). It is not surprising that AI is quickly adapted and implemented in basic and clinical translational science research given its supreme power of massive data processing. For example, a trained AI algorithm can now accurately predict cancer diagnosis and prognosis in various cancers [275-277]. Deep machine learning and neural networks develop new paradigm to stratify patient treatment based on risk factors in prostate cancer [278]. AI is also at the frontier of basic and translational science, with the capability to identify genetic mutations, therapeutic targets, and new drugs for cancer treatment [279]. With its exponential growth and vast potential in research, it will not be long before AI could assist in identifying a personalized treatment option for inoperable, metastatic GEP-NETs, as illustrated in Figure 4-1.

4.5 Final thoughts

GEP-NET was once considered a rare entity and management for advanced-stage, metastatic disease was limited. With its increasing incidence and further understanding of the disease, GEP-NET research is now becoming more diversified. In this thesis, we

investigated two mechanisms of radiosensitization with X-ray radiation in GEP-NET tumors. This represents one unique research and approach to improve treatment efficacy and enhance the therapeutic ratio of radiotherapy among advanced-stage, metastatic GEP-NET patients. There are several underlying messages within this thesis that would provoke further discussions and new perspectives in understanding this complex subject.

Radiotherapy has not been a mainstay in treating GEP-NET for decades, and the utility of radiotherapy is limited under palliative settings. Palliative radiotherapy was primarily performed with external beam radiation, which is a type of artificial ionizing radiation utilizing X-ray photon energy. This is still being recommended as a treatment option for symptomatic focal lesions and currently practiced in clinical settings. Since the role of radiotherapy was extremely limited, the radiosensitizer research in GEP-NET was virtually non-existent. However, the landscape of GEP-NET treatment drastically changed since PRRT research has gained momentum and quickly taking center stage in the GEP-NET research. The treatment efficacy has been shown to be at least effective as other systemic treatments such as long-acting somatostatin analogs and systemic chemotherapy. The NETTER-1 clinical trial was a landmark study that established the role of PRRT in metastatic GEP-NETs. This brought much attention to implementing a systemic agent with radiosensitizing property to improve the efficacy of PRRT. We recognized that radiosensitizer research has a narrow, but important application.

The most common radioisotope used in the PRRT nowadays is Lutetium-177, a beta-emitter with a half-life of 6.7 days. It is considered a low linear energy transfer (LET) ionizing radiation and causes mostly single-strand sublethal DNA damage; and thus, radiation response follows the linear-quadratic survival model for tumor cell kill.

Therefore, the concept of radiosensitization can be applied here to either increase susceptibility of DNA damage or impair DNA repair to induce more synthetic lethality from radiotherapy. A radiosensitizer could ideally enhance the therapeutic ratio between tumor and normal tissue by inducing either one of the mechanisms mentioned above. This forms the basis for all the radiosensitizers research, and thus has several limitations.

The concept of radiosensitization applies mostly with low LET ionizing radiation. If a newer generation with high-LET of isotope, such as Actinium-225, was used instead, the same concept would no longer be valid. These radioisotopes are alpha emitters, which primarily cause lethal double-stranded DNA damage. The radiation response curve, thus exhibits a predominantly linear relationship with a given dose. The radiation modality is also likely going to change. As we have seen in recent years, Stereotactic Body Radiotherapy (SBRT) or hypofractionated regimen has been utilized more frequently in the clinical setting. High-dose rate ionizing radiotherapy also operates on the linear portion of cell survival curve and similar to the concept of high LET ionizing radiotherapy. Heavy ion therapy, such as proton, neutron and carbon ion, are currently being researched and can be applied in clinical setting as well. These modalities will depend less on synthetic lethality, thus the topic of concurrent radiosensitization would not apply.

However, it does not mean that there are no other mechanisms to function synergistically with these newer modalities. The radiosensitizer research still demand much attention, though the definition and concept of radiosensitization would have to evolve over time. For instance, it was theorized that immunotherapy could induce bystander or Episcopal effect with high-dose-rate radiotherapy. Though, not a direct

radiosensitizer, immunotherapy or targeted therapy could induce more tumor antigen responses to achieve synergy when combined with radiotherapy. The bottom line is, there has to be a feasible underlying radiobiology to support the concept of radiosensitization or proposed mechanism of induced cell kills, instead of simply combining a cytotoxic agent with any modality of radiotherapy.

Another consideration and also evolving concept that this thesis has explored on is the schedule-dependence of radiosensitization. Traditionally-speaking, a radiosensitizer is administered to a therapeutic dose at the time of radiotherapy. However, this might not be necessary considering the radiobiology of cells. As mentioned in Chapter II of this thesis, PFO exhibited a schedule-dependent effect post-radiotherapy instead of concurrently with radiotherapy, indicating that PFO primarily works in preventing DNA damage repair and cellular survival, which occurs hours to days later after radiotherapy. By minimizing exposure to these cytotoxic systemic treatments, we could potentially mitigate side effects when combing a radiosensitizer and radiotherapy. Therefore, it is not only important to know "what and how" to sensitize, but also to know "when" when the biological events occur in the context of radio-sensitization. This is extremely crucial for researchers to design a safe and tolerable treatment regimen.

Last, but not least, personalization has been a profound topic for many areas of research. We have realized that tumor behaves differently on an individual level. In addition, we now have harbored the tools to examine and utilize this information efficiently. Clinical practice has shifted towards a more individualized approach and there is no doubt that radiosensitizer research will soon follow the suit. So far, we have seen biology-directed radiosensitizer research in other malignancies, but not in GEP-NET.

Genetics is likely going to play a major role in driving the future of radiosensitizer research.

In summary, radiosensitization research has a narrow, but important implication to improve treatment efficacy in managing advanced-stage, metastatic GEP-NET patients. We have witnessed the rapid development of many innovative radiosensitizers and continues to discover novel concepts to advance the field of GEP-NET research. The notion of radiosensitizer is likely going to evolve over time as our knowledge and technology advances. The future generation of radiosensitizer is going to be safe, effective, and personalized.

Table 4-1 On-going clinical trials combining a radiosensitizing agent with PRRT

Therapeutic agents	Reference number[e]	Phase	Status
Capectaibine	NCT02736448	II	Unknown
	NCT02358356	II	Completed, not yet reported
	NCT02736500	I/II	Unknown
CAPTEM[a]	NCT04194125	II	Unknown
	NCT05247905	II	Recruiting
Everolimus	NCT02205515	I/II	Completed, not yet reported
PARP[b] inhibitor	NCT05870423	I	Recruiting
	NCT05053854	I	Recruiting
	NCT04375267	I	Unknown
	NCT04086485	I/II	Recruiting
Sunitinib	NCT05687123	I	Recruiting
Cabozantinib	NCT05249114	I	Recruiting
Cabozantinib/TMZ[c]	NCT04893785	II	Recruiting
Pembrolizumab	NCT03457948	II	Recruiting
Nivolumab	NCT04525638	II	Recruiting
ASTX727[d]	NCT05178693	I	Recruiting
Triapine	NCT04234568	I	Active
	NCT05724108	II	Recruiting
Peposertib	NCT04750954	I	Recruiting

a, Capecitabine and Temozolomide combination treatment; b, Poly(ADP-ribose) polymerase; c, Temozolomide; d, fixed dose Decitabine and Cedazuridine compound; e, reference number as recorded per www.clinicaltrials.gov.

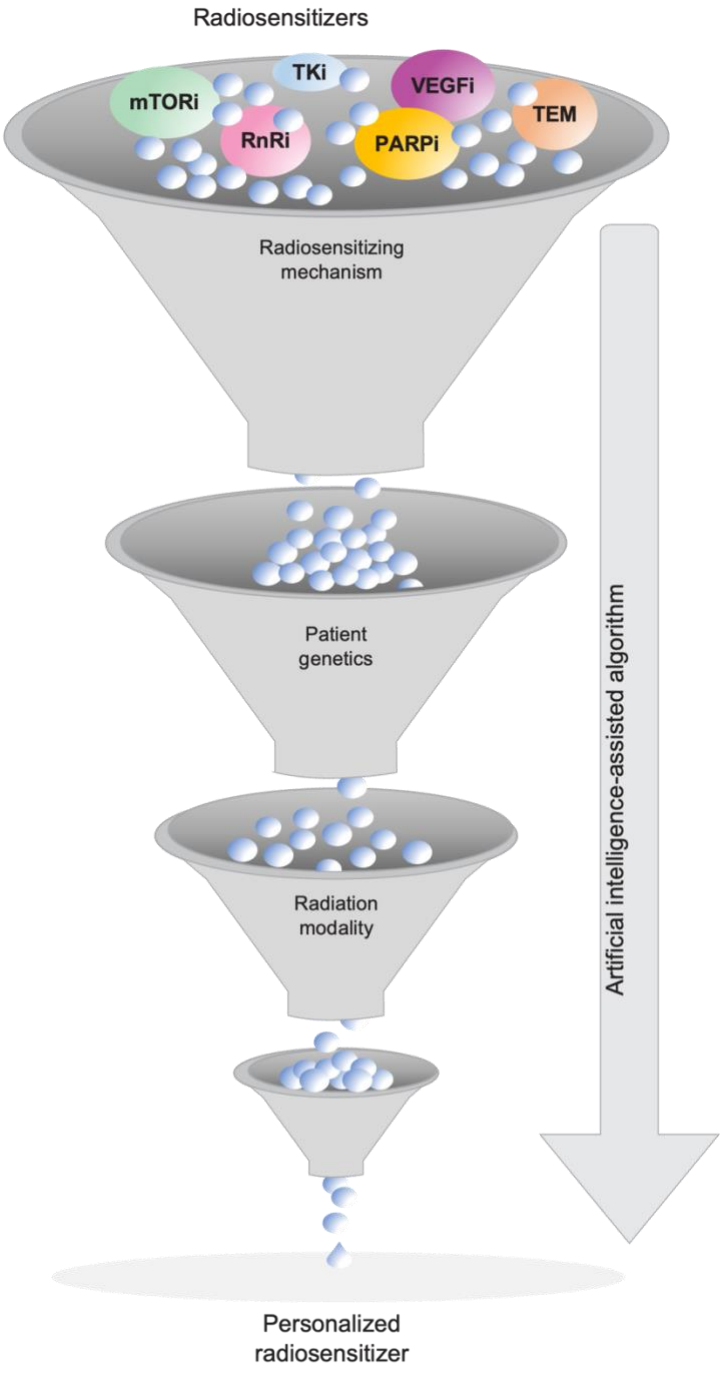

Figure 4-1 Schematics of utilizing artificial intelligence to identify a personalized radiosensitizer

REFERENCES

1. Modlin, I.M., et al., *Gastroenteropancreatic neuroendocrine tumours.* The lancet oncology, 2008. 9(1): p. 61-72.
2. Cives, M. and J.R. Strosberg, *Gastroenteropancreatic neuroendocrine tumors.* CA: a cancer journal for clinicians, 2018. 68(6): p. 471-487.
3. Vortmeyer, A.O., et al., *Non-islet origin of pancreatic islet cell tumors.* The Journal of Clinical Endocrinology & Metabolism, 2004. 89(4): p. 1934-1938.
4. Díez, M., A. Teulé, and R. Salazar, *Gastroenteropancreatic neuroendocrine tumors: diagnosis and treatment.* Annals of Gastroenterology: Quarterly Publication of the Hellenic Society of Gastroenterology, 2013. 26(1): p. 29.
5. Schimmack, S., et al., *The diversity and commonalities of gastroenteropancreatic neuroendocrine tumors.* Langenbeck's archives of surgery, 2011. 396: p. 273-298.
6. Cives, M. and J. Strosberg, *The expanding role of somatostatin analogs in gastroenteropancreatic and lung neuroendocrine tumors.* Drugs, 2015. 75: p. 847-858.
7. Kanakis, G. and G. Kaltsas, *Biochemical markers for gastroenteropancreatic neuroendocrine tumours (GEP-NETs).* Best practice & research Clinical gastroenterology, 2012. 26(6): p. 791-802.
8. Wiedenmann, B., et al., *Synaptophysin: a marker protein for neuroendocrine cells and neoplasms.* Proceedings of the National Academy of Sciences, 1986. 83(10): p. 3500-3504.
9. Scarpa, A., et al., *Whole-genome landscape of pancreatic neuroendocrine tumours.* Nature, 2017. 543(7643): p. 65-71.
10. Jiao, Y., et al., *DAXX/ATRX, MEN1, and mTOR pathway genes are frequently altered in pancreatic neuroendocrine tumors.* Science, 2011. 331(6021): p. 1199-1203.
11. Banck, M.S., et al., *The genomic landscape of small intestine neuroendocrine tumors.* The Journal of clinical investigation, 2013. 123(6): p. 2502-2508.
12. Terris, et al., *Expression of vascular endothelial growth factor in digestive neuroendocrine tumours.* Histopathology, 1998. 32(2): p. 133-138.
13. Xu, Z., et al., *Epidemiologic trends of and factors associated with overall survival for patients with gastroenteropancreatic neuroendocrine tumors in the United States.* JAMA Network Open, 2021. 4(9): p. e2124750-e2124750.
14. Dasari, A., et al., *Trends in the incidence, prevalence, and survival outcomes in patients with neuroendocrine tumors in the United States.* JAMA oncology, 2017. 3(10): p. 1335-1342.
15. Whipple, A.O., *Islet cell tumours of pancreas.* Canadian Medical Association Journal, 1952. 66(4): p. 334.
16. van Beek, A.P., et al., *The glucagonoma syndrome and necrolytic migratory erythema: a clinical review.* European journal of endocrinology, 2004. 151(5): p. 531-537.
17. Jensen, R.T., *Gastrinoma.* Baillière's clinical gastroenterology, 1996. 10(4): p. 603-643.
18. Krejs, G.J., *VIPoma syndrome.* The American Journal of Medicine, 1987. 82(5): p. 37-48.

19. Öberg, K., *Management of functional neuroendocrine tumors of the pancreas.* Gland Surg, 2018. 7(1): p. 20-27.
20. Strosberg, J.R., et al., *Prognostic validity of the American Joint Committee on Cancer staging classification for midgut neuroendocrine tumors.* Journal of clinical oncology, 2013. 31(4): p. 420-425.
21. Waisberg, J., et al., *Carcinoid tumor of the duodenum.* Arquivos de Gastroenterologia, 2013. 50: p. 3-9.
22. Jetmore, A.B., et al., *Rectal carcinoids: the most frequent carcinoid tumor.* Diseases of the colon & rectum, 1992. 35: p. 717-725.
23. Partelli, S., et al., *Antibes Consensus Conference participants. ENETS consensus guidelines for standard of care in neuroendocrine tumours: surgery for small intestinal and pancreatic neuroendocrine tumours.* Neuroendocrinology, 2017. 105(3): p. 255-265.
24. Skoura, E., et al., *The impact of 68Ga-DOTATATE PET/CT imaging on management of patients with neuroendocrine tumors: experience from a national referral center in the United Kingdom.* Journal of Nuclear Medicine, 2016. 57(1): p. 34-40.
25. Rinzivillo, M., et al., *Clinical usefulness of 18F-fluorodeoxyglucose positron emission tomography in the diagnostic algorithm of advanced entero-pancreatic neuroendocrine neoplasms.* The Oncologist, 2018. 23(2): p. 186-192.
26. Cherif, R., et al., *Parenchyma-sparing resections for pancreatic neuroendocrine tumors.* Journal of Gastrointestinal Surgery, 2012. 16: p. 2045-2055.
27. Moertel, C.G., et al., *Carcinoid tumor of the appendix: treatment and prognosis.* New England Journal of Medicine, 1987. 317(27): p. 1699-1701.
28. Singh, S., et al., *Follow-up recommendations for completely resected gastroenteropancreatic neuroendocrine tumours (GEP-NETs): Consensus guidelines from the Commonwealth NET collaboration (CommNETs) in conjunction with the North American NET Society (NANETS).* Annals of Oncology, 2017. 28: p. v147.
29. Lk, K., *Treatment of the malignant carcinoid syndrome. Evaluation of a long-acting somatostatin analogue.* N Engl J Med, 1986. 315: p. 663-666.
30. Rinke, A., et al., *Placebo-controlled, double-blind, prospective, randomized study on the effect of octreotide LAR in the control of tumor growth in patients with metastatic neuroendocrine midgut tumors: a report from the PROMID Study Group.* J Clin Oncol, 2009. 27(28): p. 4656-4663.
31. Caplin, M.E., et al., *Lanreotide in metastatic enteropancreatic neuroendocrine tumors.* New England Journal of Medicine, 2014. 371(3): p. 224-233.
32. Yao, J.C., et al., *Efficacy of RAD001 (everolimus) and octreotide LAR in advanced low-to intermediate-grade neuroendocrine tumors: results of a phase II study.* Journal of Clinical Oncology, 2008. 26(26): p. 4311.
33. Castellano, D., et al., *Everolimus plus octreotide long-acting repeatable in patients with colorectal neuroendocrine tumors: A subgroup analysis of the phase III RADIANT-2 study.* The oncologist, 2013. 18(1): p. 46-53.
34. Yao, J.C., et al., *Everolimus for advanced pancreatic neuroendocrine tumors.* New England Journal of Medicine, 2011. 364(6): p. 514-523.

35. Yao, J.C., et al., *Everolimus for the treatment of advanced, non-functional neuroendocrine tumours of the lung or gastrointestinal tract (RADIANT-4): a randomised, placebo-controlled, phase 3 study.* The Lancet, 2016. 387(10022): p. 968-977.
36. Raymond, E., et al., *Sunitinib malate for the treatment of pancreatic neuroendocrine tumors.* New England Journal of Medicine, 2011. 364(6): p. 501-513.
37. Daskalakis, K., et al., *Anti-tumour activity of everolimus and sunitinib in neuroendocrine neoplasms.* Endocrine Connections, 2019. 8(6): p. 641-653.
38. Hobday, T., et al., *MC044h, a phase II trial of sorafenib in patients (pts) with metastatic neuroendocrine tumors (NET): A Phase II Consortium (P2C) study.* Journal of Clinical Oncology, 2007. 25(18_suppl): p. 4504-4504.
39. Abdel-Rahman, O. and M. Fouad, *Bevacizumab-based combination therapy for advanced gastroenteropancreatic neuroendocrine neoplasms (GEP-NENs): a systematic review of the literature.* Journal of cancer research and clinical oncology, 2015. 141: p. 295-305.
40. Berruti, A., et al., *Bevacizumab plus octreotide and metronomic capecitabine in patients with metastatic well-to-moderately differentiated neuroendocrine tumors: the XELBEVOCT study.* BMC cancer, 2014. 14(1): p. 1-10.
41. Chan, J.A., et al., *Prospective study of bevacizumab plus temozolomide in patients with advanced neuroendocrine tumors.* Journal of Clinical Oncology, 2012. 30(24): p. 2963.
42. Kulke, M.H., et al., *A prospective phase II study of 2-methoxyestradiol administered in combination with bevacizumab in patients with metastatic carcinoid tumors.* Cancer chemotherapy and pharmacology, 2011. 68: p. 293-300.
43. Yao, J.C., et al., *Targeting vascular endothelial growth factor in advanced carcinoid tumor: a random assignment phase II study of depot octreotide with bevacizumab and pegylated interferon alfa-2b.* Journal of Clinical Oncology, 2008. 26(8): p. 1316-1323.
44. Castellano, D., et al., *Sorafenib and bevacizumab combination targeted therapy in advanced neuroendocrine tumour: a phase II study of Spanish Neuroendocrine Tumour Group (GETNE0801).* European Journal of Cancer, 2013. 49(18): p. 3780-3787.
45. Firdaus, I., et al., *Bevacizumab, pertuzumab, and sandostatin for patients (pts) with advanced neuroendocrine cancers (NET)*. 2012, American Society of Clinical Oncology.
46. Koumarianou, A., et al., *Combination treatment with metronomic temozolomide, bevacizumab and long-acting octreotide for malignant neuroendocrine tumours.* Endocrine-related cancer, 2012. 19(1): p. L1-L4.
47. Hobday, T.J., et al., *Multicenter phase II trial of temsirolimus (TEM) and bevacizumab (BEV) in pancreatic neuroendocrine tumor (PNET).* Journal of Clinical Oncology, 2012. 30(4_suppl): p. 260-260.
48. Lapuerta, P., et al., *Telotristat etiprate, a novel inhibitor of serotonin synthesis for the treatment of carcinoid syndrome.* Clinical Investigation, 2015. 5(5): p. 447-456.
49. Kulke, M.H., et al., *Telotristat ethyl, a tryptophan hydroxylase inhibitor for the treatment of carcinoid syndrome.* J Clin Oncol, 2017. 35(1): p. 14-23.

50. Pavel, M., et al., *Telotristat ethyl in carcinoid syndrome: safety and efficacy in the TELECAST phase 3 trial.* Endocrine-Related Cancer, 2018. 25(3): p. 309-322.
51. Faiss, S., et al., *Prospective, randomized, multicenter trial on the antiproliferative effect of lanreotide, interferon alfa, and their combination for therapy of metastatic neuroendocrine gastroenteropancreatic tumors—the International Lanreotide and Interferon Alfa Study Group.* Journal of Clinical Oncology, 2003. 21(14): p. 2689-2696.
52. Mirvis, E., et al., *Role of interferon-alpha in patients with neuroendocrine tumors: a retrospective study.* Anticancer research, 2014. 34(11): p. 6601-6607.
53. Nicolas, G.P., et al., *New developments in peptide receptor radionuclide therapy.* Journal of Nuclear Medicine, 2019. 60(2): p. 167-171.
54. Cives, M. and J. Strosberg, *Radionuclide therapy for neuroendocrine tumors.* Current oncology reports, 2017. 19: p. 1-9.
55. Strosberg, J., et al., *Phase 3 trial of 177Lu-Dotatate for midgut neuroendocrine tumors.* New England Journal of Medicine, 2017. 376(2): p. 125-135.
56. *Neuroendocrine and Adrenal Tumors*. 2022: NCCN Clinical Practice Guidelines in Oncology.
57. Waldherr, C., et al., *The clinical value of [90Y-DOTA]-D-Phe1-Tyr3-octreotide (90Y-DOTATOC) in the treatment of neuroendocrine tumours: a clinical phase II study.* Annals of Oncology, 2001. 12(7): p. 941-945.
58. Paganelli, G., et al., *Receptor-mediated radiotherapy with 90 Y-DOTA-D-Phe 1-Tyr 3-octreotide.* European journal of nuclear medicine, 2001. 28: p. 426-434.
59. Vinjamuri, S., et al., *Peptide receptor radionuclide therapy with 90Y-DOTATATE/90Y-DOTATOC in patients with progressive metastatic neuroendocrine tumours: assessment of response, survival and toxicity.* British journal of cancer, 2013. 108(7): p. 1440-1448.
60. Cwikla, J., et al., *Efficacy of radionuclide treatment DOTATATE Y-90 in patients with progressive metastatic gastroenteropancreatic neuroendocrine carcinomas (GEP-NETs): a phase II study.* Annals of Oncology, 2010. 21(4): p. 787-794.
61. Ballal, S., et al., *Survival outcomes in metastatic gastroenteropancreatic neuroendocrine tumor patients receiving concomitant 225Ac-DOTATATE targeted alpha therapy and capecitabine: a real-world scenario management based long-term outcome study.* Journal of Nuclear Medicine, 2022.
62. Chan, D., et al., *External beam radiotherapy in the treatment of gastroenteropancreatic neuroendocrine tumours: a systematic review.* Clinical Oncology, 2018. 30(7): p. 400-408.
63. Saif, M.W., et al., *Radiotherapy in the management of pancreatic neuroendocrine tumors (PNET): experience at three institutions.* Anticancer Research, 2013. 33(5): p. 2175-2177.
64. Zagar, T.M., et al., *Resected pancreatic neuroendocrine tumors: patterns of failure and disease-related outcomes with or without radiotherapy.* International Journal of Radiation Oncology* Biology* Physics, 2012. 83(4): p. 1126-1131.
65. Arvold, N.D., et al., *Pancreatic neuroendocrine tumors with involved surgical margins: prognostic factors and the role of adjuvant radiotherapy.* International Journal of Radiation Oncology* Biology* Physics, 2012. 83(3): p. e337-e343.

66. Strosberg, J., et al., *Effective treatment of locally advanced endocrine tumors of the pancreas with chemoradiotherapy.* Neuroendocrinology, 2007. 85(4): p. 216-220.
67. Lee, J., et al., *Role of radiotherapy for pancreatobiliary neuroendocrine tumors.* Radiation Oncology Journal, 2013. 31(3): p. 125.
68. Brieau, B., et al., *Radiochemotherapy versus surgery in nonmetastatic anorectal neuroendocrine carcinoma: a multicenter study by the Association des Gastro-Enterologues Oncologues.* Medicine, 2015. 94(42).
69. Contessa, J.N., et al., *Radiotherapy for pancreatic neuroendocrine tumors.* International Journal of Radiation Oncology* Biology* Physics, 2009. 75(4): p. 1196-1200.
70. Kennedy, A.S., et al., *Radioembolization for unresectable neuroendocrine hepatic metastases using resin 90Y-microspheres: early results in 148 patients.* American journal of clinical oncology, 2008. 31(3): p. 271-279.
71. Kim, H.S., et al., *Phase 1b study of pasireotide, everolimus, and selective internal radioembolization therapy for unresectable neuroendocrine tumors with hepatic metastases.* Cancer, 2018. 124(9): p. 1992-2000.
72. King, J., et al., *Radioembolization with selective internal radiation microspheres for neuroendocrine liver metastases.* Cancer, 2008. 113(5): p. 921-929.
73. Rhee, T.K., et al., *90Y radioembolization for metastatic neuroendocrine liver tumors: preliminary results from a multi-institutional experience.* Annals of surgery, 2008. 247(6): p. 1029-1035.
74. Jia, Z. and W. Wang, *Yttrium-90 radioembolization for unresectable metastatic neuroendocrine liver tumor: A systematic review.* European journal of radiology, 2018. 100: p. 23-29.
75. Ngo, L., et al., *Chemoembolization versus radioembolization for neuroendocrine liver metastases: a meta-analysis comparing clinical outcomes.* Annals of Surgical Oncology, 2021. 28: p. 1950-1958.
76. Strosberg, J.R., et al., *177Lu-Dotatate plus long-acting octreotide versus high-dose long-acting octreotide in patients with midgut neuroendocrine tumours (NETTER-1): final overall survival and long-term safety results from an open-label, randomised, controlled, phase 3 trial.* The Lancet Oncology, 2021. 22(12): p. 1752-1763.
77. Park, J.H., et al., *Prospective phase II study of preoperative chemoradiation with capecitabine in locally advanced rectal cancer.* Cancer Res Treat, 2004. 36(6): p. 354-9.
78. Chu, E. and C.J. Allegra, *The role of thymidylate synthase in cellular regulation.* Adv Enzyme Regul, 1996. 36: p. 143-63.
79. Lawrence, T.S., A.W. Blackstock, and C. McGinn, *The mechanism of action of radiosensitization of conventional chemotherapeutic agents.* Semin Radiat Oncol, 2003. 13(1): p. 13-21.
80. van Essen, M., et al., *Report on short-term side effects of treatments with 177Lu-octreotate in combination with capecitabine in seven patients with gastroenteropancreatic neuroendocrine tumours.* European journal of nuclear medicine and molecular imaging, 2008. 35(4): p. 743-748.
81. Claringbold, P.G., et al., *Phase II study of radiopeptide 177Lu-octreotate and capecitabine therapy of progressive disseminated neuroendocrine tumours.*

European journal of nuclear medicine and molecular imaging, 2011. 38(2): p. 302-311.
82. Nicolini, S., et al., *Combined use of 177Lu-DOTATATE and metronomic capecitabine (Lu-X) in FDG-positive gastro-entero-pancreatic neuroendocrine tumors.* European Journal of Nuclear Medicine and Molecular Imaging, 2021. 48(10): p. 3260-3267.
83. Villano, J.L., T.E. Seery, and L.R. Bressler, *Temozolomide in malignant gliomas: current use and future targets.* Cancer chemotherapy and pharmacology, 2009. 64(4): p. 647-655.
84. Claringbold, P.G., R.A. Price, and J.H. Turner, *Phase I-II study of radiopeptide 177Lu-octreotate in combination with capecitabine and temozolomide in advanced low-grade neuroendocrine tumors.* Cancer Biotherapy and Radiopharmaceuticals, 2012. 27(9): p. 561-569.
85. Claringbold, P.G. and J.H. Turner, *Pancreatic neuroendocrine tumor control: durable objective response to combination 177Lu-octreotate-capecitabine-temozolomide radiopeptide chemotherapy.* Neuroendocrinology, 2016. 103(5): p. 432-439.
86. Mauceri, H.J., et al., *Everolimus exhibits efficacy as a radiosensitizer in a model of non-small cell lung cancer.* Oncology reports, 2012. 27(5): p. 1625-1629.
87. Castellano, D., et al., *Everolimus plus octreotide long-acting repeatable in patients with colorectal neuroendocrine tumors: a subgroup analysis of the phase III RADIANT-2 study.* Oncologist, 2013. 18(1): p. 46-53.
88. Lombard-Bohas, C., et al., *Impact of prior chemotherapy use on the efficacy of everolimus in patients with advanced pancreatic neuroendocrine tumors: a subgroup analysis of the phase III RADIANT-3 trial.* Pancreas, 2015. 44(2): p. 181.
89. Yao, J.C., et al., *Efficacy of RAD001 (everolimus) and octreotide LAR in advanced low- to intermediate-grade neuroendocrine tumors: results of a phase II study.* J Clin Oncol, 2008. 26(26): p. 4311-8.
90. Yao, J.C., et al., *Everolimus for the treatment of advanced, non-functional neuroendocrine tumours of the lung or gastrointestinal tract (RADIANT-4): a randomised, placebo-controlled, phase 3 study.* Lancet, 2016. 387(10022): p. 968-977.
91. Exner, S., et al., *mTOR inhibitors as radiosensitizers in neuroendocrine neoplasms.* Frontiers in oncology, 2021. 10: p. 578380.
92. Claringbold, P.G. and J.H. Turner, *NeuroEndocrine tumor therapy with lutetium-177-octreotate and everolimus (NETTLE): a phase I study.* Cancer Biotherapy and Radiopharmaceuticals, 2015. 30(6): p. 261-269.
93. Aljubran, A., et al., *Efficacy of Everolimus Combined with 177Lu-Dotatate in the Treatment of Neuroendocrine Tumors.* Cancer Biotherapy & Radiopharmaceuticals, 2022.
94. LoPiccolo, J., et al., *Targeting the PI3K/Akt/mTOR pathway: effective combinations and clinical considerations.* Drug Resistance Updates, 2008. 11(1-2): p. 32-50.
95. Harrington, L.S., et al., *The TSC1-2 tumor suppressor controls insulin–PI3K signaling via regulation of IRS proteins.* The Journal of cell biology, 2004. 166(2): p. 213-223.

96. Shah, O.J., Z. Wang, and T. Hunter, *Inappropriate activation of the TSC/Rheb/mTOR/S6K cassette induces IRS1/2 depletion, insulin resistance, and cell survival deficiencies.* Current biology, 2004. 14(18): p. 1650-1656.
97. Sarbassov, D.D., et al., *Phosphorylation and regulation of Akt/PKB by the rictor-mTOR complex.* Science, 2005. 307(5712): p. 1098-1101.
98. Verhoef, S., et al., *Malignant pancreatic tumour within the spectrum of tuberous sclerosis complex in childhood.* European journal of pediatrics, 1999. 158: p. 284-287.
99. Tan, C., et al., *Ampullary somatostatinoma associated with von Recklinghausen's neurofibromatosis presenting as obstructive jaundice.* European Journal of Surgical Oncology (EJSO), 1996. 22(3): p. 298-301.
100. Yoshida, A., et al., *Von Recklinghausen's Disease Associated with Somatostatin-rich Duodenal Carcinoid (Somatostatinoma), Medullary Thyroid Carcinoma and Diffuse Adrenal Medullary Hyperplasia.* Pathology International, 1991. 41(11): p. 847-856.
101. Kasajima, A., et al., *mTOR expression and activity patterns in gastroenteropancreatic neuroendocrine tumours.* Endocrine-related cancer, 2011. 18(1): p. 181.
102. Horn, D., et al., *Targeting EGFR-PI3K-AKT-mTOR signaling enhances radiosensitivity in head and neck squamous cell carcinoma.* Expert opinion on therapeutic targets, 2015. 19(6): p. 795-805.
103. Sarkaria, J.N., et al., *Inhibition of phosphoinositide 3-kinase related kinases by the radiosensitizing agent wortmannin.* Cancer research, 1998. 58(19): p. 4375-4382.
104. Mardanshahi, A., et al., *The PI3K/AKT/mTOR signaling pathway inhibitors enhance radiosensitivity in cancer cell lines.* Molecular Biology Reports, 2021. 48: p. 1-14.
105. Albert, J.M., et al., *Targeting the Akt/mammalian target of rapamycin pathway for radiosensitization of breast cancer.* Molecular cancer therapeutics, 2006. 5(5): p. 1183-1189.
106. Caron, R.W., et al., *Activated forms of H-RAS and K-RAS differentially regulate membrane association of PI3K, PDK-1, and AKT and the effect of therapeutic kinase inhibitors on cell survival.* Molecular cancer therapeutics, 2005. 4(2): p. 257-270.
107. Gupta, A.K., et al., *Radiation sensitization of human cancer cells in vivo by inhibiting the activity of PI3K using LY294002.* International Journal of Radiation Oncology* Biology* Physics, 2003. 56(3): p. 846-853.
108. Miyasaka, A., et al., *PI3K/mTOR pathway inhibition overcomes radioresistance via suppression of the HIF1-α/VEGF pathway in endometrial cancer.* Gynecologic oncology, 2015. 138(1): p. 174-180.
109. Edwards, E., et al., *Phosphatidylinositol 3-kinase/Akt signaling in the response of vascular endothelium to ionizing radiation.* Cancer Research, 2002. 62(16): p. 4671-4677.
110. Wu, X., et al., *Recent advances in dual PI3K/mTOR inhibitors for tumour treatment.* Frontiers in Pharmacology, 2022. 13: p. 875372.
111. Papadopoulos, K.P., et al., *Phase I safety, pharmacokinetic, and pharmacodynamic study of SAR245409 (XL765), a novel, orally administered PI3K/mTOR inhibitor*

in patients with advanced solid tumors. Clinical Cancer Research, 2014. 20(9): p. 2445-2456.
112. Wen, P.Y., et al., *Paxalisib in patients with newly diagnosed glioblastoma with unmethylated MGMT promoter status: Final phase 2 study results*. 2022, American Society of Clinical Oncology.
113. Sweeney, C.J., et al., *Phase Ib/II study of enzalutamide with samotolisib (LY3023414) or placebo in patients with metastatic castration-resistant prostate cancer.* Clinical Cancer Research, 2022. 28(11): p. 2237-2247.
114. Parsons, D.W., et al., *Actionable tumor alterations and treatment protocol enrollment of pediatric and young adult patients with refractory cancers in the National Cancer Institute–Children's Oncology Group pediatric MATCH trial.* Journal of Clinical Oncology, 2022. 40(20): p. 2224-2234.
115. Nordlund, P. and P. Reichard, *Ribonucleotide reductases.* Annu. Rev. Biochem., 2006. 75: p. 681-706.
116. Jordan, A. and P. Reichard, *Ribonucleotide reductases.* Annual review of biochemistry, 1998. 67(1): p. 71-98.
117. Grolmusz, V.K., et al., *Cell cycle dependent RRM2 may serve as proliferation marker and pharmaceutical target in adrenocortical cancer.* American journal of cancer research, 2016. 6(9): p. 2041.
118. Yang, B., et al., *The high expression of RRM2 can predict the malignant transformation of endometriosis.* Advances in Therapy, 2021. 38(10): p. 5178-5190.
119. Morikawa, T., et al., *Expression of ribonucleotide reductase M2 subunit in gastric cancer and effects of RRM2 inhibition in vitro.* Human pathology, 2010. 41(12): p. 1742-1748.
120. Mazzu, Y.Z., et al., *A novel mechanism driving poor-prognosis prostate cancer: overexpression of the DNA repair gene, ribonucleotide reductase small subunit M2 (RRM2).* Clinical Cancer Research, 2019. 25(14): p. 4480-4492.
121. Zhang, K., et al., *Overexpression of RRM2 decreases thrombspondin-1 and increases VEGF production in human cancer cells in vitro and in vivo: implication of RRM2 in angiogenesis.* Molecular cancer, 2009. 8(1): p. 1-12.
122. Jin, C.-Y., et al., *High expression of RRM2 as an independent predictive factor of poor prognosis in patients with lung adenocarcinoma.* Aging (Albany NY), 2021. 13(3): p. 3518.
123. Sun, H., et al., *RRM2 is a potential prognostic biomarker with functional significance in glioma.* International journal of biological sciences, 2019. 15(3): p. 533.
124. Wang, S., et al., *Overexpression of RRM2 is related to poor prognosis in oral squamous cell carcinoma.* Oral Diseases, 2021. 27(2): p. 204-214.
125. Rahman, M.A., et al., *RRM2 regulates Bcl-2 in head and neck and lung cancers: a potential target for cancer therapy.* Clinical cancer research, 2013. 19(13): p. 3416-3428.
126. Ohmura, S., et al., *Translational evidence for RRM2 as a prognostic biomarker and therapeutic target in Eawing sarcoma.* Molecular Cancer, 2021. 20: p. 1-7.

127. Morikawa, T., et al., *Ribonucleotide reductase M2 subunit is a novel diagnostic marker and a potential therapeutic target in bladder cancer.* Histopathology, 2010. 57(6): p. 885-892.
128. Das, B., N. Jain, and B. Mallick, *Ribonucleotide reductase subunit M2 is a potential prognostic marker and therapeutic target for soft tissue sarcoma.* Gene, 2022. 808: p. 145988.
129. Guittet, O., et al., *Mammalian p53R2 protein forms an active ribonucleotide reductasein vitro with the R1 protein, which is expressed both in resting cells in response to DNA damage and in proliferating cells.* Journal of Biological Chemistry, 2001. 276(44): p. 40647-40651.
130. Yamaguchi, T., et al., *p53R2-dependent pathway for DNA synthesis in a p53-regulated cell cycle checkpoint.* Cancer research, 2001. 61(22): p. 8256-8262.
131. Wang, X., et al., *Regulation of p53R2 and its role as potential target for cancer therapy.* Cancer letters, 2009. 276(1): p. 1-7.
132. Jiang, C., et al., *p53R2 overexpression in cervical cancer promotes AKT signaling and EMT, and is correlated with tumor progression, metastasis and poor prognosis.* Cell Cycle, 2017. 16(18): p. 1673-1682.
133. Uramoto, H., et al., *P53R2, p53 inducible ribonucleotide reductase gene, correlated with tumor progression of non-small cell lung cancer.* Anticancer research, 2006. 26(2A): p. 983-988.
134. Byun, D.S., et al., *Expression and mutation analyses of P53R2, a newly identified p53 target for DNA repair in human gastric carcinoma.* International journal of cancer, 2002. 98(5): p. 718-723.
135. Khan, P., et al., *MicroRNA-1 attenuates the growth and metastasis of small cell lung cancer through CXCR4/FOXM1/RRM2 axis.* Molecular cancer, 2023. 22(1): p. 1.
136. Chen, X., et al., *Identification of potential target genes and crucial pathways in small cell lung cancer based on bioinformatic strategy and human samples.* Plos one, 2020. 15(11): p. e0242194.
137. Hofsli, E., et al., *Identification of novel growth factor-responsive genes in neuroendocrine gastrointestinal tumour cells.* British journal of cancer, 2005. 92(8): p. 1506-1516.
138. Kuo, M.-L. and T.J. Kinsella, *Expression of ribonucleotide reductase after ionizing radiation in human cervical carcinoma cells.* Cancer research, 1998. 58(10): p. 2245-2252.
139. Kuo, M.-L., et al., *Overexpression of the R2 subunit of ribonucleotide reductase in human nasopharyngeal cancer cells reduces radiosensitivity.* The Cancer Journal, 2003. 9(4): p. 277-285.
140. Chapman, T.R. and T.J. Kinsella, *Ribonucleotide reductase inhibitors: a new look at an old target for radiosensitization.* Frontiers in oncology, 2012. 1: p. 56.
141. Faderl, S., et al., *New nucleoside analogues in clinical development.* Cancer chemotherapy and biological response modifiers, 2002. 20: p. 37-58.
142. Shao, J., et al., *Ribonucleotide reductase inhibitors and future drug design.* Current cancer drug targets, 2006. 6(5): p. 409-431.
143. Manegold, C., *Gemcitabine (Gemzar®) in non-small cell lung cancer.* Expert review of anticancer therapy, 2004. 4(3): p. 345-360.

144. Storniolo, A.M., et al., *An investigational new drug treatment program for patients with gemcitabine: results for over 3000 patients with pancreatic carcinoma.* Cancer, 1999. 85(6): p. 1261-1268.
145. de Wit, R. and J. Bellmunt, *Overview of gemcitabine triplets in metastatic bladder cancer.* Critical reviews in oncology/hematology, 2003. 45(2): p. 191-197.
146. Dent, S., H. Messersmith, and M. Trudeau, *Gemcitabine in the management of metastatic breast cancer: a systematic review.* Breast cancer research and treatment, 2008. 108: p. 319-331.
147. Doyle, T.H., F. Mornex, and W.G. McKenna, *The clinical implications of gemcitabine radiosensitization*. 2001, AACR. p. 226-228.
148. Huff, S.E., J.M. Winter, and C.G. Dealwis, *Inhibitors of the cancer target ribonucleotide reductase, past and present.* Biomolecules, 2022. 12(6): p. 815.
149. Long, J., et al., *Overcoming drug resistance in pancreatic cancer.* Expert opinion on therapeutic targets, 2011. 15(7): p. 817-828.
150. Nigović, B., N. Kujundžić, and K. Sanković, *Electron transfer in N-hydroxyurea complexes with iron (III).* European journal of medicinal chemistry, 2005. 40(1): p. 51-55.
151. Donehower, R.C. *An overview of the clinical experience with hydroxyurea*. in *Seminars in oncology*. 1992.
152. Weppelmann, B., et al., *Treatment of recurrent head and neck cancer with 5-fluorouracil, hydroxyurea, and reirradiation.* International Journal of Radiation Oncology* Biology* Physics, 1992. 22(5): p. 1051-1056.
153. Morris, M., et al., *Pelvic radiation with concurrent chemotherapy compared with pelvic and para-aortic radiation for high-risk cervical cancer.* New England Journal of Medicine, 1999. 340(15): p. 1137-1143.
154. Zhou, B., et al., *Human ribonucleotide reductase M2 subunit gene amplification and transcriptional regulation in a homogeneous staining chromosome region responsible for the mechanism of drug resistance.* Cytogenetics and cell genetics, 2001. 95(1-2): p. 34-42.
155. Aye, Y., M.J. Long, and J. Stubbe, *Mechanistic studies of semicarbazone triapine targeting human ribonucleotide reductase in vitro and in mammalian cells: tyrosyl radical quenching not involving reactive oxygen species.* Journal of Biological Chemistry, 2012. 287(42): p. 35768-35778.
156. Kunos, C.A., et al., *Randomized phase II trial of triapine-cisplatin-radiotherapy for locally advanced stage uterine cervix or vaginal cancers.* Frontiers in oncology, 2019. 9: p. 1067.
157. Kunos, C.A., et al., *Phase I trial of triapine–cisplatin–paclitaxel chemotherapy for advanced stage or metastatic solid tumor cancers.* Frontiers in Oncology, 2017. 7: p. 62.
158. Nutting, C., et al., *Phase II study of 3-AP Triapine in patients with recurrent or metastatic head and neck squamous cell carcinoma.* Annals of oncology, 2009. 20(7): p. 1275-1279.
159. Mehta, M.P., et al., *Motexafin gadolinium combined with prompt whole brain radiotherapy prolongs time to neurologic progression in non–small-cell lung cancer patients with brain metastases: results of a phase III trial.* International Journal of Radiation Oncology* Biology* Physics, 2009. 73(4): p. 1069-1076.

160. Bradley, K.A., et al., *Motexafin-gadolinium and involved field radiation therapy for intrinsic pontine glioma of childhood: a children's oncology group phase 2 study.* International Journal of Radiation Oncology* Biology* Physics, 2013. 85(1): p. e55-e60.
161. Chen, M.-C., et al., *The novel ribonucleotide reductase inhibitor COH29 inhibits DNA repair in vitro.* Molecular pharmacology, 2015. 87(6): p. 996-1005.
162. Lee, Y., et al., *GTI-2040, an antisense agent targeting the small subunit component (R2) of human ribonucleotide reductase, shows potent antitumor activity against a variety of tumors.* Cancer research, 2003. 63(11): p. 2802-2811.
163. Modlin, I.M., et al., *Priorities for Improving the Management of Gastroenteropancreatic Neuroendocrine Tumors.* JNCI: Journal of the National Cancer Institute, 2008. 100(18): p. 1282-1289.
164. Campana, D. and P. Tomassetti, *Incidence, Epidemiology, Aetiology and Staging, Classification, Clinical Presentation/Signs and Symptoms, Diagnosis, Staging Procedures/Investigation*, in *PET/CT in Neuroendocrine Tumors*. 2016, Springer. p. 1-5.
165. Baum, R.P., et al., *[177Lu-DOTA] 0-D-Phe1-Tyr3-octreotide (177Lu-DOTATOC) for peptide receptor radiotherapy in patients with advanced neuroendocrine tumours: a phase-II study.* Theranostics, 2016. 6(4): p. 501.
166. Ezziddin, S., et al., *Targeted radiotherapy of neuroendocrine tumors using Lu-177-DOTA octreotate with prolonged intervals.* Journal of Nuclear Medicine, 2007. 48(supplement 2): p. 394P-394P.
167. Limouris, G., et al., *Comparison of 111in-[DTPA0] octreotide versus non carrier added 177lu-[DOTA0, Tyr3]-octreotate efficacy in patients with GEP-NET treated intra-arterially for liver metastases.* Clinical nuclear medicine, 2016. 41(3): p. 194-200.
168. Nicolas, G., et al., *Targeted radiotherapy with radiolabeled somatostatin analogs.* Endocrinology and Metabolism Clinics, 2011. 40(1): p. 187-204.
169. Strosberg, J.R., et al., *NETTER-1 phase III: Progression-free survival, radiographic response, and preliminary overall survival results in patients with midgut neuroendocrine tumors treated with 177-Lu-dotatate*. 2016, American Society of Clinical Oncology.
170. Van Essen, M., et al., *Peptide-receptor radionuclide therapy for endocrine tumors.* Nature Reviews Endocrinology, 2009. 5(7): p. 382.
171. Reubi, J.C., *Peptide receptor expression in GEP-NET.* Virchows Archiv, 2007. 451(1): p. 47-50.
172. van Essen, M., et al., *Report on short-term side effects of treatments with 177 Lu-octreotate in combination with capecitabine in seven patients with gastroenteropancreatic neuroendocrine tumours.* European journal of nuclear medicine and molecular imaging, 2008. 35(4): p. 743-748.
173. Bison, S.M., et al., *Optimization of combined temozolomide and peptide receptor radionuclide therapy (PRRT) in mice after multimodality molecular imaging studies.* EJNMMI research, 2015. 5(1): p. 62.
174. Kong, G., et al., *High-administered activity In-111 octreotide therapy with concomitant radiosensitizing 5FU chemotherapy for treatment of neuroendocrine*

tumors: preliminary experience. Cancer Biotherapy and Radiopharmaceuticals, 2009. 24(5): p. 527-533.
175. Zaytseva, Y.Y., et al., *mTOR inhibitors in cancer therapy.* Cancer letters, 2012. 319(1): p. 1-7.
176. Yao, J.C., et al., *Daily oral everolimus activity in patients with metastatic pancreatic neuroendocrine tumors after failure of cytotoxic chemotherapy: a phase II trial.* Journal of clinical oncology, 2010. 28(1): p. 69.
177. Pavel, M.E., et al., *Everolimus plus octreotide long-acting repeatable for the treatment of advanced neuroendocrine tumours associated with carcinoid syndrome (RADIANT-2): a randomised, placebo-controlled, phase 3 study.* The Lancet, 2011. 378(9808): p. 2005-2012.
178. Pavel, M., et al., *Efficacy of everolimus plus octreotide LAR in patients with advanced neuroendocrine tumor and carcinoid syndrome: final overall survival from the randomized, placebo-controlled phase 3 RADIANT-2 study.* Annals of Oncology, 2017. 28(7): p. 1569-1575.
179. Yao, J.C., et al., *Everolimus for the treatment of advanced pancreatic neuroendocrine tumors: overall survival and circulating biomarkers from the randomized, phase III RADIANT-3 study.* Journal of Clinical Oncology, 2016. 34(32): p. 3906.
180. Prasad, V., et al., *Somatostatin agonist and mTOR inhibitors as potential radioprotectors or radiosensitizers in neuroendocrine tumor cells.* Journal of Nuclear Medicine, 2016. 57(supplement 2): p. 1435-1435.
181. Aljubran, A.H., et al., *Combination of everolimus and lu-177 PRRT in treatment of G1-2 neuroendocrine tumors (NET): Phase 1-2 study*. 2019, American Society of Clinical Oncology.
182. Yuan, J., et al., *PF-04691502, a potent and selective oral inhibitor of PI3K and mTOR kinases with antitumor activity.* Molecular cancer therapeutics, 2011. 10(11): p. 2189-2199.
183. Britten, C.D., et al., *Phase I study of PF-04691502, a small-molecule, oral, dual inhibitor of PI3K and mTOR, in patients with advanced cancer*. Investigational new drugs, 2014. 32(3): p. 510-517.
184. del Campo, J.M., et al., *A randomized phase II non-comparative study of PF-04691502 and gedatolisib (PF-05212384) in patients with recurrent endometrial cancer*. Gynecologic oncology, 2016. 142(1): p. 62-69.
185. Dowsett, M., et al., *104P Phase II Randomized Study of Pre-Operative Pf-04691502 Plus Letrozole Compared with Letrozole (L) In Patients with Estrogen Receptor-Positive, Her2-Negative Early Breast Cancer (Bc).* Annals of Oncology, 2012. 23: p. ii44.
186. María, J., et al., *A randomized phase II non-comparative study of PF-04691502 and gedatolisib (PF-05212384) in patients with recurrent endometrial cancer*. 2016.
187. Fazio, N., et al., *A phase II study of BEZ235 in patients with everolimus-resistant, advanced pancreatic neuroendocrine tumours.* Anticancer research, 2016. 36(2): p. 713-719.
188. *CytoScanTM SRB Cell Cytotoxicity Assay*. Available from: https://www.gbiosciences.com/image/pdfs/protocol/786-213_protocol.pdf.

189. Evers, B.M., et al., *Establishment and characterization of a human carcinoid in nude mice and effect of various agents on tumor growth.* Gastroenterology, 1991. 101(2): p. 303-11.
190. Parekh, D., et al., *Characterization of a human pancreatic carcinoid in vitro: morphology, amine and peptide storage, and secretion.* Pancreas, 1994. 9(1): p. 83-90.
191. Doihara, H., et al., *QGP-1 cells release 5-HT via TRPA1 activation; a model of human enterochromaffin cells.* Mol Cell Biochem, 2009. 331(1-2): p. 239-45.
192. Benten, D., et al., *Establishment of the first well-differentiated human pancreatic neuroendocrine tumor model.* Molecular Cancer Research, 2018. 16(3): p. 496-507.
193. Rychahou, P.G., et al., *Targeted molecular therapy of the PI3K pathway: therapeutic significance of PI3K subunit targeting in colorectal carcinoma.* Ann Surg, 2006. 243(6): p. 833-42; discussion 843-4.
194. Allred, D.C., et al., *Association of p53 protein expression with tumor cell proliferation rate and clinical outcome in node-negative breast cancer.* J Natl Cancer Inst, 1993. 85(3): p. 200-6.
195. Allred, D.C., et al., *Prognostic and predictive factors in breast cancer by immunohistochemical analysis.* Mod Pathol, 1998. 11(2): p. 155-68.
196. Johnson, J., et al., *Targeting PI3K and AMPKα Signaling Alone or in Combination to Enhance Radiosensitivity of Triple Negative Breast Cancer.* Cells, 2020. 9(5): p. 1253.
197. Chen, Q., et al., *Impact of backscatter material thickness on the depth dose of orthovoltage irradiators for radiobiology research.* Phys Med Biol, 2019. 64(5): p. 055001.
198. Jiao, Y., et al., *DAXX/ATRX, MEN1, and mTOR pathway genes are frequently altered in pancreatic neuroendocrine tumors.* Science, 2011. 331(6021): p. 1199-203.
199. Tran, C.G., et al., *Metastatic pancreatic neuroendocrine tumors have decreased somatostatin expression and increased Akt signaling.* Surgery, 2020.
200. Capdevila, J., et al., *Translational research in neuroendocrine tumors: pitfalls and opportunities.* Oncogene, 2017. 36(14): p. 1899-1907.
201. Stueven, A.K., et al., *Somatostatin Analogues in the Treatment of Neuroendocrine Tumors: Past, Present and Future.* Int J Mol Sci, 2019. 20(12).
202. Bundschuh, R.A., et al., *Therapy of Patients with Neuroendocrine Neoplasia-Evidence-Based Approaches and New Horizons.* Journal of clinical medicine, 2019. 8(9): p. 1474.
203. Nisa, L., G. Savelli, and R. Giubbini, *Yttrium-90 DOTATOC therapy in GEP-NET and other SST2 expressing tumors: a selected review.* Annals of nuclear medicine, 2011. 25(2): p. 75-85.
204. Kwekkeboom, D.J., et al., *Somatostatin receptor-based imaging and therapy of gastroenteropancreatic neuroendocrine tumors.* Endocrine-related cancer, 2010. 17(1): p. R53-R73.
205. Bergsma, H., et al., *Peptide receptor radionuclide therapy (PRRT) for GEP-NETs.* Best Practice & Research Clinical Gastroenterology, 2012. 26(6): p. 867-881.

206. Lamberti, G., et al., *The role of mTOR in neuroendocrine tumors: future cornerstone of a winning strategy?* International journal of molecular sciences, 2018. 19(3): p. 747.
207. Zoncu, R., A. Efeyan, and D.M. Sabatini, *mTOR: from growth signal integration to cancer, diabetes and ageing.* Nature reviews Molecular cell biology, 2011. 12(1): p. 21-35.
208. Liu, L., et al., *Rapamycin inhibits cell motility by suppression of mTOR-mediated S6K1 and 4E-BP1 pathways.* Oncogene, 2006. 25(53): p. 7029-7040.
209. Kim, S.-H., et al., *Prognostic significance and function of phosphorylated ribosomal protein S6 in esophageal squamous cell carcinoma.* Modern Pathology, 2013. 26(3): p. 327-335.
210. Qin, X., B. Jiang, and Y. Zhang, *4E-BP1, a multifactor regulated multifunctional protein.* Cell Cycle, 2016. 15(6): p. 781-786.
211. Robb, V.A., A. Astrinidis, and E.P. Henske, *Frequent of ribosomal protein S6 hyperphosphorylation in lymphangioleiomyomatosis-associated angiomyolipomas.* Modern pathology, 2006. 19(6): p. 839-846.
212. Benjamin, D., et al., *Rapamycin passes the torch: a new generation of mTOR inhibitors.* Nature reviews Drug discovery, 2011. 10(11): p. 868-880.
213. Houghton, P.J., *Everolimus.* Clinical cancer research, 2010. 16(5): p. 1368-1372.
214. Kuger, S., et al., *Radiosensitization of glioblastoma cell lines by the dual PI3K and mTOR inhibitor NVP-BEZ235 depends on drug-irradiation schedule.* Translational oncology, 2013. 6(2): p. 169.
215. Masuda, M., et al., *Growth inhibition by NVP-BEZ235, a dual PI3K/mTOR inhibitor, in hepatocellular carcinoma cell lines.* Oncology reports, 2011. 26(5): p. 1273-1279.
216. Wong, C.H., et al., *Preclinical evaluation of the PI3K-mTOR dual inhibitor PF-04691502 as a novel therapeutic drug in nasopharyngeal carcinoma.* Investigational new drugs, 2013. 31(6): p. 1399-1408.
217. Serra, V., et al., *NVP-BEZ235, a dual PI3K/mTOR inhibitor, prevents PI3K signaling and inhibits the growth of cancer cells with activating PI3K mutations.* Cancer research, 2008. 68(19): p. 8022-8030.
218. Hu, X., et al., *Dual PI3K/mTOR inhibitor PKI-402 suppresses the growth of ovarian cancer cells by degradation of Mcl-1 through autophagy.* Biomedicine & Pharmacotherapy, 2020. 129: p. 110397.
219. Oishi, T., et al., *The PI3K/mTOR dual inhibitor NVP-BEZ235 reduces the growth of ovarian clear cell carcinoma.* Oncology reports, 2014. 32(2): p. 553-558.
220. Carlo, M.I., et al., *A phase Ib study of BEZ235, a dual inhibitor of phosphatidylinositol 3-kinase (PI3K) and mammalian target of rapamycin (mTOR), in patients with advanced renal cell carcinoma.* The oncologist, 2016. 21(7): p. 787.
221. Salazar, R., et al., *Phase II Study of BEZ235 versus Everolimus in Patients with Mammalian Target of Rapamycin Inhibitor-Naïve Advanced Pancreatic Neuroendocrine Tumors.* The oncologist, 2018. 23(7): p. 766.
222. Ma, Y., Y. Vassetzky, and S. Dokudovskaya, *mTORC1 pathway in DNA damage response.* Biochimica et Biophysica Acta (BBA)-Molecular Cell Research, 2018. 1865(9): p. 1293-1311.

223. Olive, P.L., *The role of DNA single-and double-strand breaks in cell killing by ionizing radiation.* Radiation research, 1998. 150(5s): p. S42-S51.
224. Zhuang, H.-Q., et al., *The different radiosensitivity when combining erlotinib with radiation at different administration schedules might be related to activity variations in c-MET-PI3K-AKT signal transduction.* OncoTargets and therapy, 2013. 6: p. 603.
225. Li, Q., et al., *Sorafenib modulates the radio sensitivity of hepatocellular carcinoma cells in vitro in a schedule-dependent manner.* BMC cancer, 2012. 12(1): p. 485.
226. Ezziddin, S., et al., *Outcome of peptide receptor radionuclide therapy with 177 Lu-octreotate in advanced grade 1/2 pancreatic neuroendocrine tumours.* European journal of nuclear medicine and molecular imaging, 2014. 41: p. 925-933.
227. Jordan, A. and P. Reichard, *Ribonucleotide reductases.* Annu Rev Biochem, 1998. 67: p. 71-98.
228. Elledge, S.J., et al., *DNA damage and cell cycle regulation of ribonucleotide reductase.* Bioessays, 1993. 15(5): p. 333-9.
229. Aye, Y., et al., *Ribonucleotide reductase and cancer: biological mechanisms and targeted therapies.* Oncogene, 2015. 34(16): p. 2011-2021.
230. Souglakos, J., et al., *Ribonucleotide reductase subunits M1 and M2 mRNA expression levels and clinical outcome of lung adenocarcinoma patients treated with docetaxel/gemcitabine.* British journal of cancer, 2008. 98(10): p. 1710-1715.
231. Boukovinas, I., et al., *Tumor BRCA1, RRM1 and RRM2 mRNA expression levels and clinical response to first-line gemcitabine plus docetaxel in non-small-cell lung cancer patients.* PloS one, 2008. 3(11): p. e3695.
232. Zhou, B.S., et al., *Overexpression of ribonucleotide reductase in transfected human KB cells increases their resistance to hydroxyurea: M2 but not M1 is sufficient to increase resistance to hydroxyurea in transfected cells.* Cancer Res, 1995. 55(6): p. 1328-33.
233. Corrales-Guerrero, S., et al., *Inhibition of RRM2 radiosensitizes glioblastoma and uncovers synthetic lethality in combination with targeting CHK1.* Cancer Letters, 2023: p. 216308.
234. Tang, Q., et al., *Osalmid, a novel identified RRM2 inhibitor, enhances radiosensitivity of esophageal cancer.* International Journal of Radiation Oncology* Biology* Physics, 2020. 108(5): p. 1368-1379.
235. Shao, J., et al., *A Ferrous-Triapine complex mediates formation of reactive oxygen species that inactivate human ribonucleotide reductase.* Molecular cancer therapeutics, 2006. 5(3): p. 586-592.
236. Finch, R.A., et al., *Triapine (3-aminopyridine-2-carboxaldehyde-thiosemicarbazone): A potent inhibitor of ribonucleotide reductase activity with broad spectrum antitumor activity.* Biochemical pharmacology, 2000. 59(8): p. 983-991.
237. Kunos, C.A., et al., *Radiochemotherapy plus 3-aminopyridine-2-carboxaldehyde thiosemicarbazone (3-AP, NSC #663249) in advanced-stage cervical and vaginal cancers.* Gynecol Oncol, 2013. 130(1): p. 75-80.
238. Mackenzie, M., et al., *A Phase II study of 3-aminopyridine-2-carboxaldehyde thiosemicarbazone (3-AP) and gemcitabine in advanced pancreatic carcinoma. A*

trial of the Princess Margaret hospital Phase II consortium. Investigational new drugs, 2007. 25: p. 553-558.
239. Ma, B., et al., *A multicenter phase II trial of 3-aminopyridine-2-carboxaldehyde thiosemicarbazone (3-AP, Triapine®) and gemcitabine in advanced non-small-cell lung cancer with pharmacokinetic evaluation using peripheral blood mononuclear cells.* Investigational new drugs, 2008. 26: p. 169-173.
240. Evers, B.M., et al., *Establishment and characterization of a human carcinoid in nude mice and effect of various agents on tumor growth.* Gastroenterology, 1991. 101(2): p. 303-311.
241. Doihara, H., et al., *QGP-1 cells release 5-HT via TRPA1 activation; a model of human enterochromaffin cells.* Molecular and cellular biochemistry, 2009. 331: p. 239-245.
242. Benten, D., et al., *Establishment of the First Well-differentiated Human Pancreatic Neuroendocrine Tumor Model.* Mol Cancer Res, 2018. 16(3): p. 496-507.
243. Chow, Z., et al., *PI3K/mTOR dual inhibitor PF-04691502 is a schedule-dependent radiosensitizer for gastroenteropancreatic neuroendocrine tumors.* Cells, 2021. 10(5): p. 1261.
244. Ding, N., et al., *Peroxiredoxin IV plays a critical role in cancer cell growth and radioresistance through the activation of the Akt/GSK3 signaling pathways.* J Biol Chem, 2022. 298(7): p. 102123.
245. Sukati, S., et al., *Extracellular vesicles released after cranial radiation: An insight into an early mechanism of brain injury.* Brain Res, 2022. 1782: p. 147840.
246. Rychahou, P.G., et al., *Targeted molecular therapy of the PI3K pathway: therapeutic significance of PI3K subunit targeting in colorectal carcinoma.* Annals of surgery, 2006. 243(6): p. 833.
247. Allred, D., et al., *Prognostic and predictive factors in breast cancer by immunohistochemical analysis.* Modern pathology: an official journal of the United States and Canadian Academy of Pathology, Inc, 1998. 11(2): p. 155-168.
248. G-Biosciences. *CytoScanTM SRB Cell Cytotoxicity Assay*. Available from: https://www.gbiosciences.com/image/pdfs/protocol/786-213_protocol.pdf.
249. Beckman Coulter. *Cell Cycle Staining Protocol*. Available from: https://www.beckman.com/reagents/coulter-flow-cytometry/cell-health-research-assays/staining-protocol.
250. BD Biosciences. *Annexin V Staining Protocol*. 2023; Available from: https://www.bdbiosciences.com/en-us/resources/protocols/annexin-v-staining-protocol.
251. Rychahou, P., et al., *Colorectal cancer lung metastasis treatment with polymer-drug nanoparticles.* J Control Release, 2018. 275: p. 85-91.
252. Menolfi, D. and S. Zha, *ATM, ATR and DNA-PKcs kinases—the lessons from the mouse models: inhibition ≠ deletion.* Cell & Bioscience, 2020. 10(1): p. 8.
253. Paull, T.T., *Mechanisms of ATM activation.* Annual review of biochemistry, 2015. 84: p. 711-738.
254. Buisson, R., et al., *Distinct but concerted roles of ATR, DNA-PK, and Chk1 in countering replication stress during S phase.* Molecular cell, 2015. 59(6): p. 1011-1024.

255. Eaton, J.S., et al., *Ataxia-telangiectasia mutated kinase regulates ribonucleotide reductase and mitochondrial homeostasis.* The Journal of clinical investigation, 2007. 117(9): p. 2723-2734.
256. Huang, J., et al., *Heat shock transcription factor 1 binds selectively in vitro to Ku protein and the catalytic subunit of the DNA-dependent protein kinase.* Journal of Biological Chemistry, 1997. 272(41): p. 26009-26016.
257. Lin, Z.P., et al., *Excess ribonucleotide reductase R2 subunits coordinate the S phase checkpoint to facilitate DNA damage repair and recovery from replication stress.* Biochemical pharmacology, 2007. 73(6): p. 760-772.
258. Zhan, Y., et al., *Inhibiting RRM2 to enhance the anticancer activity of chemotherapy.* Biomedicine & Pharmacotherapy, 2021. 133: p. 110996.
259. Bartek, J. and J. Lukas, *Chk1 and Chk2 kinases in checkpoint control and cancer.* Cancer cell, 2003. 3(5): p. 421-429.
260. Yang, J., et al., *ATM, ATR and DNA-PK: initiators of the cellular genotoxic stress responses.* Carcinogenesis, 2003. 24(10): p. 1571-1580.
261. Smith, J., et al., *The ATM–Chk2 and ATR–Chk1 pathways in DNA damage signaling and cancer.* Advances in cancer research, 2010. 108: p. 73-112.
262. Corrales-Guerrero, S., et al., *Inhibition of RRM2 radiosensitizes glioblastoma and uncovers synthetic lethality in combination with targeting CHK1.* Cancer Letters, 2023. 570: p. 216308.
263. Kim, J.C., et al., *Preoperative concurrent radiotherapy with capecitabine before total mesorectal excision in locally advanced rectal cancer.* International Journal of Radiation Oncology* Biology* Physics, 2005. 63(2): p. 346-353.
264. De Paoli, A., et al., *Capecitabine in combination with preoperative radiation therapy in locally advanced, resectable, rectal cancer: a multicentric phase II study.* Annals of oncology, 2006. 17(2): p. 246-251.
265. Kim, J.-S., et al., *Preoperative chemoradiation using oral capecitabine in locally advanced rectal cancer.* International Journal of Radiation Oncology* Biology* Physics, 2002. 54(2): p. 403-408.
266. Stupp, R., et al., *Radiotherapy plus concomitant and adjuvant temozolomide for glioblastoma.* New England journal of medicine, 2005. 352(10): p. 987-996.
267. Yordanova, A., et al., *Peptide receptor radionuclide therapy combined with chemotherapy in patients with neuroendocrine tumors.* Clinical nuclear medicine, 2019. 44(5): p. e329-e335.
268. Pavlakis, N., et al., *Australasian Gastrointestinal Trials Group (AGITG) CONTROL NET Study: 177Lu-DOTATATE peptide receptor radionuclide therapy (PRRT) and capecitabine plus temozolomide (CAPTEM) for pancreas and midgut neuroendocrine tumours (pNETS, mNETS)—Final results*. 2022, American Society of Clinical Oncology.
269. Cao, Y., et al., *Whole exome sequencing of insulinoma reveals recurrent T372R mutations in YY1.* Nature communications, 2013. 4(1): p. 2810.
270. Verdugo, A.D., et al., *Global DNA methylation patterns through an array-based approach in small intestinal neuroendocrine tumors.* Endocrine-Related Cancer, 2014. 21(1): p. L5-7.
271. Hijioka, S., et al., *Rb loss and KRAS mutation are predictors of the response to platinum-based chemotherapy in pancreatic neuroendocrine neoplasm with grade*

3: a Japanese multicenter pancreatic NEN-G3 study. Clinical Cancer Research, 2017. 23(16): p. 4625-4632.
272. Delbart, W., et al., *Understanding the Radiobiological Mechanisms Induced by 177Lu-DOTATATE in Comparison to External Beam Radiation Therapy.* International journal of molecular sciences, 2022. 23(20): p. 12369.
273. Graf, F., et al., *DNA double strand breaks as predictor of efficacy of the alpha-particle emitter Ac-225 and the electron emitter Lu-177 for somatostatin receptor targeted radiotherapy.* PloS one, 2014. 9(2): p. e88239.
274. Slatko, B.E., A.F. Gardner, and F.M. Ausubel, *Overview of next-generation sequencing technologies.* Current protocols in molecular biology, 2018. 122(1): p. e59.
275. Sidey-Gibbons, J.A. and C.J. Sidey-Gibbons, *Machine learning in medicine: a practical introduction.* BMC medical research methodology, 2019. 19: p. 1-18.
276. Huang, S., et al., *Mining prognosis index of brain metastases using artificial intelligence.* Cancers, 2019. 11(8): p. 1140.
277. Huang, S., et al., *Artificial intelligence in cancer diagnosis and prognosis: Opportunities and challenges.* Cancer letters, 2020. 471: p. 61-71.
278. Van Booven, D.J., et al., *A systematic review of artificial intelligence in prostate cancer.* Research and reports in urology, 2021: p. 31-39.
279. Bhinder, B., et al., *Artificial intelligence in cancer research and precision medicine.* Cancer discovery, 2021. 11(4): p. 900-915.

VITA

Zeta Chow

EDUCATION

University of Colorado School of Medicine 08.2013-05.2017
Degree: M.D.

University of Wisconsin – Madison 08.2012-05.2013
Degree: M.S.
Major: Biomedical Engineering

University of Wisconsin – Madison 08.2008-05.2012
Degree: B.S.
Major: Biomedical Engineering
Minor: Biology

PROFESSIONAL POSITION

Administrative Chief Resident – Radiation Medicine	04.2024-present
GME representative of Radiation Medicine	07.2023-present
Resident Physician – Radiation Medicine	07.2021-present
Member of ASTRO	07.2021-present
Member of ABR	07.2021-present
GME Committee of Research Representative	07.2022-07.2023
T32 Surgeon Scientist Fellow	07.2019-06.2021

Markey Cancer Center Graduate Student Committee Member	07.2019 – 06.2021
Resident Physician – General Surgery	06.2017 – 06.2021

SCHOLASTIC AND PROFESSIONAL HONORS

T32 Surgeon Scientist Training Grant Award Receipt	2019-2021
ORIEN Research Network Travel Grant Receipt	2020
Graduated with Honros in Biomedical Engineering	2012
Tong Biomedical Engineering Capstone Design Award	2009

PUBLICATIONS

Chow, Z. and Fabian, D., 2024. Cervical cancer with vaginal recurrence and prior pelvic radiation. *International Journal of Radiation Oncology, Biology, Physics*, *118*(4), pp.886-887.

Chow, Z., Amoah, E., Hao, Z. and Kudrimoti, M., 2023. Radiotherapy in Managing Metastatic Hepatocellular Carcinoma With Cardiac Involvement and Pulmonary Tumor Thromboemboli: A Case Report. *Cureus*, *15*(3).

Chow, Z., Johnson, J., Chauhan, A., Izumi, T., Cavnar, M., Weiss, H., Townsend, C.M., Anthony, L., Wasilchenko, C., Melton, M.L. and Schrader, J., 2021. PI3K/mTOR dual inhibitor PF-04691502 is a schedule-dependent radiosensitizer for gastroenteropancreatic neuroendocrine tumors. Cells, 10 (5), 1261.

Johnson, J., Chow, Z., Lee, E., Weiss, H.L., Evers, B.M. and Rychahou, P., 2021. Role of AMPK and Akt in triple negative breast cancer lung colonization. *Neoplasia*, *23*(4), pp.429-438.

Johnson, J., Chow, Z., Napier, D., Lee, E., Weiss, H.L., Evers, B.M. and Rychahou, P., 2020. Targeting PI3K and AMPKα signaling alone or in combination to enhance radiosensitivity of triple negative breast cancer. *Cells*, *9*(5), p.1253.

Chow, Z., Osterhaus, P., Huang, B., Chen, Q., Schoenberg, N., Dignan, M., Evers, B.M. and Bhakta, A., 2021. Factors contributing to delay in specialist care after colorectal cancer diagnosis in Kentucky. *Journal of Surgical Research*, *259*, pp.420-430.

Chow, Z., Gan, T., Chen, Q., Huang, B., Schoenberg, N., Dignan, M., Evers, B.M. and Bhakta, A.S., 2020. Nonadherence to standard of care for locally advanced colon cancer

as a contributory factor for high mortality rates in Kentucky. *Journal of the American College of Surgeons*, *230*(4), pp.428-439.

Furbish, S.M., Kroehl, M.E., Loeb, D.F., Lam, H.M., Lewis, C.L., Nelson, J., Chow, Z. and Trinkley, K.E., 2017. A pharmacist–physician collaboration to optimize benzodiazepine use for anxiety and sleep symptom control in primary care. *Journal of pharmacy practice*, *30*(4), pp.425-433.

Bhat, S., Kroehl, M.E., Trinkley, K.E., Chow, Z., Heath, L.J., Billups, S.J. and Loeb, D.F., 2018. Evaluation of a clinical pharmacist-led multidisciplinary antidepressant telemonitoring service in the primary care setting. *Population Health Management*, *21*(5), pp.366-372.

PRESENTATIONS

Evers, B. M., Chow, Z., Zaytseva, Y., Lee, E. Y., Townsend, C. M., Gao, T., ... & Rychahou, P. G. (2024). Role of FASN in pancreatic neuroendocrine cancer cells survival. Cancer Research, 84(6_Supplement), 1796-1796. Poster presentation at the annual AACR conference, San Diego, CA, 2024.

Chauhan, A., Arnold, S., Kolesar, J., Carson, W., Weiss, H., Jayswal, R., Yan, D., Khouli, R.E., Khurana, A., Beumer, J. and Soares, H., Chow, Z., Abstract CT194: ETCTN 10388: a first in human phase I trial of triapine and lutetium Lu 177 DOTATATE in well-differentiated somatostatin receptor-positive gastroenteropancreatic neuroendocrine tumors (GEP-NETs). *Cancer Research*, *83*(8_Supplement), pp.CT194-CT194. Poster presentation at the annual AACR conference, Orlando, FL, 2023.

Chow, Z., Kunos, C. A., & Fabian, D. (2023). Cesium-131 Low-Dose Rate Interstitial Brachytherapy as a Salvage Re-Irradiation Technique in Treating Cervical and Uterine Cancer Pelvic Recurrence with Prior History of Pelvic Radiation. International Journal of Radiation Oncology, Biology, Physics, 117(2), e507-e508. Poster presentation at the ASTRO annual conference, San Diego, CA, 2023.

Chow, Z., Johnson, J., Chauhan, A., Izumi, T., Cavnar, M., Weiss, H., Rychahou, P. (2022). Inhibition of Ribonucleotide Reductase Subunit 2 (RRM2) Induces Radiosensitization in Gastroenteropancreatic Neuroendocrine Tumors. *International Journal of Radiation Oncology, Biology, Physics*, *114*(3), S160. Oral presentation at the ASTRO annual conference, San Antonio, TX, 2022.

Johnson, J., Chow, Z., Soleimani-Meigooni, A., & Fabian, D. (2023). PO31: Definitive Treatment of Locally Advanced Vulvar Squamous Cell Carcinoma in an Elderly with External Beam Radiotherapy, Chemotherapy, and Cesium-131 Interstitial and Iridium-192 Intracavitary Brachytherapy: A Case Report. Brachytherapy, 22(5), S80-S81. Poster presentation at the ABS annual conference, Vancouver, Canada in 2022.

Chow, Z., Synergistic Cytotoxic Effect of a Novel mTOR/PI3K Dual Inhibitor PF-04691502 and Radiation Therapy on Neuroendocrine Tumor Cells. *International Journal of Radiation Oncology, Biology, Physics*, *108*(3), e527. Poster presentation at the ASTRO virtual annual conference, 2020.

Chow, Z., Chauhan, A., Anthony, L., Townsend, C., Evers, B. M., & Rychahou, P. (2020). Effect of 3AP on neuroendocrine tumor cell proliferation, apoptosis and activation of DNA repair pathway. *Cancer Research*, *80*(16_Supplement), 6269-6269. Poster presentation at the AACR virtual annual conference, 2020.

Chow, Z., Townsend, C., Evers, B. M., & Rychahou, P. Effect of novel mTOR-PI3K dual inhibitors on neuroendocrine tumor cell proliferation and apoptosis. *Cancer Research*, *80*(16_Supplement), 676-676. Poster presentation at the AACR virtual annual conference, 2020.

Rychahou, P., Chauhan, A., Chow, Z., Izumi, T., Chen, Q., Lee, E.Y., Napier, D., Anthony, L.B., Cavnar, M.J., Kunos, C. and Evers, B.M., DNA-PK inhibitor, M3814, as a radiation sensitizer in the treatment of neuroendocrine tumors. *Cancer Research*, *80*(16_Supplement), pp.6402-6402. Poster presentation the AACR virtual annual conference, 2020.

Chow, Z., Townsend, C., Evers, B. M., & Rychahou, P. (2020). Effect of novel mTOR-PI3K dual inhibitors on neuroendocrine tumor cell proliferation and apoptosis. Cancer Research, 80(16_Supplement), 676-676. Presented at the Academic Surgical Congress, Orlando, FL, 2019.